

allCardAt

1

TDA

U.S. DEPARTMENT OF ENERGY
FEDERAL ENERGY TECHNOLOGY CENTER

99 JUN 11 AM 11:18 BLD

Volume I - Topical Report

A Novel CO₂ Separation System

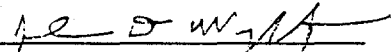
by Robert J. Copeland
Gokhan Alptekin
Mike Cesario
Steven Gebhard
Yevgenia Gershanovich

Prepared by

TDA Research, Inc.
12345 West 52nd Avenue
Wheat Ridge, Colorado 80033

For the U.S. Department of Energy
Federal Energy Technology Center
Contract No. DE-AC26-98FT40421 ✓

U.S. Department of Energy PRDA No. DE-RA26-98FT35008 ✓
Global Climate change - Novel Concepts for Management of Greenhouse
Gases


John D. Wright, Vice President

RECEIVED
DEC 11 2000
USTI

DISCLAIMER

This report was prepared as an account of work sponsored by an agency of the United States Government. Neither the United States Government nor any agency thereof, nor any of their employees, make any warranty, express or implied, or assumes any legal liability or responsibility for the accuracy, completeness, or usefulness of any information, apparatus, product, or process disclosed, or represents that its use would not infringe privately owned rights. Reference herein to any specific commercial product, process, or service by trade name, trademark, manufacturer, or otherwise does not necessarily constitute or imply its endorsement, recommendation, or favoring by the United States Government or any agency thereof. The views and opinions of authors expressed herein do not necessarily state or reflect those of the United States Government or any agency thereof.

DISCLAIMER

Portions of this document may be illegible in electronic image products. Images are produced from the best available original document.

1. Project Summary

Because of concern over global climate change, new systems are needed that produce electricity from fossil fuels and emit less CO₂. The fundamental problem with current CO₂ separation systems is the need to separate dilute CO₂ and pressurize it for storage or sequestration. This is an energy intensive process that can reduce plant efficiency by 9-37% and double the cost of electricity.

1.1. Scientific/Technical Innovation

To reduce the cost and improve efficiency, TDA identified a power generation system in which a fossil fuel (gasified coal, petroleum fuels or natural gas) at pressure reduces a metal oxide such as copper or iron, producing a metal (or a lower valence metal oxide), CO₂ and water (Figure 1-1). The water in the stream leaving the metal reduction reactor is condensed and its energy used to raise steam, leaving behind a stream of pure CO₂ that can be readily stored or sequestered. The metal is then "burned" or re-oxidized in air from the compressor section of a gas turbine, producing a hot high pressure stream of air which drives a gas turbine and generates electricity. The turbine exhaust can in turn be used to drive a steam bottoming cycle. The oxidized particles are then recycled to the first reactor to be reduced again and repeat the cycle. This system transfers the energy of the fuel to the metal and then the air, simultaneously transferring oxygen from the air to the fuel to fully oxidize the carbon containing fuel to CO₂ and water. The key is that the carbon in the fuel is never allowed to mix with and be diluted by the "combustion air."

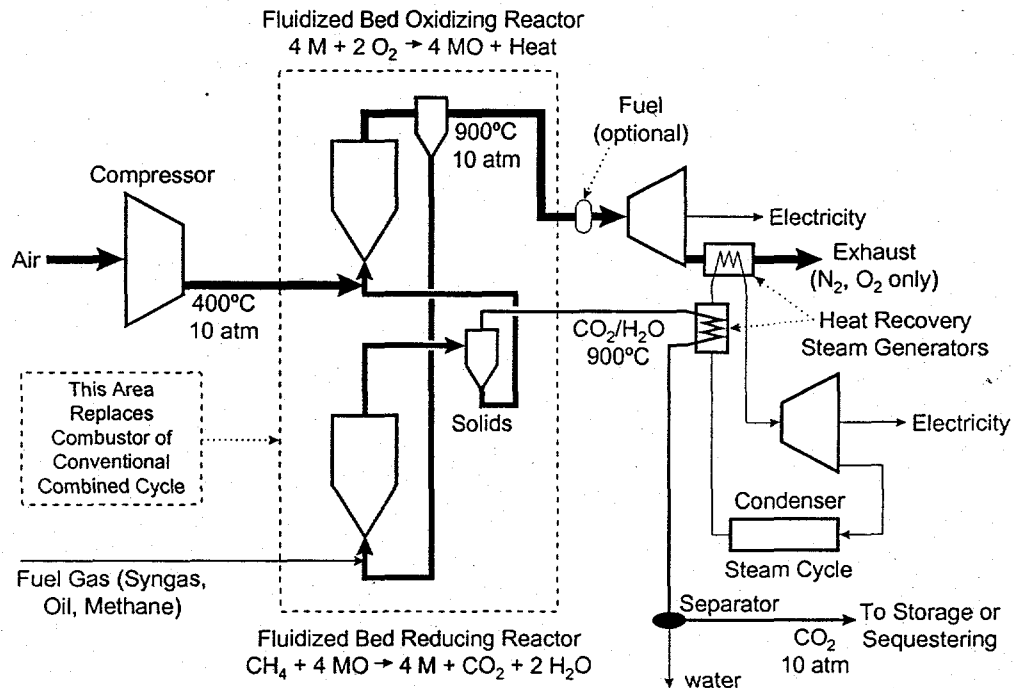


Figure 1-1. Sorbent energy transfer cycle schematic (M = metal).

TDA calls this system which transfers the energy of the fuel to the air without bringing the carbon along a Sorbent Energy Transfer System (SETS). The cycle can be run on any fuel gas (gasified coal, oil or natural gas) and does not require the development of new hardware. The power generation cycle is essentially a standard combined cycle, except that the combustor is replaced by two transport reactors (the SETS), one of which uses fuel to reduce the particulate metal oxide and one which oxidizes the metal to heat the air entering the turbine. The system was analyzed using methane (i.e., natural gas) as the fuel (because it is simplest to explain), but the cycle could also use gasified coal or petroleum.

The system can dramatically reduce or eliminate CO₂ emissions. The degree of CO₂ removal is limited only by the performance of the filters used to protect the turbine from particulates (filters that operate at higher temperatures allow the use of higher efficiency gas turbines). With the use of today's filters (a maximum filter temperature of 900°C), the cycle would reduce the CO₂ emissions of a combined cycle by 63% with natural gas and 84% with gasified coal while reducing the combined cycle efficiency by only 2.5% (i.e., 5% increase in fuel usage) from what would otherwise be a 50% combined cycle efficiency. With the use of 1300°C filters currently under development (which should be available well before our process is commercialized), the reduction in CO₂ emissions would be 100%. Since the power cycle uses only standard combined cycle generating equipment and two transport reactors (widely used in refineries), the major research needs are design optimization, sorbent development, pilot scale testing and detailed engineering and cost analyses.

1.1.1. The SETS Cycle and Components

The first step in the SETS process is to reduce a metal oxide to a metal (or a metal oxide to a lower valence metal oxide). In general, the metal (oxygen sorbent) would be supported on or contained within an inert support (such as alumina) which would provide a high surface area for reaction and good physical properties such as crush strength and attrition resistance. Reducing the metal oxide converts the energy in the fuel to energy which is stored in the reduced metal, and produces a stream which consists of 33% CO₂ and 67% water. We carry this step out at pressure (13.5 atmospheres, for example, as used in a General Electric Frame 7A gas turbine/combined cycle) in a transport reactor, and remove the steam from the CO₂ by condensing it (producing valuable mid-pressure steam which can be used to generate electricity in the steam turbine of the combined cycle) and a stream of virtually 100% pure CO₂ at high pressure. The CO₂ is sent to a storage or sequestering process with little additional compression energy.

Virtually all of the chemical energy in the original fuel gas is now incorporated into a new fuel (small particles of copper or iron on an inert support). The reduced particles enter a second reactor (also run at 13.5 atm) and are re-oxidized with air, producing large amounts of heat and heating the air to the temperatures needed to drive a gas turbine-combined cycle (900°C or greater). While transferring the energy to the air, the sorbent also transfers oxygen from the air to the fuel, fully oxidizing the fuel to CO₂ and H₂O.

Figure 1-2 shows the major components of the SETS. During Phase I, TDA found that the reducing reactor would perform best if it were subdivided into two stages: Reactor 1 oxidizes most of the fuel (~80% (e.g., natural gas; herein shown as CH_4 for simplicity) and fully reduces the sorbent, Reactor 2 completes the oxidization of the fuel with the fresh, fully oxidized oxide particles so that only very small amounts (ppm levels) of H_2 , CO , and CH_4 are sequestered with the CO_2 .

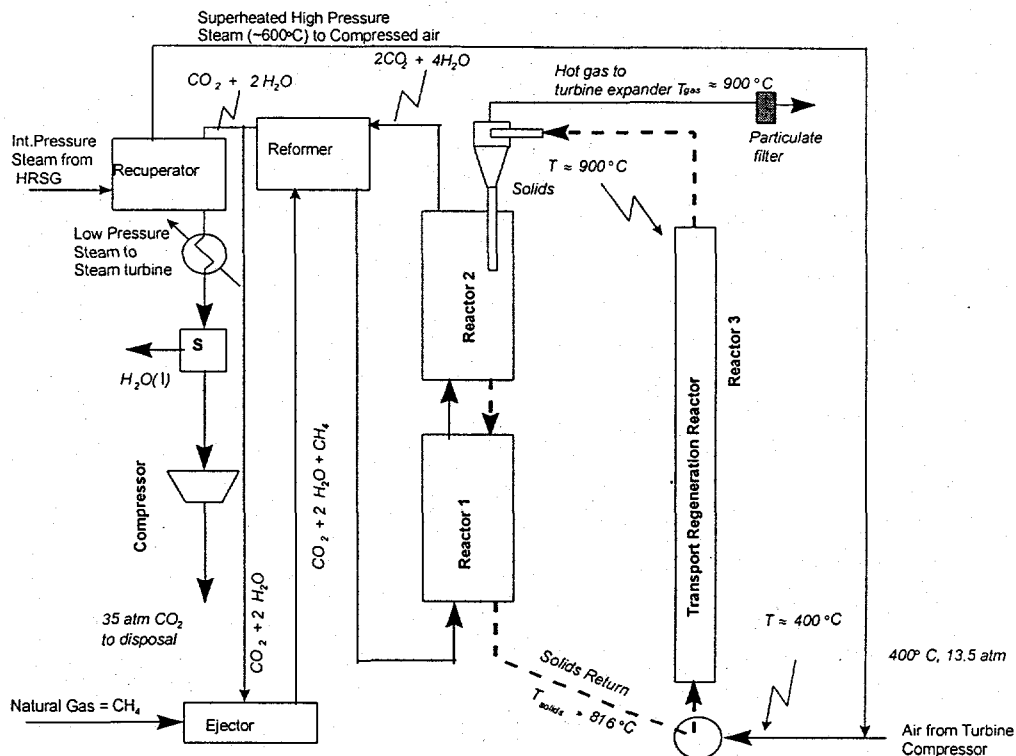


Figure 1-2. SETS components.

The air entering the oxidizing bed is the hot (400°C) high pressure (13.5 atm) air leaving the compressor stages of a standard gas turbine. The only CO_2 emissions from such a system would be produced if we burned some additional fuel to further boost the temperature of the high pressure air just before it enters the expander stages of the turbine. The oxidized sorbent particles that heated the air going to the expander section of the gas turbine would then be returned to the reducing reactor and the cycle repeated.

1.1.2. SETS Sorbents

TDA, with the aid of Dr. Doug Harrison, our consultant, investigated 77 potentially reducible metal oxides as potential oxygen sorbents for the SETS. Our objective, was to find a sorbent in which the net enthalpy change of the metal reduction and fuel oxidation reactions that occur in the reduction reactor is nearly zero (thermally neutral). We identified 13 sorbents which can operate on the SETS cycle but no one sorbent was found which would be exactly thermally

neutral in the reducing side, where there is minimal capacity to add or remove heat. While systems have been designed to use the endothermic nature of the reduction with Ni and FeO {Ishida, M. and H. Jin (1994), Ishida, M. et al. (1987), Ishida, M. et al. (1996)}, they require large heat exchangers. The use of such heat exchangers would significantly increase the capital cost of the SETS (e.g., although regenerated gas turbine cycles are known to be more efficient, most large power plants use combined cycles or simple cycles because of the high cost of the regenerative heat exchangers). TDA therefore designed the SETS to be a system which is nearly thermally neutral in the reducing side, eliminating the need for expensive heat exchangers.

To achieve a near thermally neutral reducing reactor, a mixture of two sorbents is required. One sorbent (e.g., Cu or MnO) reacts with CH₄ and releases heat in the reducing reactor. The second sorbent (e.g., Ni or FeO) absorbs heat while oxidizing CH₄ to CO₂ and H₂O. By simply controlling the relative quantities the two sorbents, we can maintain a near thermally neutral reactor. Since the oxidization of the sorbent heats the sorbent to ~900°C or more, we allow the sorbent to experience some net cooling on the reducing side (i.e., slight excess of the endothermic sorbents, Ni or FeO), so that sorbent leaves the reactor at a temperature above 700°C but less than 900°C (e.g., 816°C = 1500°F), as illustrated in Figure 1-2.

TDA reviewed the costs of the sorbents which could operate in SETS and selected four as the mostly likely to be cost effective: Cu, FeO, MnO, and Ni in the reduced state (CuO, Fe₂O₃, Mn₂O₃, and NiO oxidized). Of these, Cu and FeO are low in cost and have very good oxygen capacities. We evaluated Cu and FeO during the sorbent research in Phase I. While the reduction of Fe₂O₃ to FeO by CH₄ will not completely oxidize all CO and H₂, reduction of CuO to Cu will virtually remove all of the fuel gases (less than 100 ppm CO + H₂ are sequestered with the CO₂). Thus, the combination of sorbents provides both the desired thermally neutral reduction of the sorbent while fully oxidizing the CH₄ (or any other fuel gas)

1.1.3. Geodes for Long Sorbent Life

To make a sorbent pellet that can hold large amounts of sorbent without being destroyed by the absorption-regeneration process, TDA has developed a new sorbent structure which we call a geode (Figure 1-3). Like the geode that you buy at a gift shop, our geode has a hollow shell. The sorbent is loosely contained in, but does not fill, the hole(s) in the center. Thus, the sorbent can expand and contract indefinitely without destroying the pellet structure that surrounds it. Unlike the gem shop geode that has a single hole in the middle, our geode sorbent contains hundreds or thousands of holes in a structure that looks like a conventional catalyst support pellet on the outside. The interior structure of the geode is like a sponge, a sponge where the holes are partially filled with the chemically active material: Cu and/or FeO.

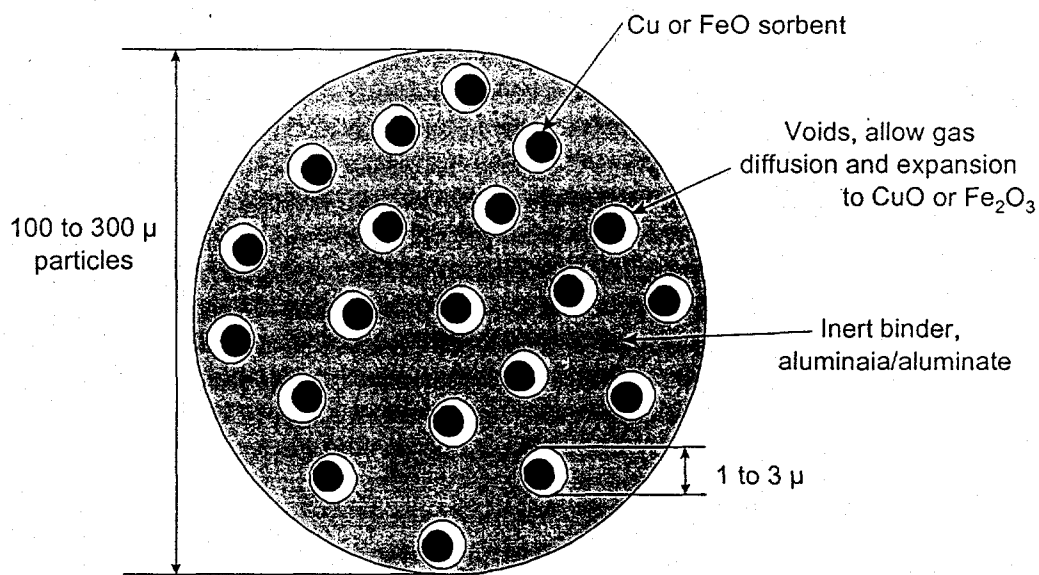


Figure 1-3. Structure of TDA's "geode."

To make the very small (e.g., 100 μ) particles required by fluidized bed and transport reactors, TDA has modified our previous methods of making the geode. The geode is made by mixing the sorbent (CuO or Fe₂O₃) with water, alumina, a low cost silica-containing material (e.g., bentonite or other natural clays or minerals), and other additives. The mixture is formed by spray drying or extruding and then firing. After firing, the water and some additives evaporate and/or burn, leaving behind a complex porous structure.

Due to the nature of this mixture, it separates upon firing into two different phases each of which are thermodynamically stable. Data from both published phase diagrams and our independent measurements show that the phases are physically separate. The size of each chemically active region of the geode (i.e., 1-3 μ m) is controlled by the selection of the starting materials. The geode structure: 1) is very strong because there is a continuous support phase, 2) effectively contains the sorbent inside small holes in the interior of the pellet, 3) allows the sorbent to expand and contract freely without disrupting the pellet structure, 4) allows the O₂ and H₂/CO/CH₄ to diffuse quickly into the interior of the pellet, and 5) can hold large quantities of sorbent. In addition, the process that we use to produce the geode is inherently inexpensive. The geode is formed by mixed metal oxide techniques, yet the geode has the continuous inert structure associated with catalyst supports, which have high strength and long lifetimes.

1.1.4. Cu and FeO Geodes for SETS

TDA, with our Dr. Doug Harrison of LSU, conducted thermodynamic analyses on several different redox metal oxides. Cu, FeO, Ni, and MnO were identified as potentially economic sorbents with a high oxygen loading as a SETS sorbents. Given the limited budget in Phase I, we selected the two lowest cost oxygen sorbents (Cu and FeO) that together can completely oxidize of the fuel gases

and for which the sum of the reactions occurring the metal reduction reaction will be nearly thermally neutral.

Sorbent Development TDA prepared ~ 30 sorbents containing copper and iron with a variety of binder materials and Cu and FeO contents. Due to the high temperatures of the SETS reactions, alumina and aluminates were the preferred binders for the geode. TDA then prepared geodes with alumina/aluminates and some silicates with either iron oxide or copper oxide or mixtures of iron and copper as the chemical sorbent. The mixtures of iron and copper were not attractive, since they turn to a very fine powder during the first reduction (at least for the high copper and iron contents in these first experiments).

Iron oxide geodes had very high iron content and were strong, porous and active. The iron based sorbents were tested for strength, porosity and surface area. The sorbents retained their strength, porosity and surface area in both oxidized and reduced state through several cycles. TDA made iron based sorbents both as geodes and by impregnating iron nitrate onto commercially FCC catalyst carriers. The iron based geodes were much better than the impregnated FCC catalyst carries; the iron based geodes were as strong as the FCC impregnates, but the iron content were much higher, more than doubling the oxygen capacity of the impregnated FCC carriers. With the geode sorbent oxygen loadings of ~9% "O" (wt.) were achieved (compared with less than 2% for the iron impregnated FCC catalyst carriers).

Strong, porous, and active copper oxide geodes were also made. While copper has a higher theoretical loading than iron, relatively larger quantities of support (i.e., alumina) are required. TDA made copper based sorbents both as geodes and by impregnating copper nitrate on to commercial FCC catalyst carriers. The copper-based geodes had much higher oxygen capacities than the impregnated FCC catalyst carries; but the copper based geodes were relatively weak when they were reduced. The copper FCC impregnates retained there strength in both oxidized and reduced conditions. With the copper impregnated FCC catalyst supports oxygen loadings of ~4.5% "O" (wt.) were achieved

Since manganese has a structure similar to iron and a slightly higher theoretical oxygen loading but like copper is exothermic during reduction, manganese (MnO) should make a better sorbent than copper. TDA is proposing to investigate MnO geodes in Phase II. Since approximately equal amounts of oxygen are carried in the iron and copper geodes, the average "O" loading in the SETS process is about 5.5% "O" for the best sorbents developed in Phase I.

Sorbent Cyclic Testing TDA then tested some of the best copper- and iron-based sorbents to determine their cyclic oxygen loading. Since the micro balance typically measures samples of less than 100 mg, we crushed and ground several pellet samples to assure that we used a powder that was representative of the sorbent.

The sorbents we selected for these tests exhibited the best combination of high porosity, crush strength and metal oxide loading. TDA selected one copper-

based sorbent and one iron-based from our earlier screenings for these microbalance tests. Both the copper and the iron based sorbents had good reaction rates. These two good sorbents are described below, and were the 28 wt% CuO on a commercial FCC catalyst support (alumina) and a high iron Fe₂O₃/Volclay geode sorbent.

Performance of a 28 wt % CuO Sorbent The extent of reduction and oxidation was measured at 800°C. Hydrogen, carbon dioxide and air were introduced to the system through separate rotameters. The rotameters were manually controlled to provide reducing or oxidizing gases at a flow rate of about 30 ml/min. Sorbent reduction was done using a mixture of 30% H₂ in CO₂ stream that was humidified to approximately P_{H₂O} = 17 Torr with a bubbler. The zero air was used without dilution for regeneration (oxidation) of the sorbent back to the metal oxide state.

The sorbent was first ground to a fine powder, and about 20 mg of sample was then placed on the platinum sample pan in our Shimadzu microbalance. The flow of 30 % H₂/CO₂ was established and then the temperature was increased to 800°C at a rate of 50°C/min. Figure 1-4 show the results of succeeding reduction and oxidation cycles on the 28% CuO sorbent. The observed weight

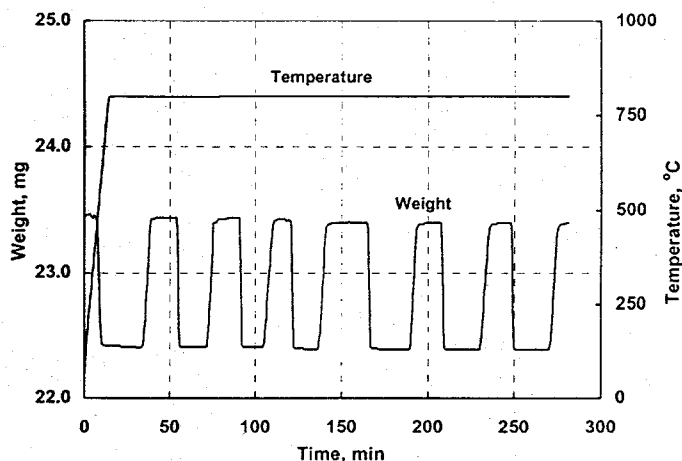


Figure 1-4. TGA results for 28 wt % CuO fluidizable sorbent.

loss upon reduction corresponds to complete reduction of CuO to metallic Cu by the hydrogen. The observed weight change was 4.4% which is the same within experimental error as the 4.8 % weight loss expected from stoichiometry. Importantly, Figure 1-4 shows that over a period of 7 cycles, the sorbent oxidation/reduction is completely reversible and no thermal history develops. This result suggests that good sorbent durability and long life can be expected when it is used at the commercial scale. Figure 1-4 shows that the original weight is regained for each cycle to within 0.1 wt %. This indicates that the reduction/oxidation capacity of the sample can be maintained over 8 cycles (about 4 h) without any significant deactivation.

Performance of a Fe₂O₃/Volclay Geode Sorbent We also tested a Fe₂O₃/Volclay geode. For this sample, we used two different reducing gases. During the first three cycles the flow of H₂/CO₂ mixture was identical to that of employed earlier. After the third cycle a gas stream of a standard mixture of CO (3.2%), CH₄ (4.7%), H₂ (10.0%), CO₂ (82.1%), (Scott Specialty Gases) to was used to reduce the sample, with air being the oxidizer for each case. The

selected gas stream simulates the composition at the outlet of the first reactor, which includes some unreacted methane and a relatively lean hydrogen concentration. This is also the composition near the middle of the natural gas reduction reactor when a transport reactor is used. At the start of the 4th cycle we switched back to the original mixture of 20% H₂/ 80% CO₂ as the reducing gas and realized an increase in the capacity to 8.5%. The oxidation and reduction rate remained unchanged through the cycles (0.3 mg/min and 0.25 mg/min for oxidation and reduction, respectively).

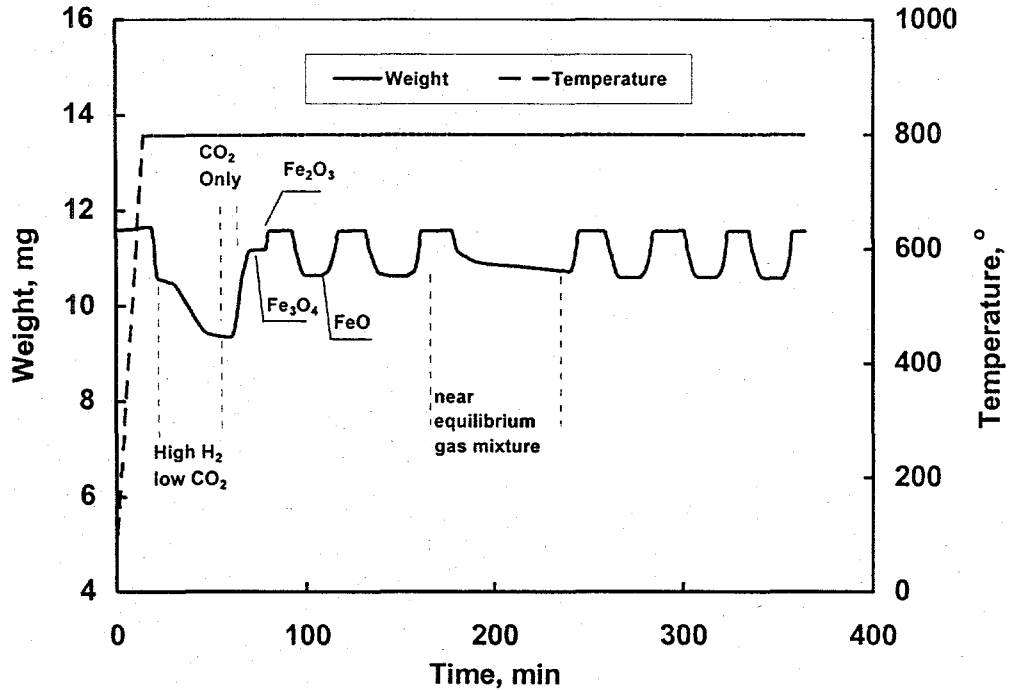


Figure 1-5. TGA results for Fe₂O₃ Voclay geode.

Note also in Figure 1-5 that when the H₂ concentration was high during the first reduction, this gave the largest weight loss. This was due to over-reduction of the sorbent to a mixture of Fe (elemental) and FeO (the weight loss was not large enough to indicate that all of the sorbent was reduced to Fe metal). Also note (labeled on Figure 1-5) that when oxidizing the sorbent from this state, the sorbent goes through the stages of oxidation: FeO (Fe^{II} oxide), Fe₃O₄ (mixed Fe^{II} and Fe^{III} oxide) and finally Fe₂O₃ (Fe^{III} oxide). Figure 1-5 shows that in both the cases of H₂ rich reducing gas (ca. 30 vol %) and the equilibrium reactor #1 gas, the oxidation and reduction of this sorbent are completely reversible with no loss in sorbent performance as the sorbent is cycled. Thus, under the condition of our SETS cycle, the cyclic capacity of this sorbent is 90%.

These results show that the TDA sorbents are highly effective for oxygen transfer and can be repeatedly cycled between the oxidized and reduced forms without any degradation in sorbent performance. We found that the Fe₂O₃/Voclay geode formulation and the 28 wt% CuO/Norton formulations gave

excellent results. Thus these sorbent formulations are ideal for application in either the two stage fluidized bed application or in the transport reactor.

1.1.5. Economic Analysis

The alternative to separating and sequestering CO₂ will probably be to pay a carbon tax. Carbon taxes are not imposed in the U.S. at this time, but various proposals would require taxes on the order of \$25 to \$50/ton of CO₂ emitted into the atmosphere. A tax of \$25 to \$50/ton CO₂ adds 10.8 to 21.6 mills/kWh to the price of electricity in a 6824 B/kWh heat rate, natural gas fired, combined cycle power plant (a roughly 20 to 40% increase in the cost of electricity). Because the carbon tax price is high, there is a significant economic incentive to develop power cycles which emit little or no CO₂.

To determine the impact of SETS on the cost of energy, TDA selected a nominal gas turbine/combined cycle, and analyzed the performance of the cycle both with and without SETS. The gas turbine has a firing temperature of 1260°C (2300°F), a gas inlet temperature to the turbine of 1200°C (2192°F), a pressure ratio of 13.5:1, and a compressor flow of 408 kg/sec (900 lb/sec). However, 2.75% of the compressor flow is used in cooling the turbine, which leaves 397 kg/sec to flow through SETS (these are approximately the operating conditions of a General Electric Frame 7A combined cycle). This combined cycle has a Lower Heating Value (LHV) efficiency of 50% of 6824 Btu/kWh when operated on natural gas. With this combined cycle, TDA calculated all of the gas, mass, and energy flows in the SETS.

System Efficiency As indicated in Figure 1-2, the fully oxidized fuel leaves reactor 2 at 900°C and has a composition of 2H₂O and 1CO₂. The gases are first cooled to ~650°C. Some of those gases mix with the natural gas in an ejector, which slightly raises the pressure of the recycling H₂O and CO₂. The mixture then flows through the reformer, reforming part of the CH₄ to CO and H₂ while cooling the outlet gases from reactor 2 to ~650°C. After cooling the gas stream splits, some is recycled and the remainder is cooled in a recuperator, generating high pressure superheated steam which is added to the high pressure air.

After superheating a stream of intermediate pressure steam, the H₂O and CO₂ are cooled, condensing the steam. Since the steam is condensed at high pressure and accounts for 63% of the gases (i.e., CH₄ + 4 "O" (from oxides) = CO₂ + 2 H₂O), the condensing of the steam with the CO₂ can be used to generate pure steam at low pressure. However, to maintain the molar flow rate in the gas turbine and steam cycle, three

Figure 1-6. SETS CO₂ separation Efficiency

KCal/CH ₄	
Low Press. ST	1.04
Lost Steam Power for H ₂ O	-3.91
CC Power	
2/3 rd s heat from SETS	62.98
1/3 rd heat Direct NG	31.93
CO ₂ compression	-0.76
Parasitic for CO ₂ separation	-0.31
Net Power (KCal /mol CH ₄)	90.97
LHV efficiency	47.48%
Loss of efficiency points	-2.52%

moles of H₂O are extracted at intermediate pressure (~ 200 psia, 13.5 ATM) from the steam cycle and added to the gas flow through the oxidizing reactor; that lost H₂O reduces the power generated in steam turbine.

The condensation of steam will generate low pressure steam (~ 1 ATM) which can generate power. The low pressure steam is assumed to generate power at 8% thermal efficiency. The extraction of intermediate pressure steam (~ 200 psia) reduces power generation in the steam turbine; we assume a power thermal efficiency penalty at 20% for intermediate pressure steam. High pressure steam (~ 600 psia) has a higher thermal efficiency (~30%) and we calculate the power gains and losses from the use of steam using these assumptions.

Additional power is lost in SETS to compress the CO₂ to high pressure and in the parasitic losses (i.e., the pressure drop of the air flowing through the reactor). Figure 1-6 presents an estimate of these efficiency losses and gains for the SETS. In comparison to the unmodified 50% LHV efficiency combined cycle (i.e., with CO₂ emissions), the use of SETS reduces the power plant efficiency by 2.5 efficiency points from 50% to 47.5% (or a 5% increase in fuel usage for the same net power output).

System Cost Based upon the use of Cu and FeO sorbents in equal proportions as the SETS sorbents, TDA estimated the flows of all of the gases and solids in all of the reactors. We estimated the size of all of the reactors and provided the data Kellogg Brown and Root, Inc. (Kellogg). Costs were calculated assuming \$3/MMBtu for natural gas, 15% \$/\$-yr Fixed Charge Rate (FCR)(for the cost of money, debt repayment, taxes, profit, insurance, and O&M), and a 75% Capacity Factor (CF).

TDA conducted a preliminary study to determine if the SETS has economic potential. Figure 1-7 presents a summary of the costs assumptions for this analysis. Natural gas at \$3/MMBtu was the fuel, and the plant efficiency was calculated as described in Figure 1-6. As of this writing, we have not received all of Kellogg's cost estimates. The capital cost analysis is based upon the preliminary data provided by Kellogg (i.e., \$50/kW based on the transport reactors at the Piñon Pine Clean Coal Technology Power Plant). Sorbent costs and loss rates were estimated based upon TDA's experience. We estimated \$5/lb for the iron based sorbent since Fe₂O₃ is very in-expensive (\$0.30/lb). Due to the higher cost of copper (\$1.21/lb for CuO) and the expensive support used in the copper based sorbent, copper sorbents were assumed to cost \$10/lb. The sorbent costs account for the largest uncertainty in the economic analysis and substantial research would be required (i.e., the DOE funded Phase II and Phase III research) to reduce the uncertainties.

Figure 1-7. Impact of SETS on the cost of electricity/CO₂ separation.

SETS capital and energy costs

\$3/MMBtu 5% efficiency penalty (loss of 2.5 per centage points) = 1.02 mill/kWh

Capital costs : @\$50/kW_e or \$10 million for a 200 MW_e power plant,
75% CF, 15% FCR =1.14 mills/kWh

Total of ~ 2.16 mills/kWh or \$5/ton CO₂ total, but 2/3^{ds} of CO₂ captured = \$7.5/ton CO₂ removed

Sorbent Cost \$11/ton CO₂ removed

Sorbent costs include the expense of the manufactured material, the oxygen loading per cycle and the loss rate of sorbent per cycle. The costs are based on an assumed price of \$5 for FeO sorbent with 9% O₂ loading and \$10/lb of Cu sorbent with 4% O₂ loadings of (5.5 lb oxygen per 100 lb of sorbent average), and an attrition rate of 2% per hour, 1.5 sec contact time per reactor pass, two reducing reactors with one pass each, and one oxidizing reactor with three passes per cycle.

Overall: \$18.5/ton of CO₂ removed

While there is a measure of uncertainty related to the capital cost of the SETS and the cost of the sorbent for CO₂ removal, there is also clearly an opportunity for SETS to reduce the carbon emissions at costs that are much lower than the proposed carbon taxes. The estimated cost of CO₂ removal is \$18.5/ton of CO₂ removed.

TDA recognizes that the cost of sequestering the CO₂ has not been included in the costs. These costs may add significantly to the cost of greenhouse gas removal. However, in some cases (e.g., for enhanced oil recovery, natural gas production), these cost may be negative, especially if the power plant is near the end user of the CO₂.

1.2. Impact

While a number of processes for separation and compression of CO₂ from stack gases have been studied, all are extremely costly and add significantly to the overall energy demand (Smelser and Booras, 1991). Herzog (1997) summarized a number of current and advanced systems for removing CO₂ from power plant flue gases. Although removing CO₂ from conventional oil or gas fired plants requires less energy than from conventional coal plants (because the carbon/hydrogen ratio of coal is higher than that of either oil or gas), the energy penalty is severe, 13-37% for current technologies and 9-15% for future systems.

SETS efficiently uses the chemical potential of the fuel to transfer the fuel energy by reducing a metal oxide. The reduced solid is then moved into a high pressure air stream which oxidizes the metal sorbent (i.e., "burns" the transferred fuel energy) to heat the air in a combined cycle power plant. Since the energy required to separate the solids from the air is very low, little of the power cycles work is lost in this separation. Similarly, since reducing the sorbents fully oxidize the fuel to CO₂ and H₂O, which are also easily separated by condensing the water and recovering the CO₂ as a high pressure gas, only a very small amount of power is required to deliver high pressure (e.g., 35 atm) CO₂ to the

sequestration system. The net result is about a 5% increase in the fuel usage for the same net power delivered to the utility grid. In comparison to the 13 to 37% energy penalty for current CO₂ separation system, SETS offers a substantial improvement in CO₂ capture technology.

Not only does SETS reduce energy consumption, it also minimizes capital costs and other operating costs. TDA estimated that SETS will increase electrical generation costs by less than 10% (e.g., \$18.5/ton CO₂) with 63% of the CO₂ capture from a natural gas combined cycle plant (in the case where current filter technology limits the SETS air outlet temperature to 900°C). In comparison Herzog and Drake (1993) estimated that CO₂ capture would increase the cost of by from 30% to 100% depending on the system. Paying CO₂ emission taxes at \$50/ton would increase the cost of a natural gas combined cycle plant by more than 20%.

For a SETS operating on natural gas and using a current technology ceramic filter, the SETS outlet temperature is limited by the temperature limits of the barrier filter downstream of the oxidizing reactor. Thus, with today's barrier filters, some additional gas must be burned (and some CO₂ released) to raise the turbine inlet temperature to 1200°C. Nevertheless, SETS removes ~63% of the CO₂ (with natural gas and 84% with gasified coal) and system can be configured to remove all of the CO₂ with a minimal increase in cost. When barrier filters capable of 1200°C operation are available (1300°C filters are already being developed), the SETS outlet temperature can be raised to 1200°C and 100% CO₂ removal can be achieved. Since 1) power plants consume ~20% of the USA energy, 2) Power plants are the largest users of coal, 3) SETS can be used with any fossil fuel (natural gas, oil, and gasified coal) and 4) SETS incorporates the most cost effective power plant now available (the combined cycle), the development of SETS could do much to mitigate greenhouse gas emissions while minimizing the costs to reduce global warming.

The installed bases of electrical generation capacity in the U.S. is 762,408 MW (1994). While it is impossible to accurately forecast growth rates for electrical generation capacity one to three decades in the future, if we assume a 2% annual growth rate and implementation beginning 15 years from now, the total annual market for new generation technology in the U.S. (and therefore the potential annual U.S. market for SETS/Combined Cycle systems) will be 20,000 MW/year.

One years worth of this electric growth represents about 51 million tons per year of CO₂, by conservatively assuming the capacity is supplied by 50% LHV natural gas fired combined cycles (i.e., the lowest carbon content fossil fuel). If the growth occurred all in coal-fired generation, the savings would be about 90 million tons of CO₂ per year. After 10 years of growth, the cumulative greenhouse gas savings are 2,500 million tons of CO₂ assuming all natural gas fueled generation (4,400 million tons savings with coal).

Assuming a 200 MW combined cycle power plant, about 100 plants are added each year. The SETS can use fossil fuels and be sited anywhere in the USA. For a ten year period this represent 1,000 SETS plants to capture CO₂ and 20% of the entire USA power generation capacity (excluding the potential for retro-fits to existing power plants). With minimal cost, many existing power plants (i.e., combined cycles and gas turbines) could also be retrofitted to incorporate SETS.

By incorporating SETS plants with improved 1200°C high temperature filters, those 1,000 power plants, which could be sited anywhere in the USA, would capture the entire 2,500 million tons of CO₂. If the CO₂ capture is required before the development of new barrier filters, SETS still captures 1,700 million tons (or more if the capacity is fired by oil or gasified coal). The applications of SETS to CO₂ is therefore available in the near term with only the development of the appropriate SETS sorbents and the demonstration of the technology, since all other portions of SETS are already in commercial use.

Table of Contents

1. Project Summary	ii
1.1. Scientific/Technical Innovation.....	ii
1.1.1. The SETS Cycle and Components.....	iii
1.1.2. SETS Sorbents	iv
1.1.3. Geodes for Long Sorbent Life	v
1.1.4. Cu and FeO Geodes for SETS.....	vi
1.1.5. Economic Analysis	x
1.2. Impact.....	xii
2. Introduction	1
2.1. The Sorbent Energy Transfer System (SETS).....	3
2.1.1. Selection of the Redox Metal	4
2.1.2. Sorbent Structure and Manufacture	6
3. Phase I Tasks, Organization, Schedule and Status	9
3.1. Phase I Organization	9
3.2. Phase I Schedule.....	10
3.3. Phase I Costs	10
4. Conceptual Design and Thermodynamic Analyses	11
4.1. Active Metal Selection	11
4.2. Use of Nickel as a Reforming Catalyst.....	16
5. Sorbent Preparation, Characterization and Testing	18
5.1. Binder Screening	18
5.2. Sorbent Screening.....	21
5.3. Sorbent Characterization	23
5.3.1. Fluidizable Norton SA5395 Support Material.....	23
5.3.2. Copper-Based Sorbents.....	25
5.3.3. Iron-Based Sorbents	27
5.4. Multiple cycle testing.....	31
5.4.1. Experimental Methods.....	31
5.4.2. Sorbent Test Results.....	33
6. Economic Analyses	40
6.1. Efficiency Impact of SETS	40
6.2. Integration of the SETS and Power Cycle.....	42
6.3. Cycle Efficiency and Cost of CO ₂ Separation.....	45
6.4. Preliminary Sizing of Sorbent Reduction and Oxidation Reactors.....	46
6.4.1. Transport Sorbent Oxidation	47
6.4.2. Stationary Fluidized Bed Reactors for Sorbent Regeneration.....	48
6.4.3. Transport Reactor for Natural Gas - Sorbent Contacting (Sorbent Reduction).....	50
6.4.4. Conclusions.....	51

7. Impact	52
7.1. Complete Removal of CO ₂ with Current Technology Barrier Filters	53
7.2. Estimated CO ₂ Capture by SETS.....	53
7.3. Conclusions	54
8. References.....	56
APPENDIX A Thermodynamic Data from Dr. D. Harrison of LSU	58

List of Figures

Figure 1-1. Sorbent energy transfer cycle schematic (M = metal).....	ii
Figure 1-2. SETS components.....	iv
Figure 1-3. Structure of TDA's "geode".....	vi
Figure 1-4. TGA results for 28 wt % CuO fluidizable sorbent.....	viii
Figure 1-5. TGA results for Fe ₂ O ₃ Voclay geode.....	ix
Figure 1-6. SETS CO ₂ separation Efficiency	x
Figure 1-7. Impact of SETS on the cost of electricity/CO ₂ separation.	xii
Figure 2-1 Schematic of TDA's geode.	6
Figure 2-2. Photomicrograph of ZnO geode.	8
Figure 3-1. Project organization.....	10
Figure 3-2 Project schedule.....	10
Figure 4-1. Oxidation of CH ₄ by NiO (virtually identical results are obtained for Fe ₂ O ₃ , see Appendix A).....	14
Figure 4-2. Oxidation of CH ₄ by CuO (similar results are obtained for Mn ₂ O ₃ see Appendix A).....	14
Figure 4-3. SETS system.....	15
Figure 5-1. Alumina & Aluminate Screening.	20
Figure 5-2. Boehmite Screening.	21
Figure 5-3. Photograph of sorbent samples analyzed with TDA's Shimadzu TGA apparatus.	23
Figure 5-4. XRD patterns for Norton SA5395 calcined at 200°C and 900°C	24
Figure 5-5. XRD patterns comparing Norton SA5395 and α-Al ₂ O ₃	25
Figure 5-6. XRD patterns for Norton support and 28 wt % CuO sorbent.....	26
Figure 5-7. XRD patterns for Norton support and 25 wt % Fe ₂ O ₃ sorbent.....	27
Figure 5-8. Shimadzu microbalance.	31
Figure 5-9. Schematic of microbalance flow apparatus.....	32
Figure 5-10. TGA results for 28 wt % CuO fluidizable sorbent.....	34
Figure 5-11. Weight change for 28 wt% fluidizable sorbent during cycling.....	34
Figure 5-12. TGA results for CuO-Fe ₂ O ₃ geode sorbent.....	36
Figure 5-13. Weight change for CuO-Fe ₂ O ₃ geode sorbent during cycling.	37
Figure 5-14. TGA results for Fe ₂ O ₃ Voclay geode.....	38
Figure 5-15. Weight change for Fe ₂ O ₃ /Voclay geode sorbent during cycling. ...	39
Figure 6-1. SETS system.....	41
Figure 6-2. Process flow diagram showing the use of stationary fluidized bed reactors for natural gas oxidation.....	46
Figure 6-3. Process using transport reactor for natural gas oxidation.	50

Figure 7-1 Reduction in CO ₂ emissions as a function of oxidation reactor outlet temperature for coal, oil and natural gas.	52
Figure 7-2. High CO ₂ removal system.....	53

List of Tables

Table 2-1. Energy penalties for CO ₂ capture.	2
Table 2-2. Reduction of redox metal oxides.....	5
Table 2-3. Oxidation of redox metal oxides.....	6
Table 4-2. Reduction of redox metal oxides.....	11
Table 4-3. Oxidation of redox metal oxides.....	12
Table 4-4. Raw material costs for redox metal oxides. Costs from Chemical Market Report of March 10, 1997, excepted as noted.	12
Table 4-5. Dependence of the cost of selected redox metal oxides on the source.	13
Table 4-1. Commercial Ni steam reforming catalysts.....	16
Table 5-1. Properties of Norton catalyst supports.....	22
Table 5-2. Impregnated sorbents.....	22
Table 5-1. Chemical analysis of Norton supports.....	24
Table 5-2. Composition of Geodes.	28
Table 5-3. Effect of cycling on geode sorbents.	29
Table 5-4. Properties of cycled sorbents.....	30
Table 5-5. Strength of reduced geodes.....	31
Table 6-1. Efficiency of two CO ₂ separation systems.....	42
Table 6-2. Nominal Compositions (mol %).	44
Table 6-3. Nominal Conditions.....	44
Table 6-4. Impact of SETS.	45
Table 6-5. Results of preliminary design calculations.	47
Table 6-6. Operating conditions for transport regeneration reactor (P = 13.5 atm).	48
Table 6-7. Operating conditions for staged fluidized bed reactors for natural gas oxidation (sorbent reduction); P = 13.5 atm.	49

2. Introduction

Fossil fuels currently supply over 85% of the world's energy needs, and will likely do so well into the 21st century. However, the high standard of living made possible by the large-scale use of fossil fuels is threatened by the real possibility of global climate change, commonly referred to as the "greenhouse effect". The major greenhouse gas is carbon dioxide (CO₂) and the major source of anthropogenic CO₂ is the combustion of fossil fuels, and in particular, the use of coal for the generation of electricity. The potential impacts of global climate change are described by Watson et al., (1996). Because of these potential impacts, the world community has adopted the Framework Convention on Climate Change.

In the near-term, significant reductions in CO₂ emissions per unit of electricity generated, and perhaps even reductions in total CO₂ emissions can be made by simply increasing the efficiency of electrical generation equipment. However, to meet probable emissions targets in the mid- to long-term, more efficient and costly mitigation technologies must be considered, specifically CO₂ capture and sequestration, nuclear, and extensive use of renewable energy.

For the capture and sequestration of CO₂, the most cost-effective targets are large stationary sources of CO₂, such as fossil fuel-fired power plants. These power plants produce about one-third of U.S. CO₂ emissions as they produce electricity for residential, commercial, and industrial customers. This share may increase in the future due to continued electrification of the industrial and building sectors. Also, over the longer-term, even the transportation sector may be electrified.

Avoidance of CO₂ emissions through physical capture of CO₂ from fossil fuel power plants was first proposed by Marchetti (1977), with disposal of the captured CO₂ in the deep ocean. In the U.S., preliminary studies were conducted at Brookhaven National Laboratory (Albanese and Steinberg, 1980; Steinberg, 1984). Other potential sequestration technologies include storage of CO₂ in depleted oil and gas reservoirs or the deep oceans (Herzog et al., 1996). The one thing all of these sequestration processes have in common is that they need a high pressure stream of CO₂.

Although it is impossible to fully understand the ultimate characteristics and costs of the sequestration systems at this time, the main options for storage are underground and ocean storage. Options for underground storage include storage in active oil reservoirs, coal bed, depleted oil and gas reservoirs, deep aquifers and mined salt domes or rock caverns. Ocean storage options include a variety of methods for injecting liquids or solids at a depth of 1000 to 4000 meters. While each of the technologies listed above has its own advantages or disadvantages, they all must be fed with a relatively pure stream of high pressure CO₂. The high pressure is needed to maximize the amount of CO₂ stored per unit volume, and purity is important simply because it is expensive to

compress gases, and we therefore do not want to waste energy compressing gases other than CO₂.

While a number of processes for separation and compression of CO₂ from stack gases have been studied, all are extremely costly and add significantly to the overall energy demand (Smelser and Booras, 1991). Herzog (1997) summarized a number of current and advanced systems for removing CO₂ from power plant flue gases. (Table 2-1). Although removing CO₂ from conventional oil or gas fired plants requires less energy than from conventional coal plants (because the carbon/hydrogen ratio of coal is higher than that of either oil or gas), the energy penalty is severe.

Table 2-1. Energy penalties for CO₂ capture.

Power Plant Type	Today	Future
Conventional Coal	27-37% (Herzog and Drake 1993)	15% (Mimura et al. 1997)
Gas	15-24% *Herzog and Drake 1993)	10-11% (Mimura et al. 1997)
Advanced Coal	13-17% (Herzog and Drake 1993)	9% (Herzog and Drake 1993)

Current CO₂ removal technology employs scrubbers, generally with aqueous amine solutions, to remove the CO₂ from the flue gas. These systems suffer from the fact that the CO₂ in the flue gas is fairly dilute (10% by volume). If we are to achieve 90% recovery of the CO₂ and produce a stream of relatively pure atmospheric pressure CO₂, we are essentially operating a compression system over a pressure ratio of 100 to 1 (power consumption for compression is proportional to the natural log of the pressure ratio). Further, in absorption based systems the separation system can be considered as a heat engine driven by the difference in temperature between the absorption and regeneration steps. As this temperature difference is relatively small, the separation system is quite energy intensive. Thus, the energy consumption of this step is roughly ten times the minimum work of compression. Although better absorption systems are under development and the potential exists to better integrate the separation system and the heat system of the power cycle, all heat driven systems that remove CO₂ from flue gases will suffer the twin problems described above (compression ratios of roughly 100 to 1 and high heat requirements).

After we separate the CO₂ from the flue gases, we still have to compress it to the pressures required for pipeline transport and sequestration. Since each sequestration technology requires a somewhat different pressure and our purpose is to develop an improved power generation cycle which reduces or eliminates CO₂ emissions, we will simply assume that the CO₂ must be further compressed to pipeline pressure of 35 atm (500 psi). This assumption does not unfairly advantage or disadvantage any technology.

Advanced coal systems that integrate CO₂ removal into the power cycle instead of removing it after it is diluted with air by the combustion process could suffer much less of a penalty. In an Integrated Gasification Combined Cycle (IGCC), the coal is gasified at high pressure and the resulting gases are cleaned and used to drive a combined cycle. If coal is gasified at pressure, the clean gas

could be shifted to using the water gas shift reaction to produce a stream which contains mainly hydrogen, steam and CO₂. Because the CO₂ would be mixed with H₂ (and probably nitrogen, depending on the type of gasifier), a chemical separation to remove the CO₂ is still necessary. However, since the partial pressure of the CO₂ is much higher (probably greater than 1 atm) than in flue gas, physical sorbents such as Selexol (dimethyl ether of polyethylene glycol) can be used, and the energy penalty is much smaller. Unfortunately, since the affinity of the sorbent for CO₂ is greater at lower temperatures, the syngas stream must be cooled to near ambient temperature before the CO₂ can be removed (a capital and energy intensive process).

While the advanced coal based system described above still has a 13-15% energy penalty associated with CO₂ removal, it does illustrate the direction we should be looking in. The important conclusions are:

- 1) The CO₂ should be removed from the system before the fuel is burned with air and thereby diluted with nitrogen (the IGCC cycle achieves this).
- 2) The partial pressure of the CO₂ should be large (well over an atmosphere if possible) to minimize not only the separation costs but the subsequent costs for compressing it to the pressure needed in the sequestration process (the advanced IGCC cycle achieves this).
- 3) If the CO₂ stream is not pure, it should not be mixed with non-condensable gases such as H₂ or N₂ that make it necessary to carry out a chemical (absorption) separation of the CO₂ (the IGCC does not achieve this).
- 4) The system should not require that a hot fuel stream (such as a syngas stream from a gasifier) be cooled to near ambient temperature in order to remove the CO₂ (the IGCC does require this).
- 5) The cycle should be applicable to all types of fuel (coal, oil and natural gas).

2.1. The Sorbent Energy Transfer System (SETS)

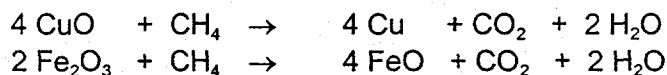
To generate power from fossil fuels while eliminating CO₂ emissions and producing a stream of concentrated, high pressure (10 atm) CO₂ which can be sent off to sequestration with only a small amount of additional compression, TDA Research, Inc. (TDA) proposes an alternate combustion system which we refer to as SETS, or Sorbent Energy Transfer System. The system can achieve up to 100% removal of CO₂ from the system with approximately a 2.5% penalty in the energy efficiency of the generating system and an incremental capital cost of roughly \$100/kW_e (assuming a 50% efficient combined cycle). The reasons for the low energy penalty and low capital cost are that the CO₂ is removed from the system at high pressure (10 atm) before air (with its diluting nitrogen) is introduced. This reduces the theoretical work of compression required to separate and compress the CO₂ to 35 atm by more than a factor of six. The theoretical work of compression when CO₂ is separated from flue gases is proportional to $\ln(35/0.01)$ or 8.1, while compression from 10 atm to 35 atm is proportional to $\ln(35/10)$ or 1.2. In practice, the reduction in the energy required to carry out the separation and compression is even greater because the highly inefficient heat driven physical or chemical sorbent based CO₂ separation step is eliminated. Because the CO₂ is mixed only with steam (which can be removed

by condensation, producing steam high pressure steam in the process), the need for energy consuming chemical separations of CO₂ from nitrogen and/or hydrogen is totally eliminated. In addition, the fuel stream (first the fuel gas, then the reduced sorbent) does not have to be cooled and reheated in order to remove CO₂. The entire process by which the fuel transfers its energy to the sorbent is carried out at high temperature. The CO₂ is eventually cooled as the water is condensed (producing useful steam in the process). However, such a step is necessary anyway; we want to efficiently recover the energy in the hot CO₂/water stream, and it is desirable to cool the CO₂ prior to the final compression to minimize the energy of compression to pipeline pressure.

2.1.1. Selection of the Redox Metal

The key to our process is to transfer the chemical energy in the fuel to a solid (sorbent) energy carrier, and then "burn" the carrier. We do this by reducing a metal oxide, producing an concentrated, high pressure stream of and steam. The metal is then re-oxidized in a stream of hot, high pressure air (from the compressor stage of a gas turbine), heating the air and without introducing any CO₂ in the process. The energy transfer process is carried out adiabatically at elevated temperature, and requires no high temperature heat exchangers. The entire SETS process is carried out in two transport reactors.

In the reducing reaction the reducing potential of the fuel (CH₄, CO, H₂, C_xH_y) is used to reduce a metal oxide to a lower valence state, in the process oxidizing the fuel to carbon dioxide and water. A number of different metals could be used as energy transfer sorbents. Representative reduction reactions are shown below, using CH₄ as an example fuel:



In the case of copper the copper oxide (CuO) is reduced from the oxide (valence state +2) to copper metal (valence state 0). In the case of iron, the ferric Fe₂O₃ (with the iron in a valence state of +3) is reduced to FeO (iron valence state of +2).

In the second step of the process the metal or lower valence state oxide (Cu, FeO) is oxidized with air, releasing large quantities of heat, and returning the metal to its original higher valence state:



There are several transition metals that can be readily oxidized and reduced as they absorb and desorb oxygen. In choosing the metal (or metals) that we will use in our cycle, we must consider their cost (it should be very low), their reactivity (the kinetics of oxidation and reduction must be fast over the temperature range 400 to 1200°C), they should have large heats of reaction per

mole (to minimize the amount of material that we use), and they must not undergo side reactions with the supports that we choose. Equally important, we would like the regeneration reaction to be as nearly thermo-neutral as possible (we want the exotherm of the oxidation of the fuel to CO₂ and H₂O to exactly balance the endotherm of the reduction of the metal).

Table 2-2 and Table 2-3 presents the heat of reaction and change in Gibbs free energy for the redox reduction of the metal oxides with methane and the oxidation reactions with air. Note that for any metal, the sum of DH and DG for the oxidation and reduction reactions is -191.5 kcal and -191.2 kcal respectively, the DH and DG of the oxidation of methane.

Delta G for all of the reduction reactions is very negative, indicating that there are no thermodynamic limits to the reduction going to completion; for any fuel the extent of reaction can go well past 99.9%. However, for some of the reactions delta H is positive (indicating that heat as well as fuel would have to be supplied to the reactor) while for other metals the reduction is exothermic (indicating that fuel would be supplied and heat would have to be removed). We do not need the reduction reaction to be perfectly thermally neutral. Any heat released during the reduction is recovered and used to generate steam to drive the steam bottoming cycle (although this is not as useful as releasing heat where it can be used in both the turbine and bottoming cycle). Likewise, a slight endotherm is not particularly harmful as long as it does not cool the solids to the point where the reduction reaction is quenched. Thus, although thermo neutrality is the ideal, as long as the endotherm or exotherm is not severe, the reaction will proceed acceptably and the overall efficiency of the power generation cycle will not be greatly reduced. Fortunately, it is easy to make the overall reduction reaction very nearly thermally neutral, simply by using the correct mixture of two transition metals (one which has an exotherm and one of which has an endotherm).

Table 2-2. Reduction of redox metal oxides.

@ 1472°F (800°C)	Delta H	Delta G
CH ₄ + 4 Fe ₂ O ₃ → CO ₂ + 2 H ₂ O (v) + 8 FeO	+ 64.6 kcal	- 59.8 kcal
CH ₄ + 4 NiO → CO ₂ + 2 H ₂ O (v) + 4 Ni	+ 33.0 kcal	- 54.6 kcal
CH ₄ + 4 Mn ₂ O ₃ → CO ₂ + 2 H ₂ O (v) + 8 MnO	- 17.0 kcal	-126.9 kcal
CH ₄ + 4 CuO → CO ₂ + 2 H ₂ O (v) + 4 Cu	- 48.2 kcal	-133.8 kcal

Table 2-3 presents the heat of reaction and change in Gibbs free energy for the oxidization of the redox metal to the higher valence state. Again all of the reactions are very favorable (i.e., Delta G is very negative) and exothermic (Delta H is negative).

Table 2-3. Oxidation of redox metal oxides.

@ 1472°F (800°C)	Delta H	Delta G
$2 \text{ O}_2 + 8 \text{ FeO} \rightarrow 4 \text{ Fe}_2\text{O}_3$	-256.1 kcal	-131.4 kcal
$2 \text{ O}_2 + 4 \text{ Ni} \rightarrow 4 \text{ NiO}$	-224.5 kcal	-136.6 kcal
$2 \text{ O}_2 + 8 \text{ MnO} \rightarrow 4 \text{ Mn}_2\text{O}_3$	-174.5 kcal	-64.3 kcal
$2 \text{ O}_2 + 4 \text{ Cu} \rightarrow 4 \text{ CuO}$	-143.3 kcal	-86.0 kcal

Again, in theory, because of the large delta G of these reactions, virtually all of the oxygen in the air stream could be oxidized. However, in practice we will not fully remove all of the oxygen from the air (as will be discussed in the next section).

2.1.2. Sorbent Structure and Manufacture

Another factor which will affect the selection of the redox metal oxide is the ability of the metal oxide to be regenerated for many cycles. The redox reactions in which Cu, Ni, FeO, and/or MnO absorb and desorb oxygen are well understood. There are no undesirable side reactions, and the kinetics of the reactions are quite fast. What we need in order for this technology to be useful is a low-cost, high capacity sorbent which can rapidly carry out the redox reaction for multiple cycles without breaking itself apart (spalling) or undergoing side reactions. Fortunately, TDA has been developing low cost, long life chemical sorbents for other applications, specifically for the removal for sulfur from gasified coal and flue gases. These sorbents are being developed for fixed bed, moving bed, and fluidized bed and transport reactors, and much of our technology and know-how is directly applicable to this project.

The trick is to make a pellet which: 1) contains a large amount of active sorbent (i.e., high surface area), yet still has the strength to be moved through absorption and regeneration, 2) will hold together during the large expansion and contraction which accompanies the absorption and removal of the oxygen, 3) is chemically stable, and 4) will withstand repeated cycling between 400°C and 900-1200°C. We achieve

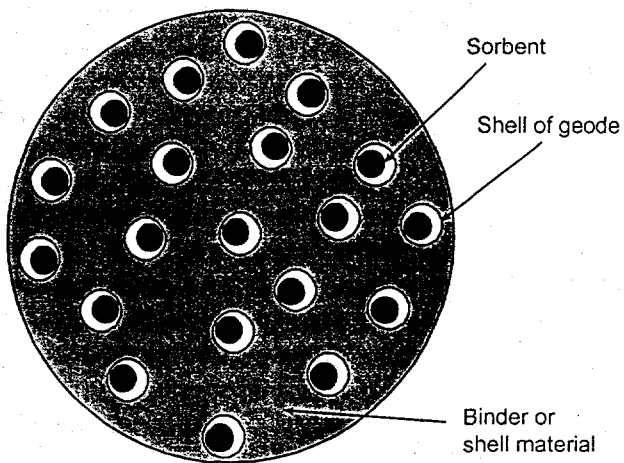


Figure 2-1 Schematic of TDA's geode.

these goals using a structure that we call a "geode" (Figure 2-1). Like the geode that you buy at a gift shop, our geode has a hollow shell. However, unlike the gem shop geode that has a single hole in the middle, our geode sorbent contains hundreds or thousands of holes in a structure that looks like a conventional catalyst pellet on the outside. The sorbent is loosely contained in, but does not fill the hole(s) in the center. Thus, the sorbent can expand and contract indefinitely without destroying the

pellet structure. In addition, since the body of the pellet contains the sorbent but does not need to have sorbent properties, we can make the shell of the pellet out of strong but highly porous materials such as high surface area alumina or titania (materials that are commonly used as catalyst and sorbent supports in applications where porosity, strength, attrition resistance and chemical inertness are essential). TDA is currently applying the geode technology in several projects which use: 1) ZnO as the H₂S chemical sorbent for gasified coal for both moving bed and fluidized bed hot gas H₂S cleanup applications, 2) Sodium aluminate for the removal of NO_x and SO_x from flue gases, and 3) Copper oxide for the removal of HCl and the recovery of Cl₂, and 4) and CaO for the removal of CO₂ from syngas.

The simplest way to make a geode is to mix the sorbent with a light oil, mix the binder with water, then mixing the oil and water slurries. Since the oil and water do not mix, the oil phase that contains the sorbent forms small micelles inside the continuous water-binder phase. The mixture is then extruded or pressed into pellets and fired. After firing, the water and oil evaporate, leaving behind a complex porous structure. The structure contains two types of voids. As the oil evaporates, it leaves behind holes in the matrix that contain the sorbent. Because the oil evaporates, the sorbent does not completely fill the holes, and, therefore, can expand and contract without breaking up the pellet structure. As the water evaporates, it leaves behind a continuous structure filled with extremely small pores (e.g., 1 μm). This structure holds the sorbent in place. Because of the porosity left behind as the water evaporates, the gas being absorbed can easily diffuse in from the exterior of the pellet to the tiny pockets of sorbent. Thus, the geode structure: 1) is very strong because there is a continuous support phase, 2) effectively contains the sorbent inside small holes in the interior of the pellet, 3) allows the sorbent to expand and contract freely without disrupting the pellet structure, 4) allows the gas to be absorbed to diffuse quickly from the exterior of the pellet, and 5) does not require that the sorbent and support be mixed. For example, we have produced ZnO/TiO₂ based geodes that do not spall (i.e., fracture) and retain their activity and their strength with cycling, even though the ZnO sorbent undergoes a 250% increase and decrease in volume over the course of the adsorption and regeneration cycles.

Since the strength and attrition resistance of the geode sorbent are provided by the continuous porous shell which surrounds the pockets of sorbent, the fact that the redox metal oxide has little strength is unimportant. In projects where we apply our geode technology to the absorption of H_2S , we have found that we can make geode pellets containing up to 50% sorbent without hurting the physical properties of the pellet.



Figure 2-2. Photomicrograph of ZnO geode.

Thus, we can make a sorbent particle which contains roughly 50% copper or iron instead of the 10% active material that is used in current commercially available sorbents which are made by standard methods such as impregnation. High loadings greatly increase the amount of O_2 which can be absorbed by the pellet and reducing the power consumption of the fluidized beds, the capital investment (the size of the fluidized beds) and the attrition losses (one of the dominant costs in regenerable sorbent systems). Finally, because our shell has a high degree of porosity, the mass transfer resistance of the pellet is low and the O_2 can easily reach the pockets of sorbent within the pellet.

A Scanning Electron Micrograph (SEM) of a geode is shown in Figure 2-2. In this geode, ZnO (used to remove H_2S from hot gases leaving a coal gasifier) is the chemically active sorbent and TiO_2 is the inert structure. The ZnO is in the center of the micrograph and is contained in regions 10 to 40 microns in diameter, surrounded by the binder. The ZnO has internal porosity; these internal 0.1 to 1.0 micron pores appear as the rough surface of the ball in the micrograph. The inert binder is also porous and the 1 micron pores can be seen in the structure surrounding the ZnO region. The most important fact shown in Figure 2-2 is that the sorbent exists as separate pockets within the matrix. It is surrounded by the inert material, but is not chemically bonded to it. This geode was produced for use in a moving bed hot gas cleanup system, under a DOE SBIR Phase II contract "A Long Life ZnO- TiO_2 Sorbent".

We have also produced smaller ZnO based geodes suitable for use in fluidized bed reactors (i.e., 70 to 250 micron particles) as part of a second DOE Phase II SBIR project. These geodes contain very small (e.g., 1 μm) regions of a chemically active region surrounded by inert shell material. For the smallest chemically active regions we simply start with chemically active material of the desired size (e.g., 1 to 5 μm) and mix with the binder material and fire; the size of the initial powder sets the size of the chemically active region. We have formed the fluidized bed sorbent by extrusion (i.e., we have a 250 μm die) and

agglomeration. The ZnO sorbents will be also produced by spray drying by Norton Chemical Process Products Corp. (Norton) under subcontract to TDA (Norton produces ceramic catalysts and its annual sales exceed \$100 million). Firing at carefully controlled temperature/time conditions produces the final material in a strong, chemically active, porous, and attrition-resistant form.

In summary, over the past several years we have produced geode structure pellets in a variety of size ranges (100 μm to 4,000 μm) using a wide range of manufacturing techniques including extrusion, pellet mills, agglomeration and spray drying. TDA has on hand the equipment needed to produce pellets several hundred pounds of a sorbent pellet. When it become time generate pellets in multi ton quantities, TDA has had them manufactured by Norton Chemical Process Products.

3. Phase I Tasks, Organization, Schedule and Status

In Phase I we conducted preliminary proof of concept experiments to determine whether the geode structure can be used to make a low-cost, long life, redox metal oxide based sorbent for use in the SETS cycle and carried out calculations to optimize the cycle and determine its efficiency and cost. The Phase I work was sub-divided into 5 tasks. In Task 1 we conducted thermodynamic analysis (equilibrium and energy requirements) to identify promising candidate redox metal oxides. In Task 2 we prepared small samples of the metal oxides and form them into geodes. We tested these samples for several cycles to verify that they retain activity during cycling. In Task 3 we analyzed the total heat and power requirements of the CO₂ capture system and the capital and operating costs. In Task 4 we prepared the Phase II proposal and in Task 5 we report the results.

3.1. Phase I Organization

To provide the necessary skills, we assembled a team which includes TDA Research, Kellogg Brown and Root, Inc., and Louisiana State University (LSU) (Figure 3-1). TDA invented the new system design. TDA manages the project, carries out the conceptual engineering and thermodynamic analysis to define the process, and develop the sorbent. Kellogg reviews the initial conceptual designs and conducts detailed engineering analyses. LSU aided in thermodynamic analyses. Kellogg, one of the largest U.S. engineering and construction contractors (with particular experience in fluidized bed and transport reactors design and construction) has the ability to provide complete commercial scale facilities based on the process.

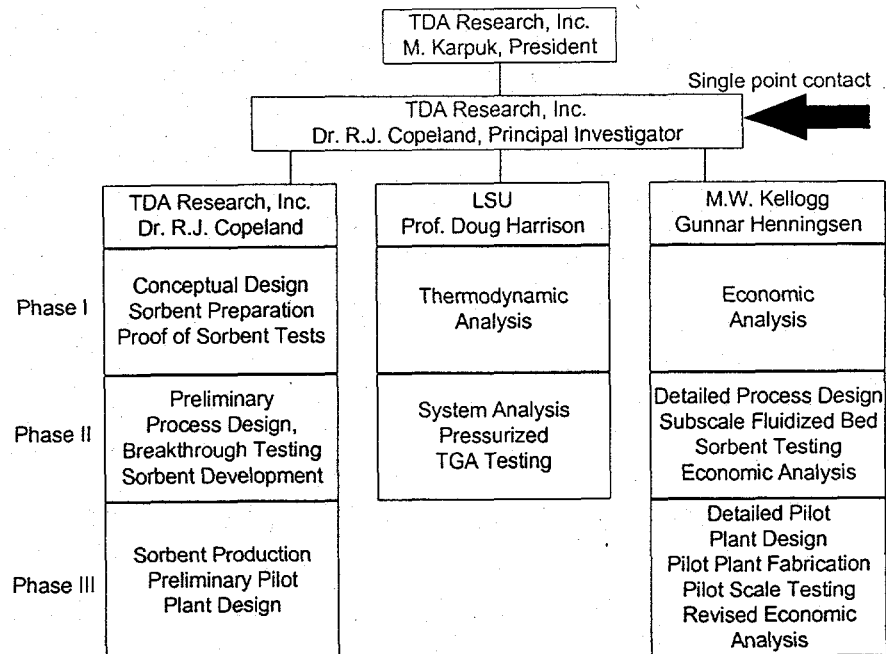


Figure 3-1. Project organization.

3.2. Phase I Schedule

The Phase I project schedule is shown in Figure 3-2.

As of the writing of this topical report Tasks 1.1, 1.2, and 1.4 have been completed. Task 1.3, economic analysis is still in progress and the final report will be finalized after receiving the cost data from Kellogg.

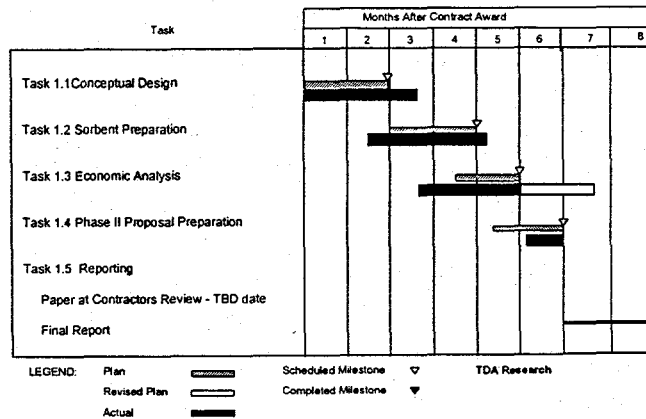


Figure 3-2 Project schedule.

3.3. Phase I Costs

As of December 31, 1998, TDA has spent \$39,801 of the \$50,000 contract. The largest item remaining is the Kellogg subcontract, which will add \$5,937 to the expenses. Total actual and committed expenses to the end of December are \$45,738. Additional expenses to prepare this report and some additional tests are being incurred in January 1999.

4. Conceptual Design and Thermodynamic Analyses

Dr. Doug Harrison of LSU, TDA's consultant, screened 77 potential redox metal oxides and identified 13 which could potentially meet the thermodynamic requirements. His results are reported in Appendix A which describe the equilibrium limitations of various redox reactions.

4.1. Active Metal Selection

Table 4-4 and Table 4-5 presents the heat of reaction and change in Gibbs free energy for the redox reduction of the metal oxides with methane and the oxidation reactions with air. Note that for any metal, the sum of ΔH and ΔG for the oxidation and reduction reactions is -191.5 kcal and -191.2 kcal respectively, the ΔH and ΔG of the oxidation of methane.

Table 4-4. Reduction of redox metal oxides.

@ 1472°F (800°C)	Delta H	Delta G
$\text{CH}_4 + 4 \text{Fe}_2\text{O}_3 \rightarrow \text{CO}_2 + 2 \text{H}_2\text{O (v)} + 8 \text{FeO}$	+ 64.6 kcal	- 59.8 kcal
$\text{CH}_4 + 12\text{Fe}_2\text{O}_3 \rightarrow \text{CO}_2 + 2 \text{H}_2\text{O (v)} + 8 \text{Fe}_3\text{O}_4$	+ 39.9 kcal	-108.7 kcal
$\text{CH}_4 + 4 \text{NiO} \rightarrow \text{CO}_2 + 2 \text{H}_2\text{O (v)} + 4 \text{Ni}$	+ 33.0 kcal	- 54.6 kcal
$\text{CH}_4 + 4 \text{Mn}_2\text{O}_3 \rightarrow \text{CO}_2 + 2 \text{H}_2\text{O (v)} + 8 \text{MnO}$	- 17.0 kcal	-126.9 kcal
$\text{CH}_4 + 4 \text{CuO} \rightarrow \text{CO}_2 + 2 \text{H}_2\text{O (v)} + 4 \text{Cu}$	- 48.2 kcal	-133.8 kcal

Delta G for all of the reduction reactions is very negative, indicating that there are no thermodynamic limits to the reduction going to completion; for any fuels the extent of reaction can go well past 99.9%. However, for some of the reactions delta H is positive (indicating that heat as well as fuel would have to be supplied to the reactor) while for other metals the reduction is exothermic (indicating that fuel would be supplied and heat would have to be removed). We do not need the reduction reaction to be perfectly thermo-neutral. Any heat released during the reduction is recovered and used to generate steam to drive the steam bottoming cycle (although this is not as useful as releasing heat where it can be used in both the turbine and bottoming cycle). Likewise, a slight endotherm is not particularly harmful as long as it does not cool the solids to the point where the reduction reaction is quenched. Thus, although thermoneutrality is the ideal, as long as the endotherm or exotherm is not severe, the reaction will proceed acceptably and the overall efficiency of the power generation cycle will not be greatly reduced. Fortunately, it is easy to make the overall reduction reaction very nearly thermo-neutral, simply by using the correct mixture of two transition metals (one which has an exotherm and one of which has an endotherm).

Table 4-5 presents the heat of reaction and change in Gibbs free energy for the oxidation of the best redox metals to the higher valence state. Again all of the reactions are very favorable (i.e., Delta G is very negative) and exothermic (Delta H is negative). Again, because of the large delta G of these reactions,

virtually all of the oxygen could be oxidized (and removed from the air) over a wide range of oxygen concentrations. However, in practice we will not fully remove all of the oxygen from the air.

Table 4-5. Oxidation of redox metal oxides.

@ 1472°F (800°C)	Delta H	Delta G
$2 \text{O}_2 + 8 \text{FeO} \rightarrow 4 \text{Fe}_2\text{O}_3$	-256.1 kcal	-131.4 kcal
$2 \text{O}_2 + 8 \text{Fe}_3\text{O}_4 \rightarrow 12 \text{Fe}_2\text{O}_3$	-231.4 kcal	- 82.6 kcal
$2 \text{O}_2 + 4 \text{Ni} \rightarrow 4 \text{NiO}$	-224.5 kcal	-136.6 kcal
$2 \text{O}_2 + 8 \text{MnO} \rightarrow 4 \text{Mn}_2\text{O}_3$	-174.5 kcal	- 64.3 kcal
$2 \text{O}_2 + 4 \text{Cu} \rightarrow 4 \text{CuO}$	-143.3 kcal	- 86.0 kcal

Thus, for both kinetics and energy balance, a two sorbent system (e.g., Fe_2O_3 and CuO being reducing to Fe_2O_3 and Cu and then re-oxidized) is preferred for the SETS. Because of its low cost and refractory nature (i.e., high melting points) of the iron oxides, there are also an option for the sorbent.

Based upon Dr. Harrison's results, TDA conducted a first order cost of sorbent assessment. Table 4-6 presents this data which 1) identifies the oxidized and reduced states of the SETS sorbent, 2) calculates the theoretical loading of each redox metal oxide, 3) reports the cost of the raw material, and 4) calculates the theoretical cost for transferring oxygen. (Since two moles of O_2 are required to fully oxidize one mole of CH_4 , the theoretical cost is equivalent to the relative cost of transferring energy). Five sorbents were identified with a cost of less than \$20/lb of O_2 capacity. Those marked with a \checkmark were selected for further study. Although the price of vanadium is comparable to nickel, vanadium requires an additional hazardous disposal cost. In addition, nickel is catalytic to the reforming of methane (which should improve the reaction rates).

Table 4-6. Raw material costs for redox metal oxides. Costs from Chemical Market Report of March 10, 1997, excepted as noted.

Oxidized State	Reduced State	Loadings wt	Cost \$/lb	\$/lb O_2	
CeO_2	Ce_2O_3	4.65%	1.21	\$ 26.03	assigned same as CuO
Cr_2O_3	CrO	10.52%	16.5	\$156.77	
Co_2O_3	CoO	9.65%	28.22	\$292.54	
CuO	Cu	20.12%	1.21	\$ 6.02	\checkmark
IrO_2	Ir_2O_3	3.57%	30	\$840.75	\$30/lb assumed
Fe_2O_3	FeO	10.02%	0.295	\$ 2.94	\checkmark
Mn_2O_3	MnO	10.13%	1.04	\$ 10.26	\checkmark
MoO_3	MoO_2	5.56%	16.5	\$296.88	
NiO	Ni	21.42%	3.93	\$ 18.35	Reforming catalyst \checkmark
RhO_2	Rh_2O_3	6.81%	30	\$440.51	\$30/lb assumed
Ru_2O_3	RuO	6.40%	30	\$469.01	\$30/lb assumed
WO_3	WO_2	6.90%	5	\$ 72.46	
VO_3	VO	38.58%	6	\$ 15.55	

Two of the selected sorbents are exothermic with the reducing reactors (CuO and Mn₂O₃) and two are endothermic (NiO and Fe₂O₃). By selecting the proper quantities of each, we can produce a reactor which is thermally neutral or slightly endothermic or exothermic.

As shown in Table 4-7 the source can influence the net cost per pound of O₂. However, the primary difference is expected to be in the loading. Based on the available data, the preferred combinations are expected to be copper or manganese with iron. Because it is costly, the use of nickel should be limited to a catalytic role unless iron oxides are not suitable. Both CuO and Mn₂O₃ are relatively low cost; they are exothermic and they fully oxidize fuel gases (< 100 ppm H₂ + CO). CuO can release some O₂ into the CO₂ at very high temperatures (i.e., >900°C).

Table 4-7. Dependence of the cost of selected redox metal oxides on the source.

• NiO		\$3.93/lb
• CuO		\$1.21/lb
• MnO ₂		
• >90% MnO ₂		\$1.04/lb
• Natural African > 74% MnO ₂		\$0.10/lb
• Iron oxides		
• FeO	Black, Synthetic	\$0.82/lb
• Fe ₂ O ₃	Red, Natural	\$0.295/lb
Source: Chemical Marketing Report March 10, 1997		

Neither iron nor nickel fully oxidize all of the fuel; at 900°C 4.45% of the exit gas will be (H₂ + CO), even with an excess of Fe₂O₃ (Figure 4-1). While copper or manganese will fully oxidize the fuel gases (Figure 4-2), in a single stage fluidized bed, the CuO or Mn₂O₃ would be reduced before the iron oxides (or NiO) are reduced, leaving the iron or nickel equilibrium level of H₂ and CO in the dry CO₂ going to disposal. This would both unacceptably increase the cost of disposal and increase the fuel costs.

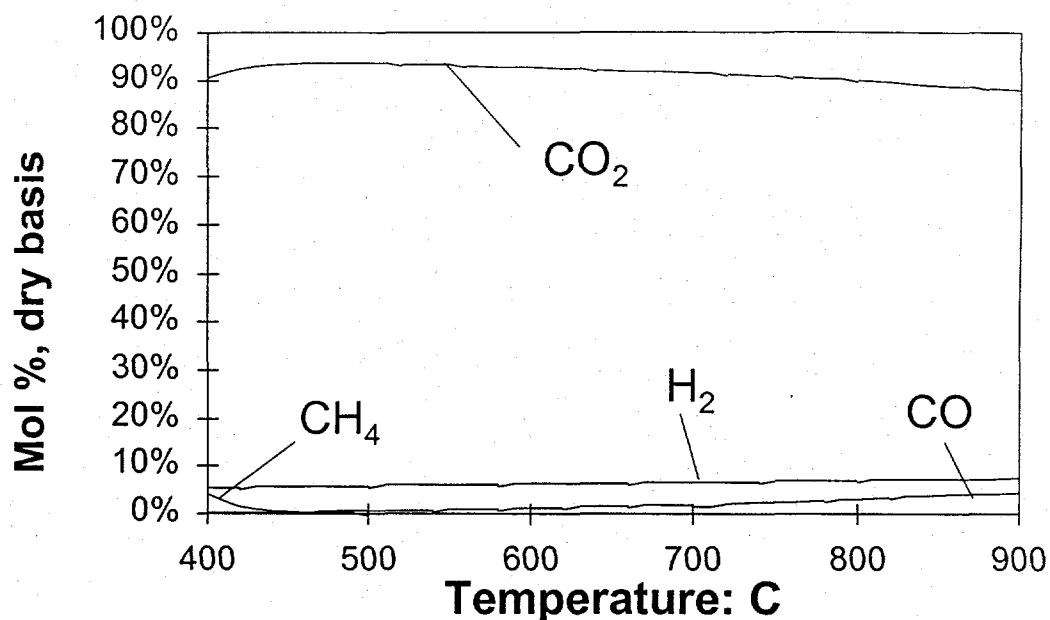


Figure 4-1. Oxidation of CH₄ by NiO (virtually identical results are obtained for Fe₂O₃, see Appendix A).

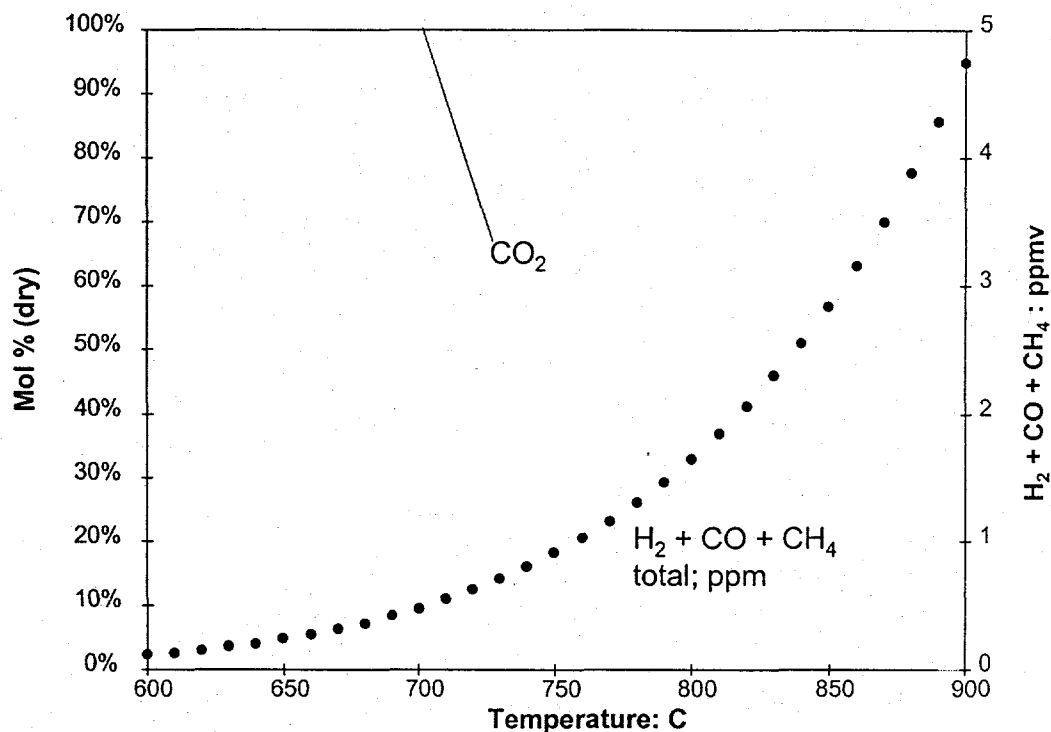


Figure 4-2. Oxidation of CH₄ by CuO (similar results are obtained for Mn₂O₃ see Appendix A).

To solve the problem of residual unreacted reducing gases in the effluent, TDA designed the SETS to use a two stage reducing reactor as illustrated in Figure 4-3. In this version of the SETS, air is compressed to ~13.5 ATM, which heats the air to ~ 400°C. The reduced sorbents (e.g., copper and iron, since they are the lowest

cost exothermic/endothermic combination) and air are mixed in a transport reactor where the sorbent is oxidized. The oxidization heats the sorbent and air to $\sim 900^{\circ}\text{C}$ and the two are separated (i.e., in the cyclone).

The sorbents (at 900°C) and partially oxidized gases leaving Reactor 1 at $\sim 700^{\circ}\text{C}$ and 67% to 90% enter transport Reactor 2 and the fuel gases are oxidized (i.e., most of the oxidation occurs in Reactor 1) and the solids are reduced. Since the solids entering Reactor 2 have a great excess of oxidation potential and CuO has the greatest reduction potential, only some of the copper oxide is reduced to copper while all of the fuel gases are oxidized to CO_2 and H_2O ; the Fe_2O_3 , due to the small quantity of H_2 , CO , and CH_4 entering Reactor 2 is not completely reduced. Due to the high flow rate of cooler gases (i.e., 700°C) and limited reaction occurring in Reactor 2 (which is actively cooling by generating steam or the reforming of the CH_4), the solids are maintained at temperatures less than 900°C . This inhibits loss of oxygen by the sorbents, and the solids leave Reactor 2 at 700 to 900°C .

The solids leaving Reactor 2, are slightly depleted in oxygen (as oxides) and enter Reactor 1. Recycled gases from the effluent of Reactor 2 are mixed with natural gas (primarily CH_4) and flow into the transport reactor (Reactor 1). This Reactor (#1) has an excess of reducing gas so that both sorbents are fully reduced to

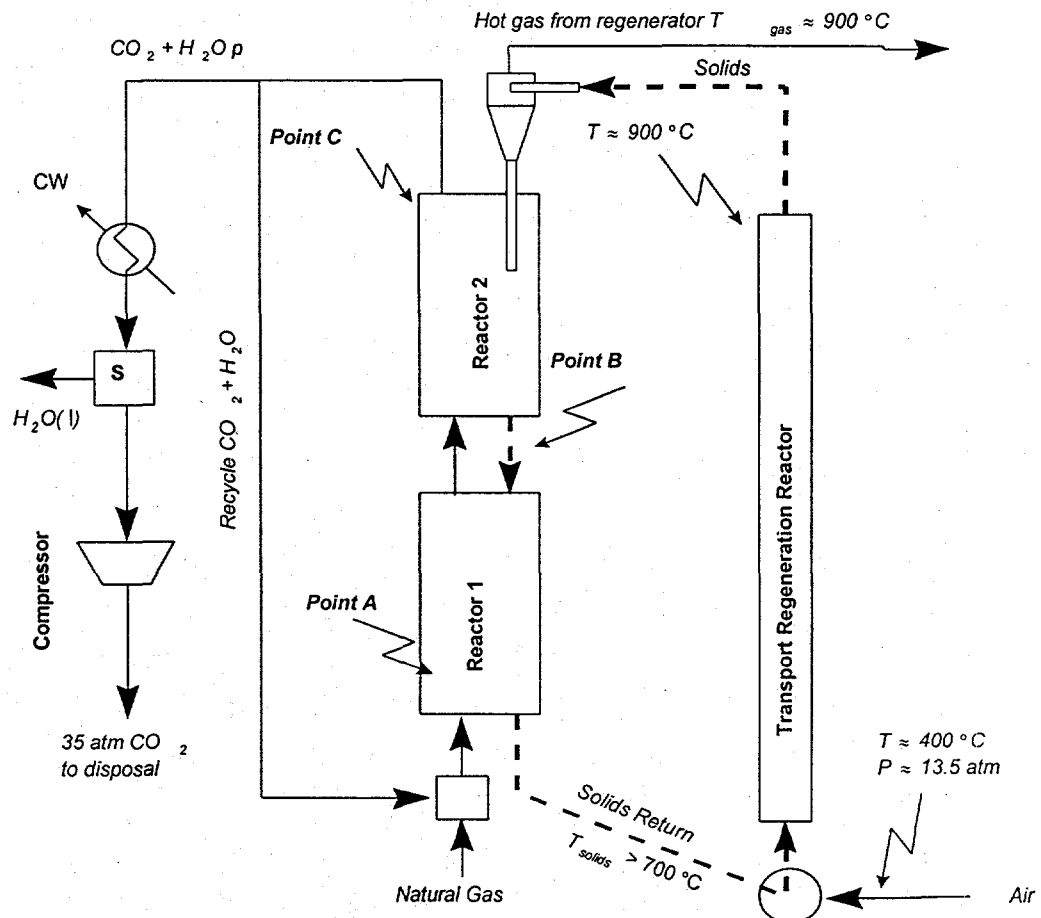


Figure 4-3. SETS system.

maximize the oxygen transfer from the oxidizing (Transport regeneration reactor) to the reducing side of the SETS. Due to the endothermic reforming the solids leave Reactor 1, at ~700°C but the exit temperature could be controlled at temperatures up to 900°C. Given that the oxidation rates are known to be low at lower temperature, TDA limited the system to a solids return temperature to the oxidizing reactor (no. 3) of at least 700°C (for kinetic considerations) but not more than 900°C (to minimize the use and cost of high alloy equipment).

4.2. Use of Nickel as a Reforming Catalyst

During our discussions we recognized that copper oxide and Fe₂O₃ will readily react with H₂ and CO, but may not react rapidly with CH₄. Simply including a reforming catalyst to start the process would avoid any reaction rate issues. Fortunately, nickel (i.e., reduced nickel oxide) is a well known reforming catalyst and a good redox sorbent for SETS.

There are a large number of commercial Ni-base steam reforming catalysts available, and this catalyst technology is quite mature. Most of the major catalyst manufacturers produce large quantities of steam reforming catalysts. United Catalysts, Imperial Chemical Industries (ICI Katalco), Haldor Topsoe and BASF are a

Table 4-1. Commercial Ni steam reforming catalysts.

Catalyst	Manufacturer	Composition	Feedstock
ICI23-series	ICI-Katalco	NiO/promoted calcium aluminate	Natural gas
ICI25-series	ICI-Katalco	NiO (K-promoted)	Associated gas/LPG
ICI46-series	ICI-Katalco	NiO (K-promoted)	Naphtha
ICI47-series	ICI-Katalco		Dual feedstocks
UCI-C11-series	UCI	NiO/calcium aluminate, titanate, alumina	Natural gas
UCI-G-91	UCI	Ni/calcium aluminate	C ₃ /C ₄ steam reforming
RKNGR	Haldor Topsoe	Nickel	Pre-reforming
RKNR,	Haldor Topsoe	Nickel	Naphtha
RK-68, & -7H	Haldor Topsoe	Nickel (K-promoted)	Naphtha
R-67, & -7H	Haldor Topsoe	Nickel	Natural gas
RK-69, & -7H	Haldor Topsoe	Nickel (K-promoted)	Natural gas
RKS-2, & -7H	Haldor Topsoe	Nickel	Secondary reforming

few of the companies that each make a variety of catalysts for different (and frequently specialized) steam reforming applications. Alkali and alkaline earth oxides are frequently incorporated into the catalyst support to retard the formation of coke due to hydrocarbon decomposition. Table 4-1 is a list of commercial nickel-based steam reforming catalyst made by several major catalyst manufacturers.

Table 4-1 shows that most of the Ni catalysts use ceramic supports, frequently calcium aluminate. Calcium aluminate is both strong (for supporting tall fixed beds of catalyst in the reformer tubes) and also retards coke lay-down by acting as a catalyst for the steam-coke reaction. For naphtha reforming, where coke formation is more of a problem than with light gases, potassium is added. This is usually incorporated into the support so that it will slowly leach out by reaction with steam to form KOH. At steam reforming temperatures, KOH acts as a carbon gasification catalyst and reduces the tendency of the nickel catalyst to coke.

In our process, the Ni is oxidized to NiO during regeneration and reduced back to the metal during reforming. Thus, the Ni catalyst used must be able to withstand this repeated cycling without a deterioration in catalytic performance or physical characteristics (such as strength). Unfortunately, the calcium aluminate support and potassium promoters can react with CO₂ forming the carbonates which would release their CO₂ into the gas stream in the oxidizing reactor. Improved supports will be needed and TDA will investigate MgO as an alkali additive to alumina to inhibit coking, since MgCO₃ is not stable at >360°C in 100% CO₂ at 10 atm.

5. Sorbent Preparation, Characterization and Testing

5.1. Binder Screening

The first step to identifying a successful geode is developing an inert binder formulation that will be stable and yield an adequate attrition resistance under the conditions of its working environment. To study the relative strengths of potential binder formulations, we have employed the isopress technique. This allows us to quickly evaluate the material properties of the resulting pellets and eliminate the majority of processing parameters that produce unacceptable pellet strengths. We prepared a variety of aluminas and fired the resulting pellets in a box furnace at a range of temperatures. The aluminas in question were then mixed with potential "active" ingredients to test for the formation of any aluminates that may occur the firing process, and to determine whether the active sorbents had any effects on the physical properties the binders. Next, the type of alumina (i.e. alpha, boehmite etc.) was varied do find the most desirable combination of physical properties, and the resulting pellets were further tested to hone in on the optimum binder formulation.

To examine relative material strengths, TDA began screening potential binders using the isopress technique. By filling a flexible, waterproof tube with the potential binder formulations, and immersing this filled tube in water before applying pressure (5000 psi in our case), you apply an equal load to all sides of the powder filled tube. The compacted powders will then slip out of this tube when the load is relieved. This technique allows us to isolate the material characteristics of each individual binder formulation under the same conditions, i.e., the same lubricant and binder contents and forming pressures. (The problem with testing extrudates of these materials is that the pressure, amount of binder and lubricant added, feed rate etc. all effect the resulting pellets physical properties, this makes it difficult to separate out the processing parameters contributions to strength versus those contributions from the material itself.)

Since the scale-up of any production process will be done out of house, on equipment that is much larger than and different from the lab scale equipment we are using for the development work, optimization of material strength is deemed more important then optimizing processing parameters that would need to be redone anyway in the final processing step. TDA will conduct some small scale processing optimization after serious sorbent candidates have been identified by the isopress, to ensure that desirable final sorbent characteristics are attainable using other, more representative size enlargement techniques and equipment. All pellets produced were fired in the range of temperatures from 1000 - 1150°C, and analyzed to determine crush strength and void percentage. Selected pellets were also subjected to x-ray diffraction, surface area, and mercury intrusion analysis.

Using the techniques described above, we identified numerous alumina precursors of each class of alumina (i.e. boehmite, alpha, gamma, hydrates.) We have chosen to start with alumina binders primarily because they are inert to the reactions of choice, are readily available at an acceptable cost, and are known for their toughness after sintering. The alumina powders were screened based on phase, suppliers, cost, and particle sizes.

After the best of each class of alumina was identified, these representatives were mixed with a stoichiometric amount of either the potential "active" ingredient or ingredients which should form an inert aluminate under the firing conditions (stoichiometric implying that a full reaction with the alumina would form 100% of the respective aluminate.) The active materials tested were copper oxide, iron oxide, and manganese oxide. Nickel oxide was excluded from these early tests because of its high cost. Zinc oxide was also added as it should form the inert zinc aluminate. Every powder was added to the two best candidate aluminas, and only two each, iron oxide and zinc oxide were added to the others, as a check that the trends identified by the best two candidates were applicable to all the aluminas in the screening. For clarity, only the best formulations are shown on Table 4-7. We found that a combination of pseudo-boehmite with iron is by far the superior binder combination, and that iron additions dramatically increased the strength of all the aluminas tested while zinc oxide actually reduced the strength of the alumina supports. The next best candidate for sorbent strength is copper oxide. Fortunately, a combination of iron oxide and copper oxide, in the correct ratio, can yield a thermo-neutral reduction in the role of greenhouse gas mediation via the SETS process. Fe_2O_3 and CuO are also the most desirable combination of "actives" in term of cost.

All of these pressings included 3.0 wt.% hectarite clay. We expect to use this clay in an extrudable formulation as it provides both lubrication (to aid extrusion) and enhances green strength of both the extrudate and the finished pellet. Under the oxidizing environment of the box furnaces, XRD analysis did not detect the presence of any aluminates in detectable quantities, we must subject these pellets to the reducing environment they will experience in the SETS process to determine any potential reactions between the support and the "actives", occur under reducing conditions.

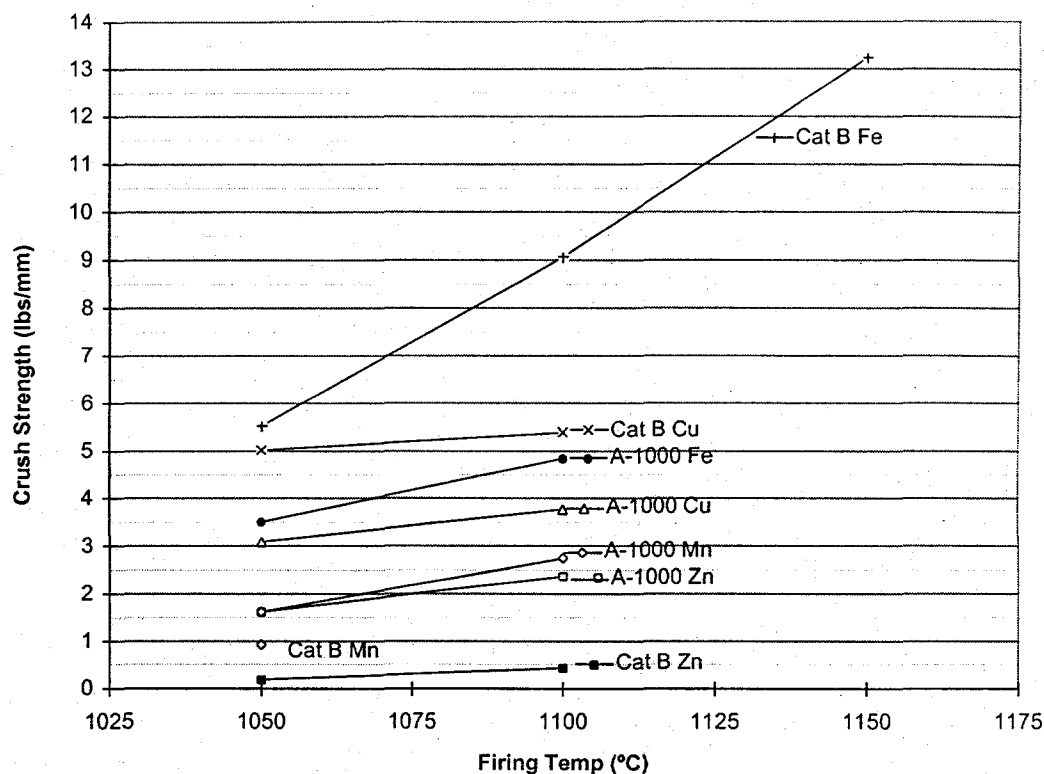


Figure 5-1. Alumina & Aluminate Screening.

Since the pseudo-boehmite appeared to make the best support material (both with and without "active" additions), a further search was conducted to identify the best and least expensive boehmite/pseudo-precursor. Since the trends for metal oxide mixtures were consistent for each alumina phase, only iron additions were tested in this next step see Figure 5-1. As an added test, a variation of the clay used as lubricant/binder was included, as was one pressing that contained no clay. A small amount of a 5% methyl cellulose solution was added to increase the compatibility of the powder mixtures as well as to further enhance green strength, this explains why CatB Fe-1 CatB and Fe-2 are significantly different in the two figures, although they are of the same composition. Several interesting conclusions were gathered from this test. The Catapal pseudo-boehmites are all better than any of the Vista series boehmites. In particular, Catapal B is the material of choice for the conditions in question, particularly at higher firing temperatures. If a lower firing temperature is need ($\leq 1050^{\circ}\text{C}$) due to reactivity concerns, any of the Catapals are excellent alumina sources. Also, clay addition is not necessarily needed for pellet strength.

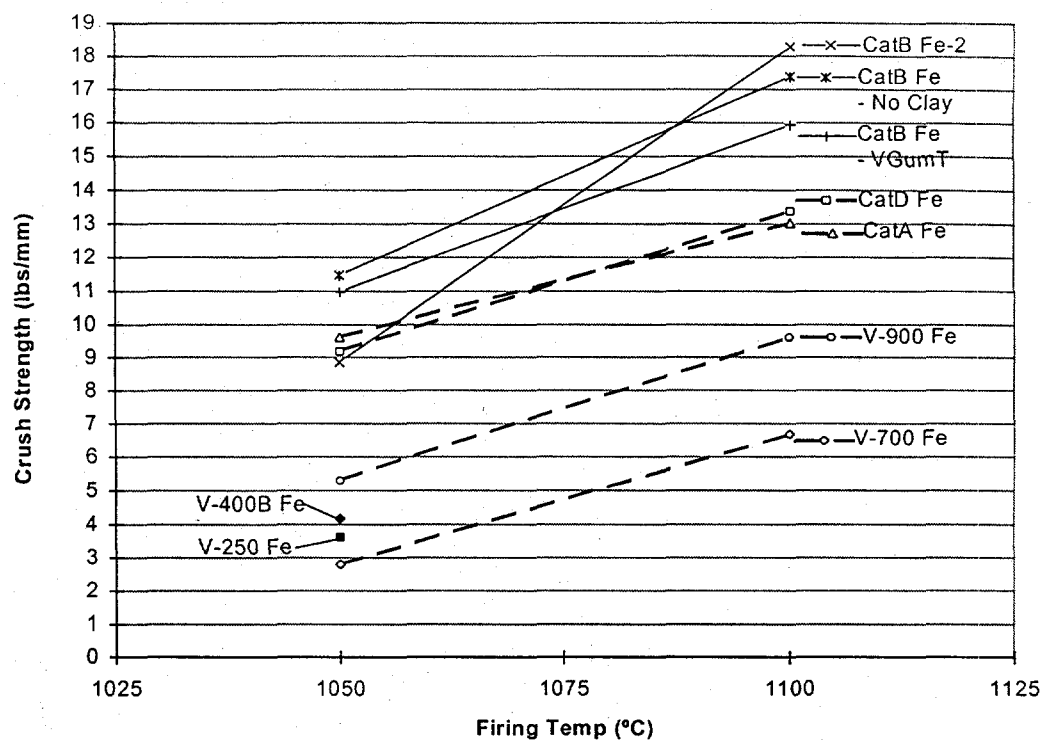


Figure 5-2. Boehmite Screening.

5.2. Sorbent Screening

In exploring various ways of forming a satisfactory pellet, we have expanded our database to include impregnation of pre-formed dense alumina substrates that already meet or exceed the allowable attrition index values for a transport reactor based system. Norton sent us five of the formulations currently on their product list. The first step was to categorize the surface area, attrition index, and void fraction of these supports to find the ones best suited for our needs. Their physical characteristics are shown in Table 5-1. The best supports were then impregnated using the incipient wetness technique with a variety of solutions containing a soluble form of the desired active metal(s). Nitrates of both copper and iron were chosen, both for their solubility and "clean" decomposition at a relatively low temperature. A range of metal loadings for each support was then prepared. If the void and solubility of the support and nitrate salt was not sufficient to allow us to use a one step impregnation, a series of impregnations was performed with intermediate drying steps. When the desired amount of metal salt had been deposited on the alumina support, the impregnated pellet was calcined at 900°C to both decompose the metal nitrate to the metal oxide

It is obviously desirable to maximize the metal oxide loading. Table 5-2 summarizes the loadings we achieved. By far the best combination was made with Norton sample #9195096, which has the largest void fraction, and unusually, the highest attrition resistance, and was easily impregnated. Using this Norton precursor, a 28% CuO sorbent was prepared for microbalance testing.

Table 5-1. Properties of Norton catalyst supports.

Norton Support	Attrition Index (wt%/hr loss)	Surface Area (m ² /g)	Void (cc/g)	Size and Shape
9016235	5.77	0.78	0.228	Fluidizable
9195093	7.46	0.19	0.274	Fluidizable
9195096	0.44	0.217	0.45	Fluidizable
9416002	0.55	0.127	0.229	Fluidizable
9816240	2.54	0.19	0.114	Fluidizable

Table 5-2. Impregnated sorbents.

Metal Oxide	Norton Support				
	9016235	9195093	9195096	9416002	981624
Loading					0
CuO	10	10	9	10	10
(wt%)	28	24		15	19
				25	25
Fe ₂ O ₃		10	10		
(wt%)		15	15	15	15
		25	25	25	25

In addition we continued to extrude with much lower binder amounts and higher "actives" loadings. We found that a sufficient strength could be achieved with < 15.0% binder by weight, even in some cases with no binder, however we think the lifetime under cycling would be poor without at least some binder skeleton to support the active ingredients during their volume changes. Pellets produced primarily consisted of either a thermoneutral ratio of Cu₂O and with different quantities of binder, high Fe₂O₃ loadings (up to 100%) and either no alumina or combinations of alumina with low levels of ZnO and hectaraite clays. We have also fired materials in a reducing environment consisting of 25 vol% each H₂O, CO₂, N₂, H₂ at 850°C in one of our HTHP reactors. Since FeO should sinter at a lower temperature than Fe₂O₃, we should be able to achieve a greater or similar strength at a lower temperature under these conditions, and indeed, that is what we see as shown in Table 5-2. Figure 5-3 is a photograph of several sorbents in pellet form.



Figure 5-3. Photograph of sorbent samples analyzed with TDA's Shimadzu TGA apparatus.

5.3. Sorbent Characterization

X-ray diffraction was used to determine the composition of the sorbent support material and the prepared Cu and Fe sorbents. The XRD patterns were recorded with a Phillips PW1229 x-ray diffractometer with Phillips APD 3520 control electronics. The x-ray source was Cu K α radiation ($\lambda = 1.544$ angstroms). The data were recorded on a 33 MHz 486 PC using Visual XRDTM (Diffraction Technology Pty. Ltd) software. The data were analyzed using TracesTM software (Diffraction Technology Pty. Ltd) and compared with the published powder diffraction files for identification purposes

5.3.1. Fluidizable Norton SA5395 Support Material

Figure 5-4 contains the XRD patterns of Norton SA5395 that has been calcined at 200°C and 900°C. Comparison with the standard powder patterns indicates that the majority phase present is α -Al₂O₃. The α -Al₂O₃ phase of aluminum oxide is the closest packed, strongest and most stable phase, and is formed by high temperature treatments of intermediate aluminas (Misra 1986). This is shown in Figure 5-5, where the XRD pattern of Norton SA5395 that has been calcined in air at 900°C is compared with the XRD pattern of a reference sample of pure α -Al₂O₃. Note that the Norton support is not pure α -Al₂O₃. This is because small amounts of SiO₂ and other oxides are added to the alumina (see Table 5-1) to improve its

physical properties. As a result, the Norton sample has minor peaks due to the presence of additional ceramic phases in addition to the main α - Al_2O_3 .

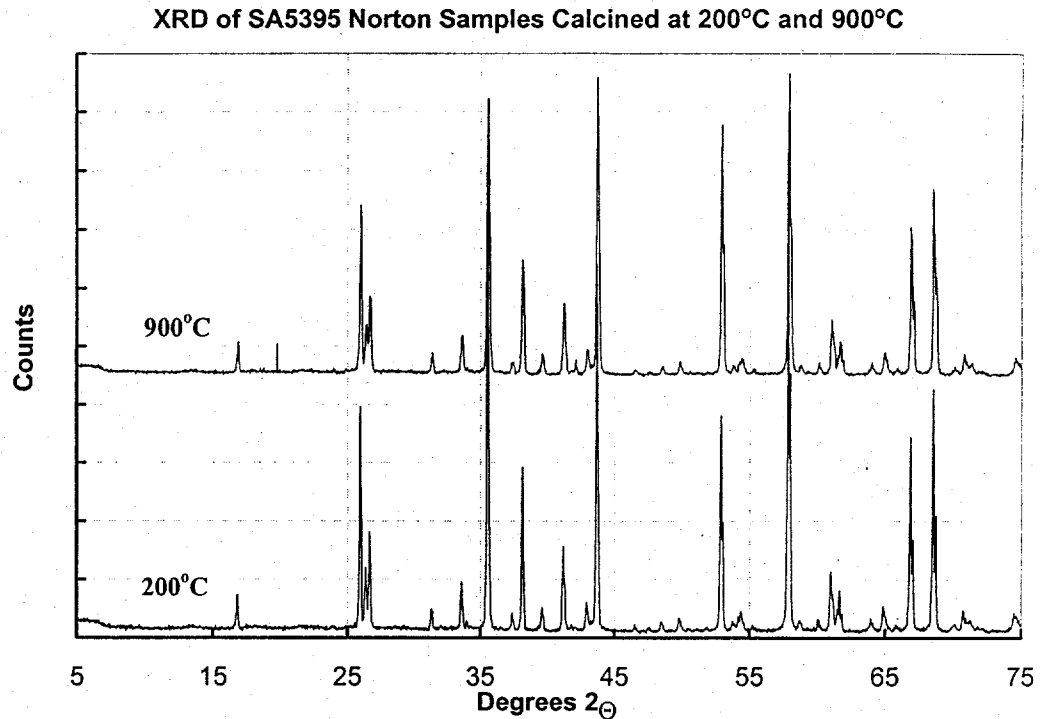


Figure 5-4. XRD patterns for Norton SA5395 calcined at 200°C and 900°C

Table 5-1. Chemical analysis of Norton supports.

Sample Number	9195096	9816240	6416002	9016235	9195093
Type	SA 5395	SA 5397	XA 16374	XA 16612	SA 5396
Size and shape	Fluidizable	Fluidizable	Fluidizable	Fluidizable	Fluidizable
Surface area m^2/g	0.217	0.19	0.127	0.78	0.19
Packing density (g/cm^3)	1.06	1.7	1.67	1.45	1.37
Particle size (μm)	96.9			47.12	80.41
Air jet attrition %/hr			0.19		0.64
Median particle diameter (μm)		90	50.9		
% SiO_2			0.13		0.97
% Al_2O_3					98.52
% Fe_2O_3			0.03		0.15
% CaO					0.08
% MgO					0.06
% Na_2O			0.04		0.15
% K_2O			< 0.01		0.01

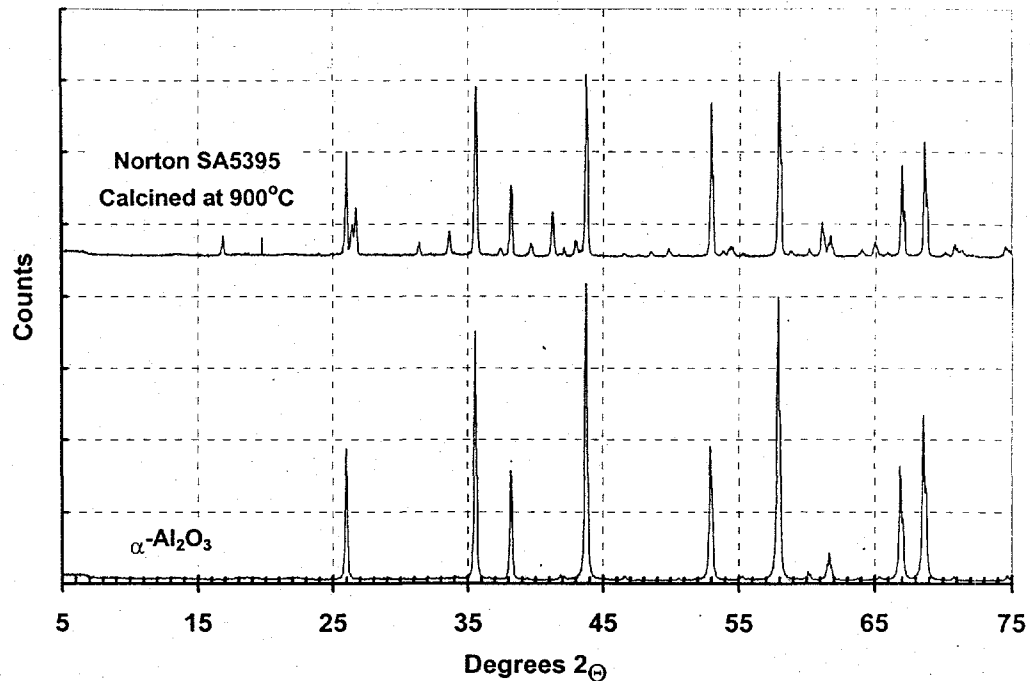


Figure 5-5. XRD patterns comparing Norton SA5395 and α - Al_2O_3 .

Figure 5-4 shows that heating the Norton support to 900°C has essentially no effect on the structure of the support. This is important because temperatures this high can be encountered during sorbent regeneration, where the metal (Cu or Fe) is reoxidized back to the oxide form with neat (21% O_2) air, with the oxidation reaction being very exothermic.

5.3.2. Copper-Based Sorbents

Figure 5-6 contains the XRD pattern for the Norton SA5395 support used to make the 28 wt% CuO sorbent and the pattern for the sorbent after calcination (heating in air) at 900°C. The peak in the sorbent at $2\theta = 39.1^\circ$ is due to the presence of bulk CuO and analysis of the peak width gives the size of the CuO crystallites as approximately 18 nm (180 Å). The crystallite size was determined from the Scherrer formula given by Equation 5-1.

$$t = \frac{0.9\lambda}{B \cos \theta}$$

Equation 5-1 Equation for crystallite size from line broadening

where t is the approximate crystallite size in \AA , λ is the x-ray wavelength (\AA) (for Cu $K\alpha$ radiation, $\lambda = 1.544 \text{\AA}$), B is the instrument line broadening in (\AA), and Θ is the diffraction angle (Cullity 1956). This line broadening occurs because in crystals that are small, the constructive and destructive interference that leads to the XRD pattern is incomplete, thus, the diffracted beam has a range of angles rather than a single angle that would be observed if the crystal were "infinitely thick" (Cullity 1956).

**XRD of Norton SA5395 plain and with 28.03 wt% of CuO
calcined at 900°C for 3h**

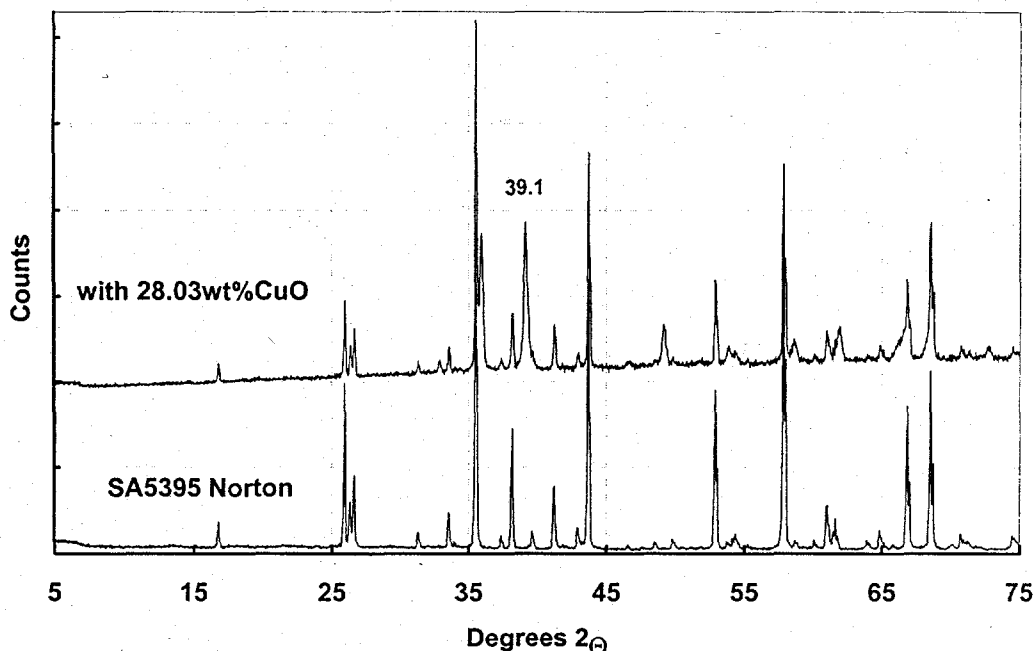


Figure 5-6. XRD patterns for Norton support and 28 wt % CuO sorbent.

The large size of the CuO crystallites is due to sintering of this material at the higher temperatures. The melting temperature of CuO is $T_m = 1508 \text{ K}$. The Tammann temperature is the temperature at which solid diffusion rates become significant, and depending on the solid is between about $\frac{1}{2} T_m$ and $\frac{2}{3} T_m$. For CuO this is 754K to 1005 K (481°C to 732°C). Not only is the pretreatment temperature above the Tammann temperature for CuO, all of the temperatures encountered by the sorbent (700-900°C) in the process application are above the Tammann temperature. As a result CuO is present as large particles. As CuO is reduced to elemental Cu by CH_4 , CO and H_2 , the metallic Cu will also sinter ($T_{\text{Tammann}} = 405^\circ\text{C} - 631^\circ\text{C}$) during the reducing phase of the process. Fortunately, the metal and oxide sintering has no deleterious effect on sorbent performance, as discussed below in the section on cyclic testing.

5.3.3. Iron-Based Sorbents

Figure 5-7 compares the XRD of the Norton support material with the sorbent made using 25 wt % Fe_2O_3 . The estimated size of the Fe_2O_3 crystallites by from the peak width at half maximum for the peak at $2\theta = 49.9^\circ$ is 47 nm (4700 Å). The melting temperatures of Fe, Fe_2O_3 and FeO are 1808 K, 1838 K, and 1642 K respectively. The Tammann temperature ranges are therefore: 631°C - 932°C for elemental Fe, 646°C - 952°C for Fe_2O_3 and 548°C - 822°C for FeO. Thus sintering will occur both in the sorbent preparation and at least during the regeneration step of the process (where Fe and FeO are reoxidized back to Fe_2O_3 where temperatures can reach 900°C and greater). As was the case with the copper based sorbent, sintering of the active phase has no detrimental effect on sorbent performance (as discussed below).

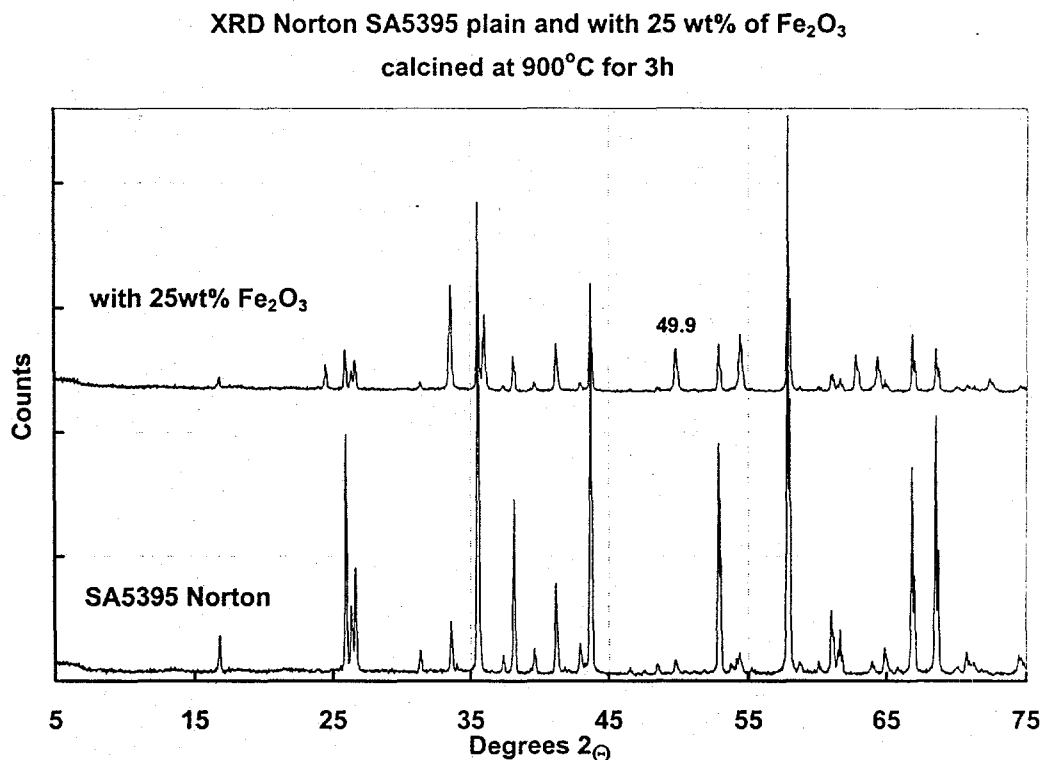


Figure 5-7. XRD patterns for Norton support and 25 wt % Fe_2O_3 sorbent.

Table 5-2. Composition of Geodes.

		Pellet Composition (wt%)		Crush Strength (lbs/mm) / Void (%)		at Firing Temperature (°C)					
		Fe ₂ O ₃	Boehmite	ZnO	Cu ₂ O	Volclay	900	1000	1050	1100	850R*
263	-	35.3	64.7							4.1 / 47	
34a											
263	-	50.0	50.0							10.6 / 53	
34b											
263	-	64.7	35.3							12.2 / 45	
34c											
263	-	61.0			39.0			8.7 / 25		12.9 / 17	
35c											
263	-	57.5	5.6		36.9			13.8 / 27	15.9 / 21	12.2 / 24	
35d											
263	-	51.4	14.4		34.2			14.8 / 24	12.2 / 25	8.7 / 32	
35e											
263	-	70.0		25.0		5.0	8.9 / 40	11.4 / 40			6.2 / 53
39a											
263	-	70.0		30.0			6.2 / 40	7.7 / 40			8.8 / 56
39b											
263	-	85.0		10.0		5.0	9.2 / 42	10.7 / 48			12.2 / 45
39c											
263	-	90.0		10.0			7.7 / 44	10.2 / 50			10.6 / 45
39d											
263	-	95.0				5.0	8.6 / 46	24.6 / 60			7.3 / 57
39e											
263	-	100.0					5.5 / 49	12.1 / 60			12.7 / 34
39f											

* Fired under reducing gas flows (25 vol% each CO₂ / H₂O / N₂ / H₂) otherwise under air.

In order to better understand their behavior we took a number of pellets we had previously fired in the oxidizing environment of the box furnaces and loaded them in the HTHP reactor and subjected them to an extreme reducing environment. We also included unfired "green" pellets to compare pellets fired in this low temperature reductive firing/cycling with those which were fired at higher temperatures under oxygen. The reactor conditions and observations are shown in Table 5-3.

Table 5-3. Effect of cycling on geode sorbents.

Reactor Conditions (4 hour exposure)

600 °C; 4000 (25 vol%/ 1000 sccm each H₂,CO,CO₂,N₂); 50-150 psig

	Formulation *	Oxidized Form	Reduced Form
263-35e-1000	15 wt%CatB (8.6wt% Al ₂ O ₃) - TN Mix	Silvery Gray Pellets	Black Powder
263-35e-Green	15 wt%CatB (8.6wt% Al ₂ O ₃) - TN Mix	Red Pellets	Dark Brown Pellets
263-30-2a-1100	Zn Al ₂ O ₄	White Pellets	White Pellets
263-30-2c-1100	Cu Al ₂ O ₄	Tan Pellets w/ black spots	Burgandy Pellets (too dark to see if spotted)
22/12-1000	65wt%CatB - 1352 Fe ₂ O ₃	Red Pellets	Black Pellets
263-35d-1050	4 wt%CatB (2.5wt% Al ₂ O ₃)- TN Mix	Silvery Gray Pellets	Black Powder w/ Pink Flakes
263-35d-1100	4 wt%CatB (2.5wt% Al ₂ O ₃) - TN Mix	Silvery Gray Pellets	Fractured Pink Pellets w/ Black Interiors
263-34b-1100	18 CatB / 18 Fe ₂ O ₃	Red Pellets	Black Pellets
CatB-No Clay-Green	CatB 1352 Stoich.	Red Rods	Black Rods
263-35e-1100	15 wt%CatB (8.6wt% Al ₂ O ₃) - TN Mix	Silvery Gray Pellets	Black Powder
263-35d-1000	4 wt%CatB (2.5wt% Al ₂ O ₃) - TN Mix	Silvery Gray Pellets	Black Powder
263-30-2b-1100	FeAl ₂ O ₄	Red Pellets w/ white spots	Black Pellets w/ white spots
263-30-2d-1100	Mn Al ₂ O ₄	Dark Tan Pellets	Lighter Tan Pellets
18/18-1000	50wt%CatB - 1352 Fe ₂ O ₃	Red Pellets	Black Pellets
263-35c-1050	TN Mix (1.00 Fe ₂ O ₃ : 0.64 Cu ₂ O)	Silvery Gray Pellets	Fractured Pink Pellets
263-34a-1100	22 CatB / 12 Fe ₂ O ₃	Red Pellets	Black Pellets
263-34c-1100	12 CatB / 22- Fe ₂ O ₃	Red Pellets	Black Pellets
CatA/1352-Green	CatA 1352 Stoich.	Red Rods	Black Rods

* TN Mix equals a thermoneutral mixture of CuO and Fe₂O₃

As is seen in the "reduced form" column, in this extremely reducing environment (2:1 reducing to non-reducing gasses), a number of the fired pellets fell apart into a powder. However only those pellets that were previously oxidized and contained both CuO and FeO fell apart. Identical compositions that were introduced in the green state stayed as pellets, as did those geodes that only included one of these active ingredients. XRD analysis indicated almost all the

iron in these deteriorated pellets was in the form of Fe_3C . This implies that the iron and copper must be put in alumina separately, or that the extreme reducing environment be avoided to prevent iron carbide formation. In addition, the void of these mixed iron copper materials is probably also too low, since we are operating well above the sintering point of copper oxide the low void contributes to spalling under these conditions. Table 5-4 shows only those pellets which "survived" this rather harsh exposure. As a final cycling simulant, the stronger pellets identified in this test were re-oxidized at 900°C after which the physical properties were again measured. The iron on alumina geodes (22/12, 263-30-2b, 263-34(a,b,c) for iron) showed little to no deterioration in pellet strength or void fraction is evident and as such are good candidates for further development.

Table 5-4. Properties of cycled sorbents.

	Oxidized	Reduced	Reoxidized			
	Crush Strength (lbs/mm)	Void (%)	Crush Strength (lbs/mm)	Void (%)	Crush Strength (lbs/mm)	Void (%)
263-35e-Grn	n/a	n/a	4.6	48	16.7	30
263-30-2a-1100	2.4	66	2.4	64	n/a	n/a
263-30-2c-1100	3.8	61	1.8	61	n/a	n/a
22/12-1000	5.25	54	4.6	56	5.6	58
263-34b-1100	10.6	53	8.3	62	14.4	53
263-30-2b-1100	4.9	52	4.9	53	5.2	53
263-30-2d-1100	2.8	55	2.0	59	n/a	n/a
263-34a-1100	4.1	47	4.5	51	10.4	49
263-34c-1100	12.2	45	6.5	58	8.8	53

To see if the inhibition of iron carbide formation degrades a pellet's strength through normal cycling, we re-exposed some of the geode compositions that powdered under the severe reducing conditions to an environment more like that they will be exposed to in the real world situation (reducing gas to non-reducing gas ratio of 1:1). This should be a non-carbide forming situation according to HSC simulations run at TDA. As shown Table 5-5, 263-35c and 263-35e which powdered in reducing cycle #1, but maintained their pellet shape and strength under normal conditions. 263-35c-1100 contains no binder, and as such would be expected to lose more of its structural integrity than 263-35e-1000 which contains approx. 10% alumina binder. We can thus conclude that in a less reducing environment, the combination of copper oxide and iron oxide should be

compatible on a single alumina supported pellet, although the amount of binder may still need to be increased.

Table 5-5. Strength of reduced geodes.

Reactor Conditions (15 Minute exposure)

4000 (25 vol%/ 1000 sccm each H₂, H₂O, CO₂, N₂) 850 °C; 0 - 25 psig

	Oxidized Form	Reduced Form
	Crush Strength (lbs/mm) / Void (%)	Crush Strength (lbs/mm) / Void (%)
263-39a-Grn	n/a	6.2 / 53
263-39b-Grn	n/a	8.8 / 56
263-39c-Grn	n/a	12.2 / 45
263-39d-Grn	n/a	10.6 / 45
263-39e-Grn	n/a	7.3 / 57
263-39f-Grn	n/a	12.7 / 34
263-34a-Grn	n/a	2.4 / 62
263-35c-1100	12.9 / 17	6.4 / 62
263-35e-Grn	n/a	14.1 / 37
263-35e-1000	14.8 / 24	11.6 / 39
263-38a-Grn	n/a	4.8 / 61
263-38a-900	7.6 / 62	21.7 / 20

5.4. Multiple cycle testing

5.4.1. Experimental Methods

The sorbent must be able to withstand repeated oxidation/reduction cycles as well as thermal cycling. Also, the amount of oxygen transferred per unit weight of sorbent (oxygen capacity) should be as high as possible to minimize sorbent costs. In Phase I, we prepared several sorbent samples and have tested them to determine 1) oxygen uptake capacity; 2) regenerability; and 3) resistance to degradation by thermal cycling. These tests were done in a microbalance system where reducing and regeneration gases could be passed over a sorbent sample at different temperatures while the weight of the sample is continuously monitored. The microbalance system was ideal for this application because it provides a direct gravimetric measurement of oxygen uptake, and the extent of reduction. Thus, comparisons with the stoichiometric weight change expected provide a direct measure of sorbent capacity.

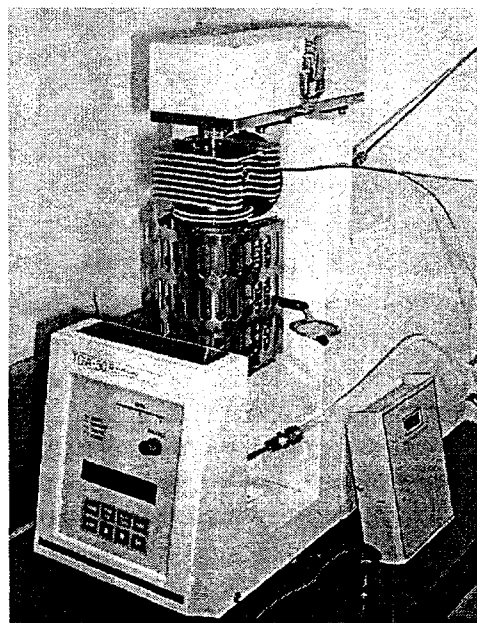


Figure 5-8. Shimadzu microbalance.

Additionally, the sample can be repeatedly subjected to cycles of reduction and oxidation to determine if there is any gradual change in oxygen uptake.

Figure 5-8 is a photograph of the Shimadzu TGA-50 microbalance, and Figure 5-9 is a schematic that shows how the TGA-50 is used in a flow system mode to measure weight changes that accompany the reduction and oxidation of sorbents. Air, CO₂ and H₂ are metered in with variable area flowmeters (rotameters). The gas streams (air and CO₂ or H₂ diluted with CO₂) are mixed and pass through a room temperature bubbler where the relative humidity of the gas is increased to 100% at 20°C (partial pressure of approximately 18 Torr). The humid gas then enters the top of the tube furnace (Figure 5-9) flows over the sample, out the bottom and is vented. The tube furnace is thoroughly purged with pure CO₂ for 5 - 10 min between regeneration and reduction experiments to ensure that no residual H₂ ever mixes with air. The instrument is computer controlled and the weight change and temperature recorded to disk as a function of time.

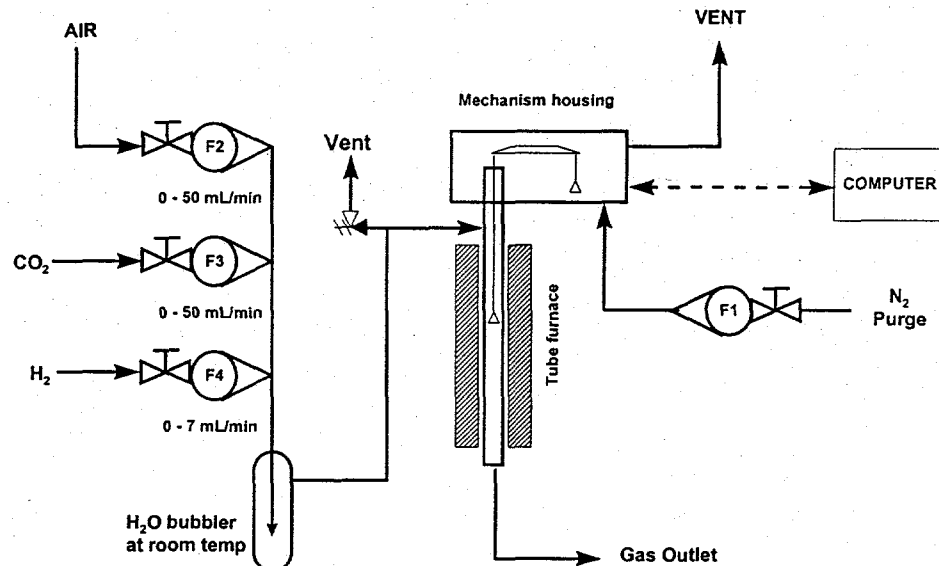


Figure 5-9. Schematic of microbalance flow apparatus.

The active components of the sorbents are transition metal oxides (CuO and Fe₂O₃). The sorbent in the oxide form is reacted with a reducing gas (10% H₂ in CO₂) at 800°C. The weight change is recorded and yields information on the extent of reduction and kinetics of the reduction process (based on the time required for reduction). After reduction, the sorbent is exposed to neat air (zero grade bottled air) and re-oxidized back to the oxide form. The weight increase indicates the quality of the regeneration procedure (i.e. weight increasing back to its value before reduction). The sorbent is subjected to several cycles of reduction and oxidation at 800°C to determine its durability and stability.

5.4.2. Sorbent Test Results

The sorbents we selected for these tests exhibited the highest porosity, crush strength and metal oxide loading level. These were the 28 wt % CuO on Norton 5395, a CuO/Fe₂O₃/Al₂O₃ geode sorbent and a Fe₂O₃/Voclav geode sorbent.

Performance of a 28 wt % CuO Sorbent First, we examined the reduction and oxidation of 28% CuO/Norton 5395 sorbent that was prepared by impregnation. The sorbent was first ground to a fine powder, and about 20 mg of sample was then placed on the platinum sample pan in the Shimadzu microbalance. The flow of 30 % H₂/CO₂ was established and then the temperature was increased to 800°C at a rate of 50°C/min. Figure 5-10 show the results of succeeding reduction and oxidation cycles on the 28% CuO sorbent. The observed weight loss upon reduction corresponds to complete reduction of CuO to metallic Cu by the hydrogen. The observed weight change was 4.4% which is the same within experimental error, of the 4.8 % weight loss expected from stoichiometry. Importantly, Figure 5-10 shows that over a period of 7 cycles, the sorbent oxidation/reduction is completely reversible and no thermal history develops. This result suggests that good sorbent durability for long life can be expected when used at the commercial scale.

The excellent reversibility of the weight is shown in Figure 5-11 which indicates that the original weight is regained for each cycle to within 0.1 wt %. This indicates that the reduction/oxidation capacity of the sample can be maintained over 8 cycles (about 4 h) without any significant deactivation.

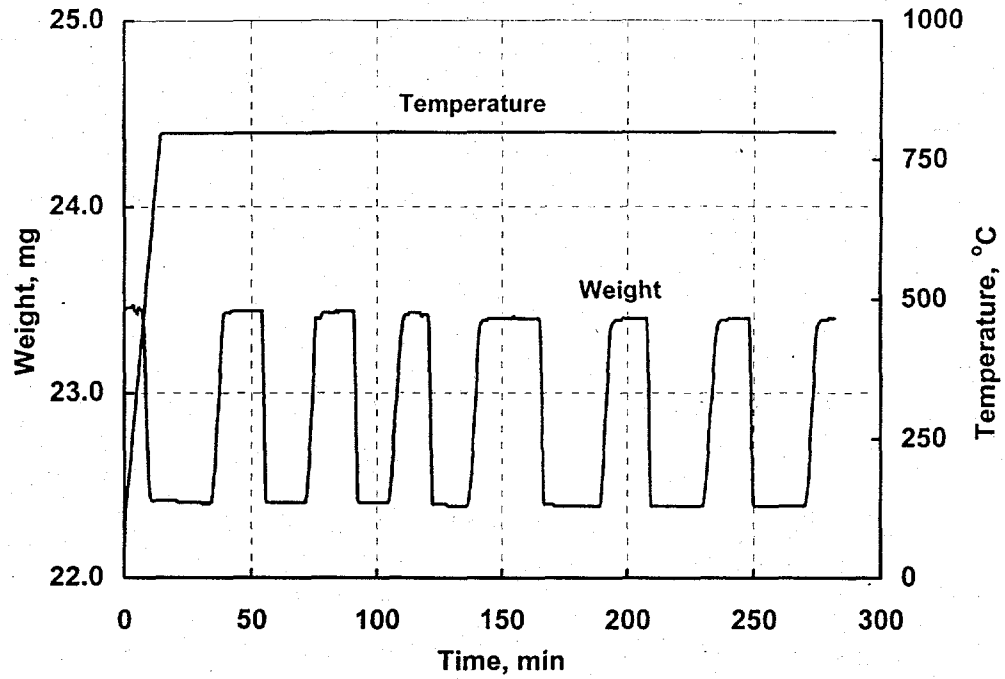


Figure 5-10. TGA results for 28 wt % CuO fluidizable sorbent.

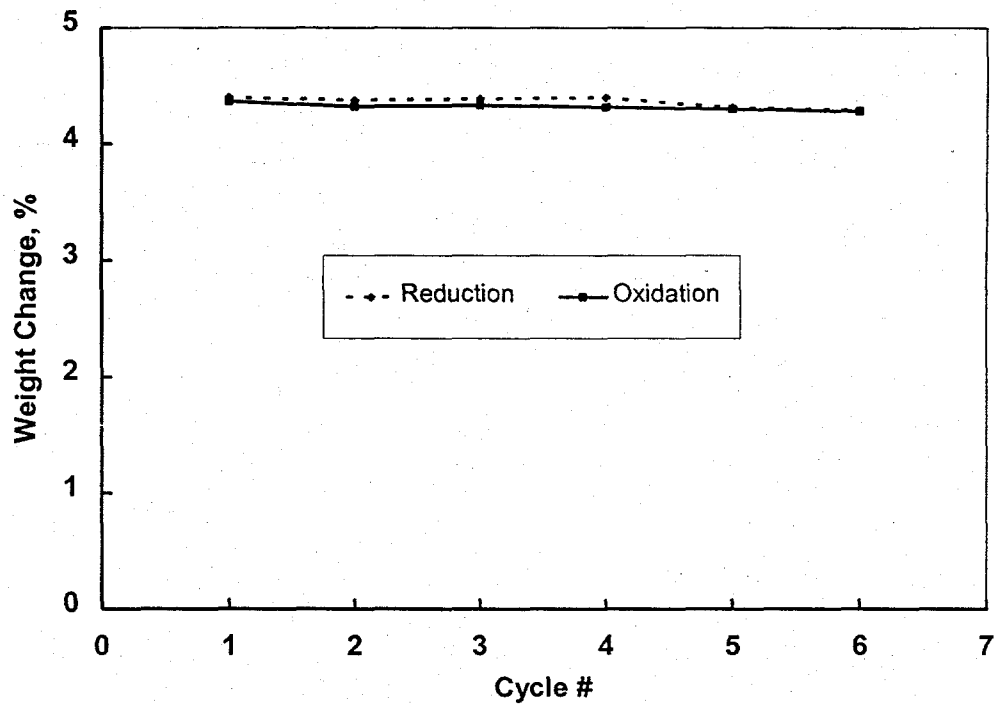


Figure 5-11. Weight change for 28 wt% fluidizable sorbent during cycling.

Examining Figure 5-10 in detail reveals that the rate of reduction of the sorbent (0.40 - 0.55 mg/min) is slightly higher than the rate of reoxidation (0.25 - 0.30 mg/min). This may be due to different rates of solid state diffusion that have to occur during reduction compared to oxidation. The CuO crystallites are rather large (ca. 1700 Å for the 28 wt% CuO sorbent), and both the reduction and oxidation (regeneration) reactions start at the surface of the particles. In the case of reduction, H₂ diffuses to the surface from the surrounding gas, adsorbs on the surface and then reacts with oxide ions to form water. At the same time electron transfer to the Cu²⁺ ions reduces them to metallic Cu atoms. Aside from the extent that H₂ diffuses into the CuO crystallites, solid state diffusion is the only mechanism that can replenish the surface region with Cu²⁺ and oxide ions so that the whole crystallite can eventually be reduced. A similar analogy holds for the oxidation step; the surface needs to be replenished with metallic copper as Cu²⁺ ions and oxide ions counter diffuse into the bulk. While the details of these atomic scale processes are complex and irrelevant to our application for this sorbent, the results presented in Figure 5-10 are completely consistent with what is known about oxidation/reduction reactions between solids and gases, and further strengthen our confidence in the quality of the data.

5.4.2.1 *Performance of a CuO-Fe₂O₃ Geode Sorbent.*

In a test that was essentially identical to the test of the 28 wt% CuO sorbent discussed above, we tested a CuO-Fe₂O₃ geode sorbent. In this test we examined the pellet form of the sorbent to determine if there were any substantial effects on the overall reduction/oxidation rates due to pore diffusion limitations. The TGA data for this bulk pellet are shown in Figure 5-12. Diffusional resistances manifest themselves by a slowing of the rates of both reduction and regeneration (oxidation). This can be seen by comparing the weight change curve in Figure 5-12 with the analogous curve in Figure 5-11. The rise and fall in weight is much more rapid in the case of the 28 wt % CuO sorbent, where the sample was a fine powder. While the rates of regeneration and oxidation of the CuO/Fe₂O₃/Al₂O₃ pellet are lower than that of the fine powdered CuO sorbent, complete reduction still occurs within 40 min which is sufficiently fast for using the pellets in a fixed bed application where reduction and oxidation would be performed in parallel reactors operated in a swing mode.

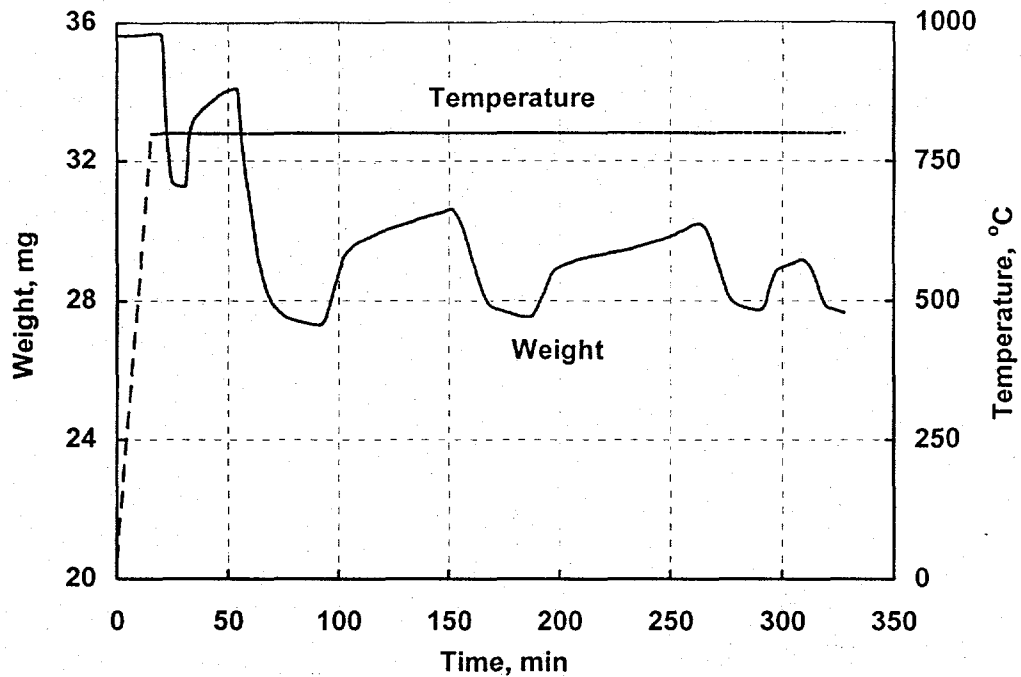


Figure 5-12. TGA results for $\text{CuO-Fe}_2\text{O}_3$ geode sorbent.

TGA pattern of the $\text{CuO-Fe}_2\text{O}_3$ geode is quite unusual. The amount of sample reduced and oxidized as well as the reduction/oxidation rates (slope of the curves) increased significantly after the first cycle. It is apparent Figure 5-12 that the reduction/oxidation capacity gradually decreases over the duration of the test. Although the weight change associated with reduction decreased substantially (from 13% to 8%), the overall weight change due to oxidation was almost constant particularly for a short waiting period (the 10 min interval immediately after the air is introduced to the system, where the oxidation was the fastest) as shown in Figure 5-13.

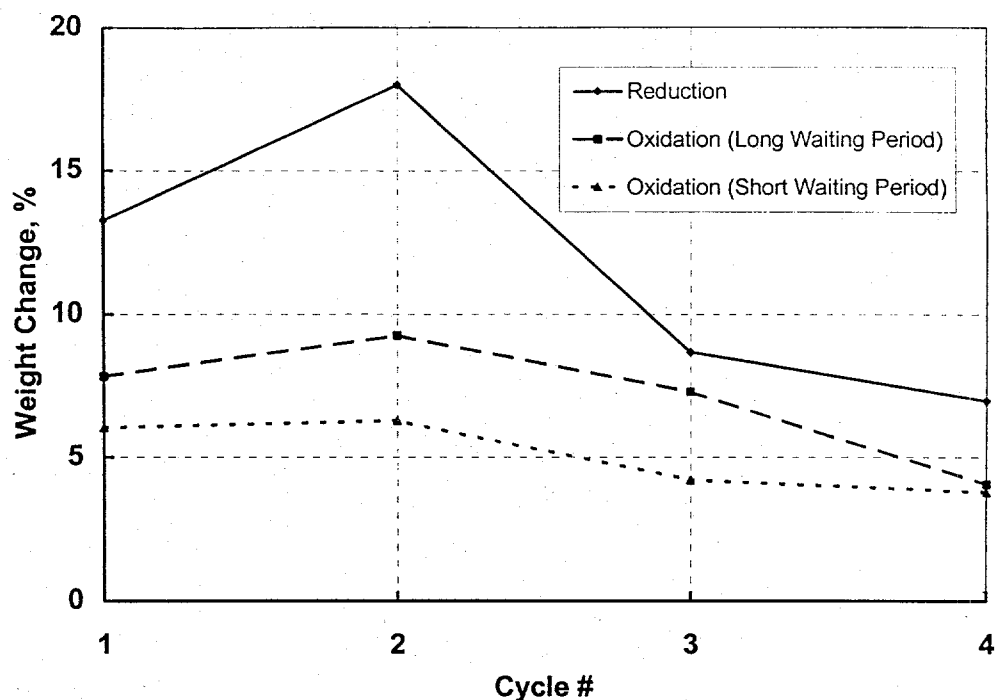


Figure 5-13. Weight change for CuO-Fe₂O₃ geode sorbent during cycling.

Based upon our previous particle size and surface area measurement results, we can speculate that the loss in activity of the CuO-Fe₂O₃ geode pellet is due to particle sintering, and perhaps more importantly in this material, and reduction in surface area of the support due to collapse of the pore structure of the Al₂O₃ due to a phase change toward α -Al₂O₃ at 800°C. In spite of the capacity loss however, the sorbent still has 4.2 wt % capacity for oxygen at the end of the 4th cycle.

5.4.2.2 Performance of a Fe₂O₃/Volclay Geode Sorbent

We also tested a Fe₂O₃/Volclay geode. For this sample, we used two different reducing gases. For the first two cycles we used a mixture of 30% H₂ in CO₂ as described previously. After the second cycle, we examined a gas stream containing 3.2 vol % CO, 4.7 vol % CH₄, 10 vol % H₂ and 82.1 vol % CO₂ (Scott Specialty Gases). The gas mixture has a composition that is similar to the equilibrium gas mixture that exists in the exit of the first reduction reactor (where methane is first contacted with partially reduced sorbent). This is also the composition near the middle of the natural gas reduction reactor when a transport reactor is used.

As before, neat air was used to regenerate the sorbent by oxidation. The thermogravimetric data and weight of change associated with the reduction/oxidation cycles are presented in Figure 5-14 and Figure 5-15. The reduction capacity of the stream with 30% H₂ (% after second cycle) was apparently higher than that of the standard gas mixture. However, the reduction/oxidation capacity of % achieved after cycles is very satisfactory.

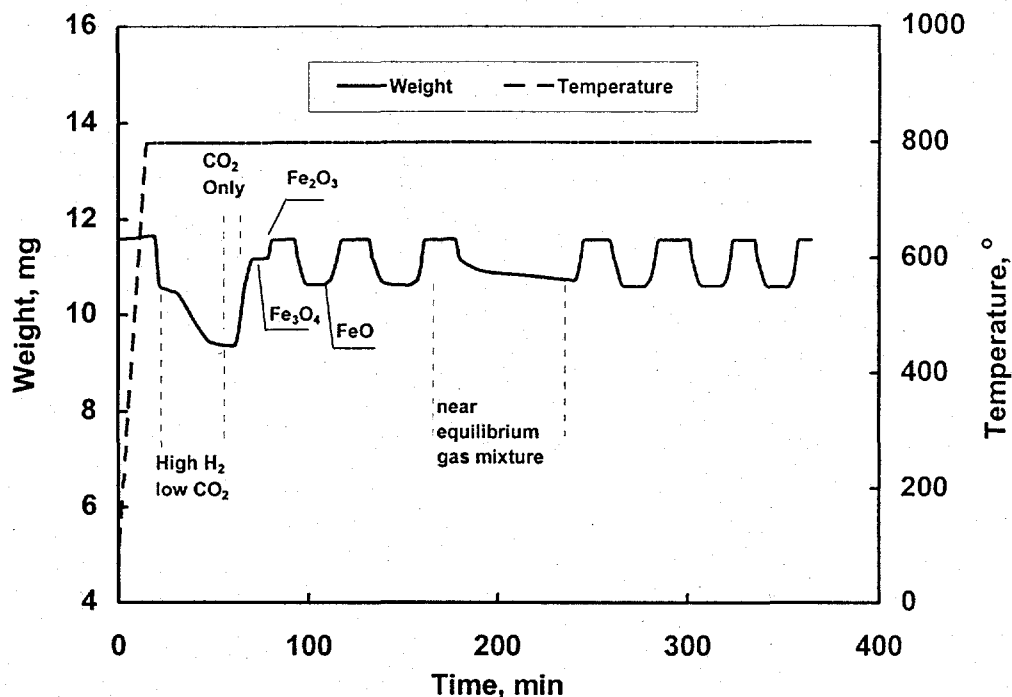


Figure 5-14. TGA results for Fe_2O_3 Voclay geode.

At the start of the 4th cycle we switched back to the original mixture of 20% H_2 /80% CO_2 as the reducing gas and realized an increase in the capacity to the 8.5% level. The oxidation and reduction rate remained unchanged through the cycles (0.3 mg/min and 0.25 mg/min for oxidation and reduction, respectively).

Note also in Figure 5-14 that when the H_2 concentration was high during the first reduction, this gave the largest weight loss. This was due to over-reduction of the sorbent to a mixture of Fe (elemental) and FeO (the weight loss was not large enough to indicate that all of the sorbent was reduced to Fe metal). Also note (labeled on Figure 5-14) that when oxidizing the sorbent from this state, the sorbent goes through the stages of oxidation: FeO (Fe^{II} oxide), Fe_3O_4 (mixed Fe^{II} and Fe^{III} oxide) and finally Fe_2O_3 (Fe^{III} oxide).

Figure 5-15 shows that in both the cases of H_2 rich reducing gas (ca. 30 vol %) as well as the equilibrium reactor #1 gas, the oxidation and reduction of this sorbent are completely reversible with no loss in sorbent performance as the sorbent is cycled.

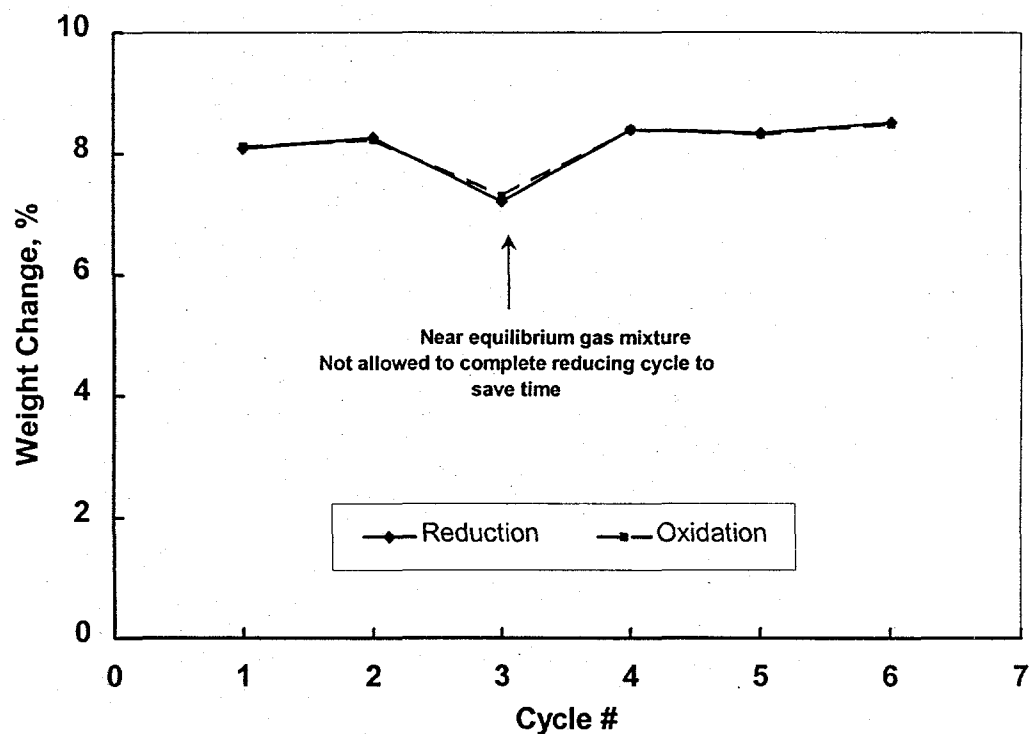


Figure 5-15. Weight change for $\text{Fe}_2\text{O}_3/\text{Voclay}$ geode sorbent during cycling.

These results show that the TDA sorbents are highly effective for oxygen transfer and can be repeatedly cycled between the oxidized and reduced forms without any degradation in sorbent performance. We found that the $\text{Fe}_2\text{O}_3/\text{Voclay}$ geode formulation and the 28 wt% CuO/Norton formulations gave excellent results. Thus these sorbent formulations are ideal for application in either the two stage fluidized bed application or in the transport reactor.

6. Economic Analyses

In this section we start by describing the SETS cycle (Section 6.1). Section 6.2 describes the integration of the SETS cycle with the power cycle. Sections 6.3 and 6.4 describe the sizing of the key components of the SETS systems, the oxidation and regeneration reactors.

6.1. Efficiency Impact of SETS

For the SETS, TDA selected a two stage reducing reactor as illustrated in Figure 6-1; Reactor 1 and Reactor 2 are transport reactors (but could be fluidized reactors). The oxidized solids and fuel are contacted in a counter-current manner in Reactors 1 and 2. The oxidized solids enter at the top of Reactor 2 and the fuel gases enter at the bottom of Reactor 1. The regeneration reactor (i.e., Reactor 3) is a transport reactor and oxidizes the sorbent while heating the air. TDA selected transport reactors, because their fast cycling time of the sorbent minimizes capital and operating costs.

Air is compressed to 13.5 ATM by the compressor stages of the gas turbine (TDA assumed a General Electric Frame 7A gas turbine for this analysis), which heats the air to $\sim 400^{\circ}\text{C}$. The reduced sorbents (e.g., copper and iron, since they are the lowest cost exothermic/endothermic combination) and air are contacted in a transport reactor where the sorbent is oxidized. The oxidation heats the sorbent and air to $\sim 900^{\circ}\text{C}$ and the two are separated in a cyclone.

The sorbents (at 900°C) then enter reactor No. 2 (a transport reactor) and contact the partially oxidized fuel gases leaving Reactor 1, which are at $\sim 700^{\circ}\text{C}$ and are 67% to 90% oxidized (i.e., most of the oxidation occurs in Reactor 1). Since Reactor 2 has a great excess of oxidation potential and CuO has the greatest reduction potential, only some of the copper oxide is reduced to copper while it fully oxidizes all of the fuel gases to CO_2 and H_2O ; the Fe_2O_3 is only partially reduced due to the small quantity of H_2 , CO , and CH_4 entering Reactor 2. Due to the high flow rate of cooler gases (i.e., 700°C) and the limited reaction occurring in Reactor 2 (and the active cooling carried out by generating steam or reforming of the CH_4), the solids are maintained at temperatures less than 900°C throughout the reactors to inhibit loss of oxygen, and the solid sorbents leave Reactor 2 at 600° to 700°C .

The solids leaving Reactor 2, as slightly depleted in oxygen (as oxides) and drop into Reactor 1, which is also a fluidized bed or transport reactor. Recycled gases from the effluent of Reactor 2 are mixed with natural gas (primarily CH_4) and flow into Reactor 1. This Reactor (#1) has an excess of reducing gas so that both sorbents are fully reduced to maximize the oxygen transfer from the oxidizing (Transport regeneration reactor) to the reducing side of the SETS. Due to the endothermic reforming (i.e., reducing of the Fe_2O_3 to FeO) the solids leave Reactor No. 1 at $\sim 700^{\circ}\text{C}$ to 816°C .

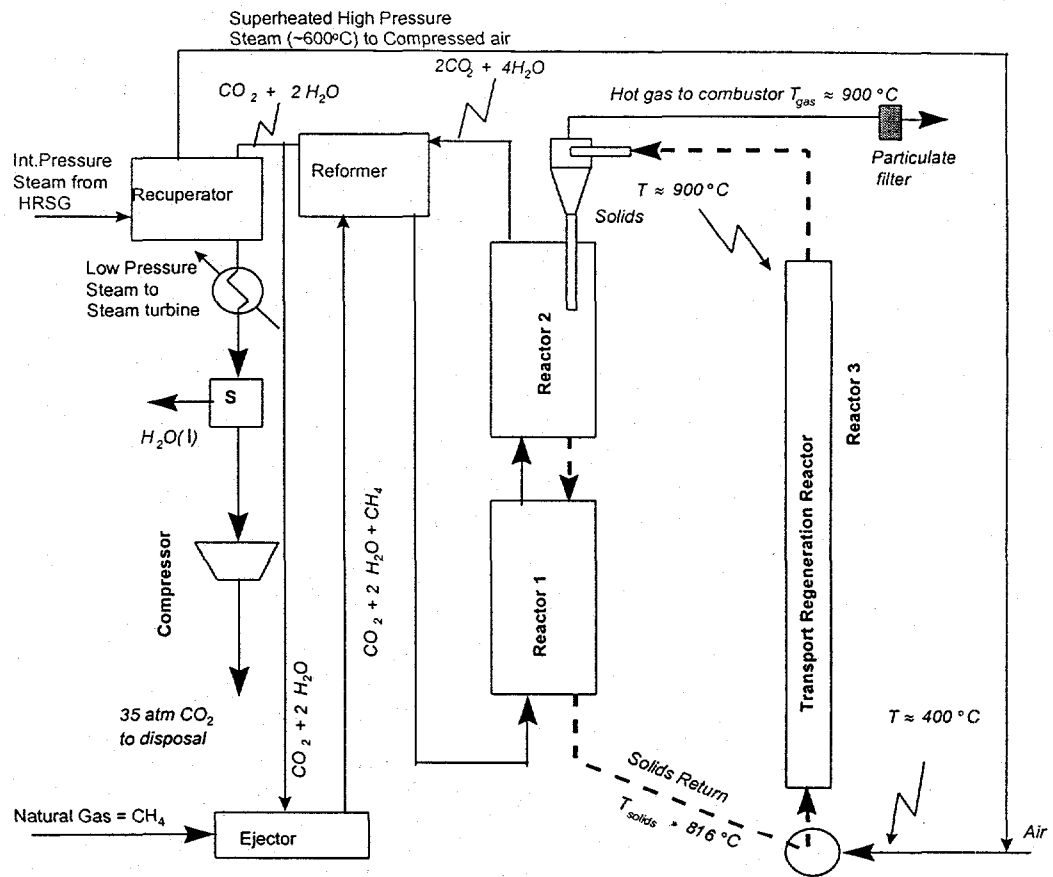


Figure 6-1. SETS system.

Figure 6-1 shows the temperatures and pressures expected in the baseline nominal SETS and the nominal reactions occurring in each reactor. The fully oxidized fuel leaves reactor 2 at 900°C containing $2\text{H}_2\text{O}$ and CO_2 . The gases are first cooled to $\sim 650^\circ\text{C}$. Some of those gases mix with the natural gas in an ejector, which slightly pressurizes the recycled H_2O and CO_2 . The mixture then flows through the pre-former, giving up their heat to drive the reforming of part of the CH_4 to CO and H_2 while cooling the outlet gases from reactor 2 to $\sim 650^\circ\text{C}$. After cooling the gas stream splits, some is recycled and the remainder is cooled in a recuperator generating high pressure superheated steam which is added to the high pressure air entering the transport regeneration reactor.

After giving up some of their heat to superheat intermediate pressure steam, the H_2O and CO_2 are cooled condensing the steam. Since the steam is condensed at high pressure and account for 67% of the gases (i.e., $\text{CH}_4 + 4\text{ "O" (from oxides)} = \text{CO}_2 + 2\text{H}_2\text{O}$), the condensing of the steam with CO_2 can be used to generate pure steam at low pressure. However, three mols of H_2O are extracted from the steam turbine at intermediate pressure ($\sim 150\text{ psia}$, 10 ATM) for use in the reformer; that lost H_2O reduces the power generated in steam turbine.

The condensation of steam will generate low pressure steam ($\sim 1\text{ ATM}$) which can generate power. The low pressure steam is assumed to generate power at 8% thermal efficiency. The extraction of intermediate pressure steam ($\sim 200\text{ psia}$)

reduces power generation in the steam turbine; we assume a power thermal efficiency penalty at 20% for intermediate pressure steam. High pressure steam (~600 psia) has a higher thermal efficiency (~30%) and we calculate the power gains and losses from the use of steam using these assumptions.

Additional power is lost in SETS in compressing the CO₂ to high pressure and in the parasitic loss (i.e., pressure drop of the air flowing through the reactor). Table 6-1 presents an estimate of these efficiency losses and gains for the SETS and a competing advanced CO₂ separation system which steam reforms the natural gas to H₂.

Table 6-1. Efficiency of two CO₂ separation systems.

Per mole methane	SETS	H ₂ from H ₂ O/CH ₄ Reformer
CH ₄ , HHV kcal	-211.12	-211.12
CH ₄ , LHV kcal	-191.58	-191.58
Heat of vaporizing H ₂ O	per mol 9.77	4 mols H ₂ O/CH ₄
Low Press. ST	1.04	1.56
Lost Steam Power for H ₂ O	-3.91	-11.72
CC Power		95.79
2/3 rd s heat from SETS	62.98	
1/3 rd heat Direct NG	31.93	
Lost steam work		
CO ₂ compression	-0.76	0.00
Parasitic for CO ₂ separation	-0.31	-0.31
Net Power (kCal /mol CH ₄)	90.97	85.31
LHV efficiency	47.48%	44.53%
HHV Efficiency	43.09%	40.41%
Relative loss in fuel efficiency	5.03%	10.94%
Loss of efficiency points from 50% LHV	-2.52%	-5.47%

The steam reformer for the H₂ producing system is assumed to operate at high pressure (e.g., 600 psia, ~40 ATM) so that no downstream compression of either H₂ or CO₂ is required. The hydrogen is assumed to be extracted at 15 ATM and burned directly in the gas turbine. However, since a large quantity (4 H₂O per CH₄) of very high pressure steam (i.e., 600 psia, ~40 ATM) is required in the reformer to prevent coking, the lost of potential power generation in the steam turbine is very large. Theoretically, 2 mol H₂O per CH₄ can react to form 4 H₂ and CO₂, but coking and equilibrium work against the completion of the reaction.

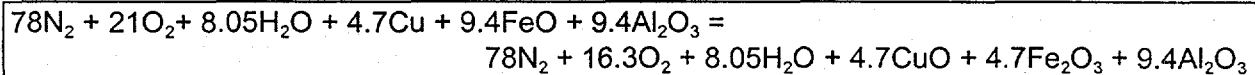
6.2. Integration of the SETS and Power Cycle

In this analysis, we used a relatively standard combined cycle as our basis for comparison. We then modified the combined cycle to incorporate the SETS cycle, and compare the cost and efficiency of the baseline and modified systems.

TDA selected a nominal gas turbine to analyze the performance of the SETS. The gas turbine has a firing temperature of 1260°C (2300°F), a gas inlet temperature to the turbine of 1200°C (2192°F), a pressure ratio of 13.5:1, and a compressor flow of 408 kg/sec (900 lb/sec). However, 2.75% of the air is used in cooling the turbine, which leaves 397 kg/sec to flow through SETS.

The SETS sorbents are assumed to be Cu and FeO in equal proportions as shown in

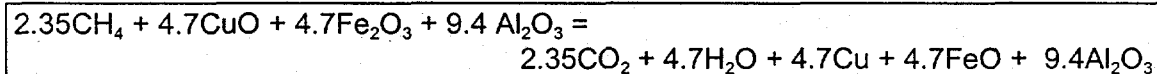
Equation 6-1. We calculate the energy required to heat 100 mols of air (assumed as 78N₂/21O₂/1.0H₂O) from 400°C to 900°C by consuming the oxygen and oxidizing the redox metal oxides (4.7 mol Cu and 9.4 mol FeO are required). We assume 9.4 mol of alumina as the inert support for the chemically active solids.



Equation 6-1. Nominal SETS oxidation (or regeneration) reaction

Since the removal of oxygen removes mass which could have been expanded in the turbine cycle, we extract intermediate pressure saturated steam (~ 200 psia) from the HRSG of the combined cycle. We add that steam in the ratio of 1.5 mol H₂O per mol O₂ removed (i.e., same number of mol which would have been generated by oxidation of methane). Since 4.7 mol O₂ are removed we add 7.05 mol H₂O to the 1.0 mol H₂O assumed in the air for a total of 8.05 mol of steam entering the oxidation or regeneration reactor (i.e., No. 3).

Equation 6-2 presents the net reduction reaction which occurs in Reactor 1 and Reactor 2. This reaction is slightly endothermic and cools the solids to provide the heat necessary for the reaction. Although TDA's geodes do yield high levels of chemically active sorbent per unit weight of inert, about one mole of alumina is needed for every mole of O⁻² transfer in SETS. Thus, since 2 O₂ (or 4 O⁻²) are transferred in oxidizing methane, 4 mol of Al₂O₃ are assumed in this analysis as shown in Equation 6-2



Equation 6-2. Nominal SETS reduction reaction

The polishing reactor (No. 2) only provides 20% of the oxygen, so there is a large excess of copper oxide to fully oxidize the fuel to CO₂ and 2 H₂O. Based upon these relationships, we calculate the compositions of the gasses throughout the cycle; Table 6-2 presents that data. Likewise, the cycle temperatures are shown in Table 6-3.

Table 6-2. Nominal Compositions (mol %)

Location	O ₂	N ₂	H ₂ O	H ₂	CO	CO ₂	CH ₄
Air Inlet Reactor 3	21%	78%	1%				
Steam to Reactor 3			100%				
Air Exit Reactor 3	15.9%	76.2%	7.9%				
Gas Inlet Reactor 2			56.70%	9.92%	3.18%	30.14%	0.06%
Gas Exit Reactor 2			66.67%			33.33%	
Gas Inlet Reactor 1			48.9%	1.2%	0.4%	24.9%	24.6%
Gas Exit Reactor 1			56.70%	9.92%	3.18%	30.14%	0.06%
Gas Exit Reformer			48.9%	1.2%	0.4%	24.9%	24.6%
Gas Inlet Reformer			50.0%			25.0%	25.0%

Our data is based upon a nominal gas turbine (nominally a General Electric MS 7001F) with a simple cycle heat rate of 10,390 Btu/kWh ISO rating of 135.7 megawatts. When operated as a combined cycle, using the exhaust gas at 593°C (1100°F) to generate steam in the HRSG, the total plant produces more than 200 megawatts with a heat rate of less than 6828 Btu/kWh.

Based on the data in Table 6-2 with the same natural gas consumption, the combined cycle which produced 200 megawatts with CO₂ removal would have a net power production of 190 megawatts and a heat rate of about 7188 Btu/kWh.

Table 6-3. Nominal Conditions.

Location	Temperature: °C (°F)	Pressure: ATM (psia)	Flow: kg/sec (lb/sec)
Air Inlet Reactor 3	390 (734)	13.5 (198)	397.0 (875.0)
Steam to Reactor 3	600 (1112)	13.5+ delta 4	17.54 (38.68)
Exit Reactor 3	900 (1652)	13.5 - delta 3	393.8 (868.35)
Gas Inlet Reactor 2	816 (1501)	13.5 - delta 1	47.80 (105.39)
Gas Exit Reactor 2	933 (1711)	13.5 - delta 2	51.95 (114.55)
Gas Inlet Reactor 1	600 (1112)	13.5 (198)	31.18 (68.75)
Gas Exit Reactor 1	816 (1501)	13.5 - delta 1	47.80 (105.39)
Solid Inlet Reactor 2	900 (1652)	13.5 - delta 2	287.7 (634.4)
Solid Exit Reactor 2	933 (1711)	13.5 - delta 1	283.5 (625.2)
Solid Inlet Reactor 1	933 (1711)	13.5 - delta 1	283.5 (625.2)
Solid Exit Reactor 1	816 (1501)	13.5 (198)	266.9 (588.5)

Assuming the natural gas fired combined cycle (i.e., without CO₂ removal) has a price of \$600/kW, the original plant would cost \$120 million. The only price increase would be for the addition of the SETS equipment when CO₂ is removed for sequestering.

6.3. Cycle Efficiency and Cost of CO₂ Separation

At some time in the future, the likely alternative to separating and sequestering CO₂ will be to pay a carbon tax. Carbon taxes are not imposed in the USA at this time, but various proposals would require on the order of \$25/ton of CO₂ emitted into the atmosphere. A tax of \$25/ton CO₂ adds ~10.8 mills/kWh to the price of electricity in a 6824 B/kWh heat rate, natural gas fired, combined cycle power plant (approximately a 20% increase in the cost of electricity). Because the carbon tax price is high, there is a significant economic incentive to avoid paying it. At minimum, to be adopted, any new cycle must be less expensive than paying the tax.

TDA conducted a very preliminary study to identify if the SETS has economic potential with the SETS approach. Table 6-4 presents a summary of the costs assumptions for this analysis. Natural gas was assumed at \$3/MMBtu with the plant efficiency calculated in Table 6-1. The capital costs were simply assigned and are the area most in need of analysis by Kellogg. Sorbent costs and loss rates were assigned based upon TDA's experience. While the sorbent costs are the largest uncertainty, substantial research would be required (i.e., the DOE funded Phase II and Phase III research) to reduce the uncertainties.

Table 6-4. Impact of SETS.

<p>SETS capital and energy costs \$3/MMBtu @5% fuel penalty (loss of 2.5 per centage points) = 1.02 mill/kWh Capital costs : @\$50/kW_e or \$10 million for a 200 MW_e power plant, 75% CF, 15% FCR = 1.14 mills/kWh Total of ~ 2.16 mills/kWh or \$5/ton CO₂ total, but 2/3rds of CO₂ captured = \$7.5/ton CO₂ removed</p> <p>Sorbent Cost \$11/ton CO₂ removed Sorbent costs include the expense of the manufactured material, the oxygen loading per cycle and the loss rate of sorbent per cycle. The costs are based on an assumed price of \$5 for FeO sorbent with 9% O₂ loading and \$10/lb of Cu sorbent with 4% O₂ loadings of (5.5 lb oxygen per 100 lb of sorbent average), and an attrition rate of 2% per hour (higher than FCC catalysts), 1.5 sec contact time per reactor pass, two reducing reactors @ one pass each, and one oxidizing reactor with three passes per cycle; total 7.5 sec per cycle in the reactors or 480 cycles per hour.</p> <p>Overall: \$18.5/ton of CO₂ removed</p>

While there is a measure of uncertainty related to the capital cost of the SETS and the cost of the sorbent for CO₂ removal, there is also clearly an opportunity for SETS to reduce the impact of carbon taxes on power plants.

6.4. Preliminary Sizing of Sorbent Reduction and Oxidation Reactors

The overall SETS process flow (with the staged reactors) is shown in Figure 6-2. The same process carried out with transport reactors is shown in Figure 6-3 (ancillary process components are omitted for clarity). Table 6-5 summarizes the results of equipment size estimates for the case where staged stationary fluidized beds are used for natural gas oxidation by the Fe_2O_3 and CuO sorbents, and where a transport reactor is used to carry out the natural gas oxidation.

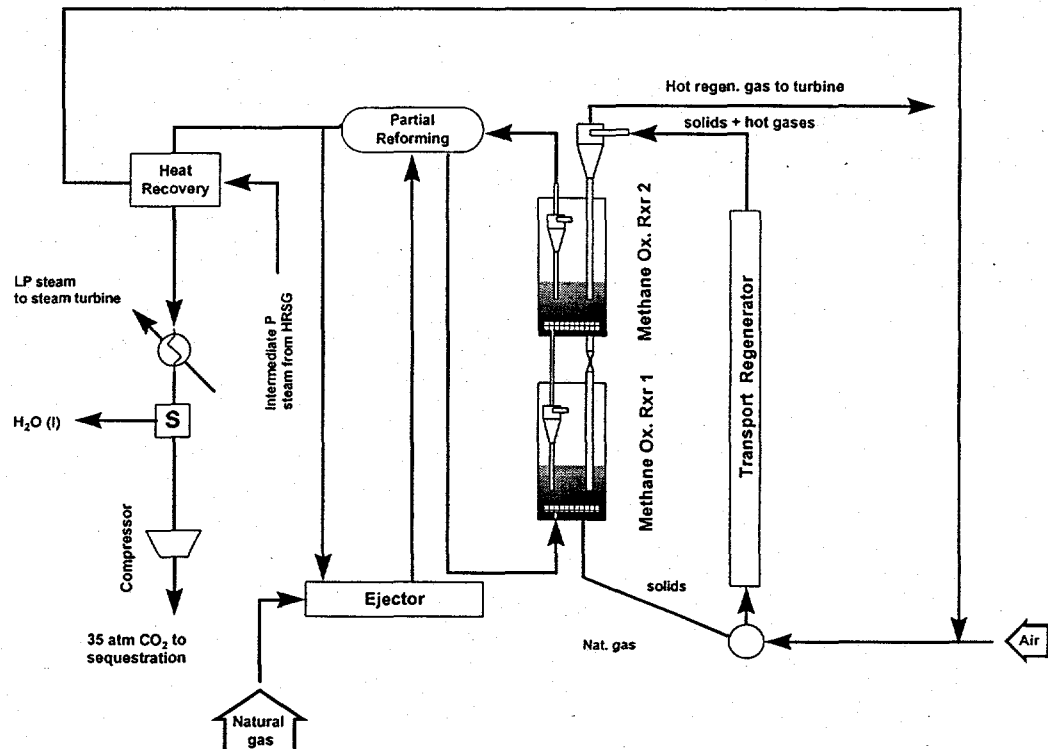


Figure 6-2. Process flow diagram showing the use of stationary fluidized bed reactors for natural gas oxidation.

Because the kinetics of sorbent reduction and regeneration are not known at this time, we have made our preliminary design calculations based on gas and solid flow rates only, with the expectation that an average residence time of at least two seconds (in the transport reactor designs) should be sufficient for both the reduction and regeneration reactions to go to completion. In both cases, we chose to use a transport reactor for the sorbent regeneration step because of the high gas throughput rate (the product gas goes to the gas turbine for power generation) and large exothermic heat of sorbent oxidation (from FeO and Cu to Fe_2O_3 and CuO).

Table 6-5. Results of preliminary design calculations.

	Transport regenerator (airreduction/ sorbent oxi- dation	Transport reactor for methane oxidation/sor- bent reduction)	Stationary fluidized bed (reactor 1)	Stationary fluidized bed (reactor 2)
Gas flow rate (kg/s)	415	52.0	47.8	52.0
Gas flow rate (m ³ /s)	61.1	14.7	12.7	14.7
Solid flow rate (kg/s)	267	284	267	284
T (K)	1089	1206	1089	1206
P (atm)	13.5	13.5	13.5	13.5
Design velocity (m/s)	12.5	12.5	0.98	0.98
Reactor Diameter (m)	2.49	1.22	4.06	4.35
Reactor height (m)	25	25	10.7*	10.9
Height/diameter ratio	10.1	20.5	0.33 (bed)	0.33 (bed)
Reactor Volume (m ³)	122	29.3	139	162
Solids inventory (kg)	535	567	34,700	42,800
Gas residence time (sec)	2.0	2.0	10.2	10.3
Solids residence time (sec)	2.0	2.0	132	155

6.4.1. Transport Sorbent Oxidation

The upper limit of the operating velocity in the transport reactor is determined by mechanical limitations of the sorbent and equipment considerations such as erosion. We used FCC riser cracker operating parameters and physical dimensions to guide us in determining feasible vessel sizes, residence times and gas velocities because FCC is proven technology (Sadeghbeigi 1995; Froment and Bischoff 1990).

The first column in Table 6-5 summarizes the design of the sorbent regenerator. For these and the other calculations, we assumed a average particle size (d_p) of 88 μm , a particle density of 3800 kg/m^3 , a particle sphericity (ϕ) of 0.8 and a void fraction at minimum fluidization (ϵ_{mf}) of 0.5. Gas transport properties (viscosity etc.) were calculate using methods outlined by Reid et al. (1987). Compressibility factors for all gas mixtures were $Z > 0.95$ so the ideal gas law was used to calculate the density at pressure. The operating parameters used in the calculations are given in Table 6-6.

Table 6-6. Operating conditions for transport regeneration reactor (P = 13.5 atm).

REGENERATION REACTOR	Units	C_p (J/gmol-K)	Density (kg/m ³)	Viscosity (kg/m-s)
Air mass flow rate	397 kg/sec	31.13	6.94	3.9E-05
Steam mass flow rate	17.54 kg/sec	39.63	3.30	2.9E-05
		Ave (C_p)	Ave. density	Ave. viscosity
Total flow rate of gas	414.54 kg/sec	31.49	6.79	3.9E-05
Volumetric gas flow	61.075 m ³ sec			
Solid properties				
Solids flow rate at	266.9 kg/sec			
Temperature	816 °C			
Epsilon min fluid	0.5			
Particle size	88 μm			
Particle density	3800 kg/m ³			
Sphericity	0.8			

The terminal velocity was calculated for particles in the size range expected for sorbent used in this system. The terminal velocities for particles with diameters between 40 μm and 150 μm were 0.07 m/s to 0.58 m/s (using average fluid density and viscosity for the gas streams (Kunii and Levenspiel 1991). An operating velocity of 12.5 m/s therefore represents from 22 to 180 times the terminal velocity of the sorbent particles. The minimum velocity needed for pneumatic transport is about 1.6 m/s (Perry et al. 1984). Using an operating velocity of 12.5 m/s and a gas flow rate of 61.1 m³/s, the diameter of the reactor is 2.49 m. A residence time of 2.0 sec can be obtained by using a 25 m tall reactor. These dimensions are similar to the dimensions of riser reactors used in fluid catalytic cracking (FCC) in petroleum refining and are thus reasonable (Sadeghbeigi 1985). The primary difference between our application and FCC is that FCC operates at 2 - 3 atm, whereas we will operate at about 13.5 atm. At 13.5 atm, the required wall thickness of the cylindrical reactor body is about 20 mm using a conservative 25% of the yield stress of stainless steel at 705°C ($\sigma_{hoop} = 206$ MPa) (Baumeister et al. 1978).

6.4.2. Stationary Fluidized Bed Reactors for Sorbent Regeneration

In our initial process layout we suggested the use of stationary, staged fluidized bed reactors for oxidation of the natural gas by hot sorbent (the sorbent is reduced to a mixture of Cu metal and FeO). Calculations of reactor size made using the mass balances for gas and solids indicate that while this type of reactor would work, a large inventory of solids is required for operation, which would lead to unacceptably long residence times for the sorbent. The operating parameters used in the calculations made for the stationary fluidized bed reactors are given in Table 6-7.

Table 6-7. Operating conditions for staged fluidized bed reactors for natural gas oxidation (sorbent reduction); P = 13.5 atm.

Bed	Temp (K)	Flow rate (kg/s)	Flow rate (m ³ /s)	C _p (J/gmol-K)	Density (kg/m ³)	Viscosity (kg/m-sec)
REACTOR 1						
Gas IN	873.15	31.18	7.13	49.07	4.37	3.36E-05
Gas OUT	1089.15	47.80	12.74	49.08	3.75	4.22E-05
Solids IN	1206.15	283.50				
Solids OUT	1089.15	266.90				
REACTOR 2						
Gas IN	1089.15	47.80	12.74	49.08	3.75	4.22E-05
Gas OUT	1206.15	51.95	14.67	47.82	3.54	4.52E-05
Solids IN	1173.15	287.70				
Solids OUT	1206.15	283.50				

Table 6-5 lists the results for both reactors 1 and 2. Most of the natural gas conversion occurs in reactor 1 by reduction of Fe₂O₃ to FeO by CH₄. Because of equilibrium limitations the product gas exiting reactor 1 contains about 3 % CO. When this gas contacts the copper containing component of the sorbent in reactor 2, the CO is fully oxidized to CO₂, and CO₂ and H₂O are the only products exiting reactor 2.

In industrial stationary fluidized bed reactors it is common to operate above the terminal velocity of the particles in the bed because internal cyclones can be added to return the solids back to the reactor vessel (Matsen et al. 1985). Thus, the limit on the fluidization velocity is set mostly by the capacity of the cyclones in the overall reactor vessel, as long as attrition of the particles and similar factors are acceptable (Matsen et al. 1985).

Again using FCC as a guideline, we chose an operational velocity of about 1 m/s (similar to FCC catalyst regeneration) and assumed that an internal cyclone assembly would be present to prevent loss of sorbent. The presence of these internals is represented schematically in Figure 6-2. The reactors were designed based on outlet conditions because the outlet has the largest gas flow rate. Reactors 1 and 2 have essentially the same dimensions, and because of this, could be combined in one pressure vessel in a staged design as discussed in the literature (Kunii and Levenspiel 1991). The shortest gas residence time (because outlet conditions were used) is about 10 sec (Table 6-5). The solids residence times are on the order of 2 min which is expected to be unacceptably long. Also, for a bed geometry of bed depth = 1/3 bed diameter (similar to FCC regeneration), the sorbent inventory becomes 35 tonne for reactor 1 and 43 tonne for reactor 2. These large solids inventories increase the residence time of the solids in the vessels and add extra requirements for the support structures of the loaded vessels which increases capital costs. From these calculations we

conclude that the use of stationary fluidized bed reactors for the natural gas-sorbent contacting will probably be unsatisfactory.

6.4.3. Transport Reactor for Natural Gas - Sorbent Contacting (Sorbent Reduction)

Because of the large solids inventories and residence times for stationary fluidized bed reactors, we performed calculations to determine if a transport reactor would be feasible for this part of the process. As expected the resulting dimensions of the reactor were similar to those of the regeneration reactor, except that the diameter of the reduction reactor is smaller because of the lower gas flow rate. For a design velocity of 12.5 m/s the reactor diameter becomes 1.22 m. A 25 m tall reactor gives a residence time of about 2 sec. Importantly, the solids inventory in the transport reactor for sorbent reduction (natural gas oxidation) is only 567 kg (which corresponds to a solids concentration in the reactor volume of 19 kg/m³). These calculations suggest that the best approach for the sorbent reduction and regeneration is likely to be the use of two transport reactors (or at least fast fluidized bed reactors).

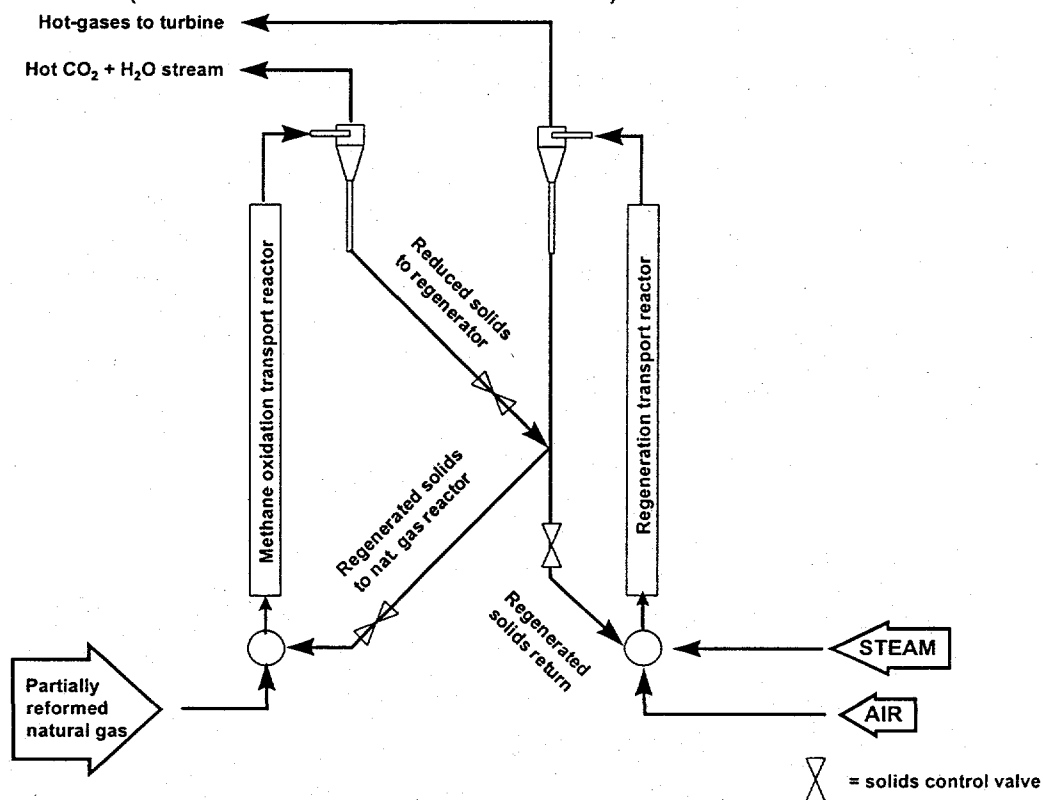


Figure 6-3. Process using transport reactor for natural gas oxidation.

In Figure 6-3 we show a simplified scheme using two transport reactors. Steam and air are fed to the regenerator which entrain the reduced sorbent, and as the sorbent and air flow up the reactor, the sorbent is reoxidized. The solids and gas are separated in a cyclone (or series of cyclones) and the hot gases (ca 900°C) go on to the gas turbine for power generation. The solids stream from the cyclone is split into a stream that returns to the transport reactor (recycle) and a

stream that goes to the reactor where natural gas is oxidized. Natural gas contacts oxidized sorbent forming CO_2 , H_2O , and reduced sorbent which are then separated in a cyclone assembly. The solids from the cyclone go to the regenerator and the hot CO_2 and H_2O gas stream goes to heat recovery, H_2O removal, and finally CO_2 sequestration (see Figure 6-3). One advantage of the dual transport reactor process is the ability to adjust the solids contact times in each reactor by controlling the relative solids flow rates which increases the flexibility of the process. Also, the size of the equipment is minimized by the dual transport design (relative to using staged stationary fluidized bed reactors).

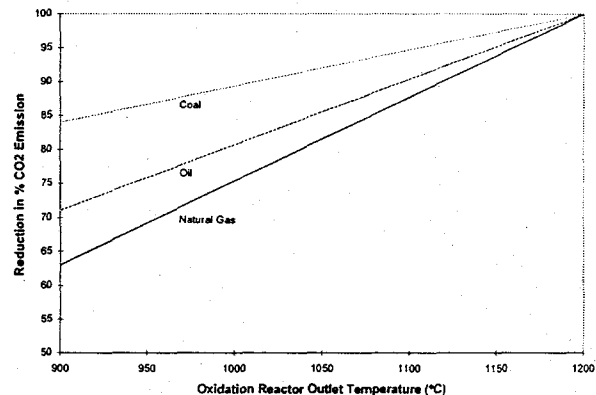
6.4.4. Conclusions

Our preliminary design calculations suggest that the best approach for indirect natural gas combustion for CO_2 emissions control is to use a transport reactor for contacting the natural gas with hot oxidized sorbent, and to use a transport reactor to regenerate the sorbent. Such a system provides maximum flexibility, simplifies the process equipment and eliminates potentially harmful effects of excessively long residence times for the solids.

7. Impact

In combination with commercially available Combined Cycle power generation technology, the Sorbent Energy Transfer System (SETS) has the potential to drastically reduce or eliminate CO₂ emissions with only a 2.5% efficiency penalty (5% fuel increase) for CO₂ capture and a 10% increase in the cost of generated electricity (accounting for both the increased capital cost and reduced generation efficiency).

The SETS technology is applicable to any fossil fuel. The degree of CO₂ reduction achieved by SETS is determined by the fuel that is used and the state of the art in barrier filter technology. The degree of CO₂ reduction that can be achieved with coal, oil and natural gas as a function of the oxidation reactor outlet temperature is shown in Figure 7-1. Savings are greatest with coal,

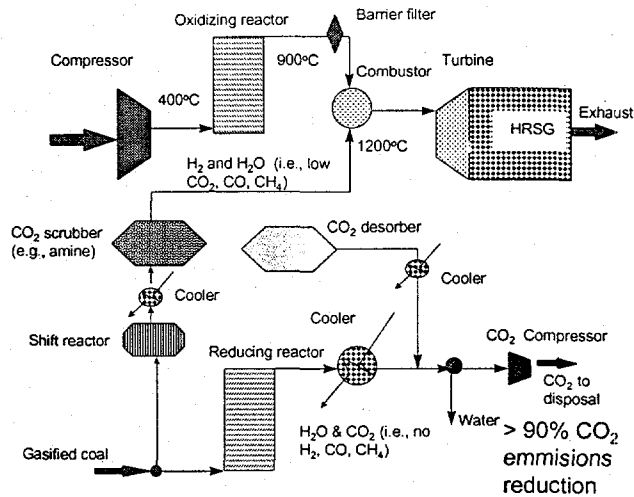


followed by oil and natural gas simply because coal has the highest C/H ratio and natural gas

has the lowest, and conventional coal burning systems therefore emit more CO₂ per kWh generated than oil or gas. As discussed earlier, the modern, high efficiency gas turbines have air inlet temperatures of 1093 to 1371°C (2000 to 2500°F). Assuming a turbine inlet temperature of 1200°C (which is the temperature of a General Electric Frame 7A gas turbine/combined cycle), the amount of fuel which must be burned to bring the air temperature to the optimum turbine inlet temperature is set by the maximum operating temperature of the particulate filters that keep trace amounts of the sorbent from being carried into the expander (not by any limitation of our sorbents). Current filters have maximum operating temperatures of 900°C, and filters capable of operation at up to 1360°C are being researched. For a given maximum filter temperature, the reduction in CO₂ emissions (compared to an identical combined cycle running on and identical fuel) are greatest for gasified coal. For a 900°C outlet temperature from the oxidation reactor, the reduction in CO₂ emissions over the standard combined cycle are 84% for gasified coal, 71% for oil, and 63% when operating on natural gas. Of course, if a 1200°C particulate filter is developed, no supplemental fuel would be needed to bring the air to the optimum turbine inlet temperature, and the reduction in CO₂ emissions would be 100% in all cases (the operating temperature of the bed is limited only by the maximum operating temperature of the filters, not by the performance of the metal oxide).

7.1. Complete Removal of CO₂ with Current Technology Barrier Filters

Although in the long run the development of improved (higher operating barrier filters) will eliminate all CO₂ emissions from SETS system, we could use a standard amine based CO₂ scrubbing system to recover the CO₂ emitted because of our wish to raise the hot gas from 900°C to 1200°C before it enters the turbine. Unfortunately those



system increase fuel consumption by the 13-17% (Herzog and Drake 1993) with current technology and 9% with advanced technology (Herzog and Drake 1993)(versus 5% with SETS). However, we could use that approach to separate CO₂ from gasified coal to achieve near 100% CO₂ capture without an improved barrier filter.

This system is shown in Figure 7-2. The amine based system does reduce the efficiency of the SETS system. However, since the gas stream is only about one third the previous case, the loss due to the amine system is only one third of what it was. However, the efficiency loss of the combined SETS/amine system is less than the amine alone but that system is still substantially higher than SETS with improved barrier filters.

7.2. Estimated CO₂ Capture by SETS

While the added capital cost of our SETS facility is not particularly large, the system is physically large. Therefore, like most or all new power cycles and cycle modifications, it is more likely to be used in new facilities than as a retrofit to older facilities. Of course, if the demands for greenhouse gas reduction become more severe, SETS systems could be installed on any combined cycle power plant, whether fueled by coal, oil or natural gas and can be retro-fitted into many existing power plants. For this analysis we simply assume that only new plants will use SETS.

The installed bases of electrical generation capacity in the US is 762,408 MW (1994). While it is impossible to accurately forecast growth rates for electrical generation capacity one to three decades in the future, if we assume a 2% annual growth rate and implementation beginning 15 years from now, the total annual market for new generation technology in the US (and therefore the annual US market for SETS/Combined Cycle systems) will be 20,000 MW/year.

One years production from 20,000 MW releases about 51 million tons of CO₂, by conservatively assuming a 50% LHV natural gas fired combined cycle (i.e., the lowest carbon content fossil fuel). If the production occurred all in coal, about 90 million tons of CO₂ per year would be emitted. For 10 years of growth in the power generation industry (i.e., 200,000 MW added releasing 510 million tons of CO₂ per year in the 10th year) during the 10 year period about 2,500 million tons of CO₂ from natural gas (4,400 million tons with coal) would be emitted into the atmosphere.

Assuming a nominal 200 MW combined cycle power plant, about 100 plants would added each year, at the above assumed growth rate. Since fossil fuels cost less than alternative energy (e.g., solar, nuclear), and fossil fuels can be sited anywhere in the USA, these plants would be constructed to use fossil fuel, unless the greenhouse taxes force the use of an alternative source. For a ten year period the assumed growth rate would add 1,000 plants to the power generation capacity of the USA. Since SETS can function with any fossil fuel source, the 1,000 plants could all be constructed to capture CO₂.

By incorporating SETS plants with improvements in high temperature filters, those 1,000 power plants, which could be sited anywhere in the USA, would capture the entire 2,500 million tons of CO₂. If the CO₂ capture is required before the development of new barrier filters, SETS still captures 1,700 million tons (or more if oil or gasified coal fired). The applications of SETS to CO₂ is therefore available in the near term with only the development of the appropriate SETS sorbents and the demonstration of the technology, since all other portions of SETS are already in commercial practice.

7.3. Conclusions

In combination with commercially available Combined Cycle power generation technology, the Sorbent Energy Transfer System (SETS) has the potential to drastically reduce or eliminate CO₂ emissions with small energy penalty for CO₂ capture and a 10% increase in the cost of generated electricity (accounting for the increased capital cost and reduced generation efficiency).

While the added capital cost of our SETS facility is not particularly large, the system is physically large. Therefore, like most or all new power cycles and cycle modifications, it is more likely to be used in new facilities than as a retrofit to older facilities. Of course, if the demands for greenhouse gas reduction become more severe, SETS systems could be installed on any combined cycle power plant, whether fueled by coal, oil or natural gas.

The installed bases of electrical generation capacity in the US is 762,408 MW (1994). While it is impossible to accurately forecast growth rates for electrical generation capacity one to three decades in the future, if we assume a 2% annual growth rate and implementation beginning 15 years from now, the total annual market for new generation technology in the US (and therefore the

annual US market for SETS/Combined Cycle systems) will be 20,000 MW/year or about \$1,000,000,000 per year for the SETS at \$50/kW_e.

The SETS technology is applicable to any fossil fuel. The degree of CO₂ reduction achieved by SETS is determined by the fuel that is used and the state of the art in barrier filter technology. Savings are greatest with coal, followed by oil and natural gas simply because coal has the highest C/H ratio and natural gas has the lowest, and conventional coal burning systems therefore emit more CO₂ per kWh generated than oil or gas. By incorporating SETS, fossil fueled plants, which could be sited anywhere in the USA, would capture about 2,500 million tons of CO₂ in the first 10 years after introduction. If the CO₂ capture is required before the development of new barrier filters, SETS still captures 1,700 million tons in ten years (or more if oil or gasified coal fired).

TDA has used relatively conservative estimates for the performance of the sorbent, the cost of the system, the cost of money and greenhouse taxes. Even with these assumptions the estimate cost for SETS can less than paying carbon taxes. Given the current high cost to separate CO₂ the SETS approach offers a very viable alternative which will allow the continue use of fossil fuels, natural gas, oil, and coal even when greenhouse gas emissions are tightly controlled.

8. References

- Albanese A.S. and M. Steinberg, *Environmental Control Technology for Atmospheric Carbon Dioxide*, DOE/EV-0079, Brookhaven National Laboratory, Brookhaven, NY (1980).
- Baumeister, T., Avallone, E.A., and Baumeister III, T., (1978) *Mark's Standard Handbook for Mechanical Engineers*, 8th ed., McGraw Hill.
- Cullity, B.D. (1956) *Elements of X-Ray Diffraction*, Addison-Wesley Publishing.
- Eggersted, P.M. (1995). "Lightweight Ceramic Filter Components: Evaluation and Application" in *Proceedings of the Advanced Coal-Fired Power Systems '95 Review Meeting*, Morgantown, West Virginia: U.S. Department of Energy Morgantown Energy Technology Center, Report No. DOE/METC-95/1018 (DE95009732).
- Froment, G.F. and Bischoff, K.B. (1990) *Chemical Reactor Analysis and Design*, 2nd ed. Wiley.
- Herzog H., E. Drake, J. Tester and R. Rosenthal, *A Research Needs Assessment for the Capture, Utilization, and Disposal of Carbon Dioxide from Fossil Fuel-Fired Power Plants*, DOE/ER-30194, U.S. Department of Energy, Washington, DC (1993).
- Herzog H.J. and E.M. Drake, *Long-Term Advanced CO₂ Capture Options*, IEA/93/0E6, IEA Greenhouse Gas R&D Programme, Cheltenham, UK (1993).
- Herzog H.J., E. Adams, D. Auerbach and J. Caulfield, *Technology Assessment of CO₂ Ocean Disposal*, Report 95-001, MIT Energy Laboratory, Cambridge, MA (1995).
- Herzog, H. et al. (1996), *Energy Conv. Mgmt.* 37, 999.
- Ishida, M. and H. Jin (1994). *J. Chem. Engng. Japan*, 27, 296.
- Ishida, M. et al. (1987). *Energy*, 20, 147.
- Ishida, M. et al. (1996). *Energy and Fuels*, 10, 958.
- Kirkpatrick, M. and R. Pike (1994). *AIChE Symposium Series*, Vol. 90, No. 298.
- Kunii, D. and Levenspiel, O. (1991) *Fluidization Engineering*, 2nd ed. Butterworth-Heinemann.
- Lippert, T.D., G.J. Bruck, Z.N. Sanjana, and R.A. Newby. (1995). "Westinghouse Advanced Particle Filter System" in *Proceedings of the Advanced Coal-Fired Power Systems '95 Review Meeting*, Morgantown, West Virginia: U.S. Department of Energy Morgantown Energy Technology Center, Report No. DOE/METC-95/1018 (DE95009732).
- Marchetti C, "On Geoengineering and the CO₂ Problem", *Climatic Change* 1(1), pp. 59-68 (1977).
- Matsen, J.M., Rossetti, S.J. and Halow, J.S. (1985) "Fluidized Beds and Gas Particle Systems," in *Encyclopedia of Chemical Processing and Design*, vol 23, Marcel Dekker.
- Mimura T., H. Simayoshi, T. Suda, M. Iijima and S. Mituoka, "Development of Energy Saving Technology for Flue Gas Carbon Dioxide Recovery by Chemical Absorption Method and Steam System in Power Plant", *Energy Convers. Mgmt.*, in press (1997).
- Misra, C. (1986) *Industrial Alumina Chemicals*, ACS Monograph 184, American Chemical Society.

- Mudd, M.J. and J.D. Huffman. (1993). "Initial Operation of the Tidd PFBC Hot Gas Clean Up Filter, *Advanced Coal-Fired Power Systems '93 Review Meeting*, Morgantown, WV: U.S. Department of Energy Morgantown Energy Technology Center, Report No. DOE/METC-93/6131 (DE93000289).
- Perry, R.H., Green, D.W. and Maloney, J.O eds. (1984) Perry's Chemical Engineers' Handbook, 6th ed. McGraw Hill.
- Reid, R.C., Prausnitz, J.M., and Poling, B.E. (1987) The Properties of Liquids and Gases, 4th ed. McGraw Hill.
- Richter, H. and K. Knoche (1983). In *Efficiency and Costing*, ACS Symposium Series 235.
- Sadeghbeigi, R. (1995) Fluid Catalytic Cracking Handbook, Gulf Publishing.
- Smelser, S. and G. Booras (1991). *Energy* 16, 1295.
- Steinberg M., "Production of Hydrogen and Methanol from Natural Gas with Reduced CO Emission", *Hydrogen Energy Progress XI*, Proc. of the 11th World Hydrogen Energy Conf., Stuttgart, 1, pp. 499-510 (1996).
- Steinberg M., *An Analysis of Concepts for Controlling Atmospheric Carbon Dioxide*,
- Weast (1981) Handbook of Chemistry and Physics, 62nd ed., CRC Press.

APPENDIX A Thermodynamic Data from Dr. D. Harrison of LSU

Dr. Doug Harrison, a professor of chemical engineering at Louisiana State University (LSU) consulted during the Phase I work. Dr. Harrison made three reports which reproduced in the following pages. The three reports are titled "Status Report: Greenhouse Project," "Status Report 2: GHG Project," and "Status Report 3: GHG Project."

"Status Report: Greenhouse Project" identifies the 77 elements considered for the redox reaction in SETS and presents data on the equilibrium of nickel and copper compounds during reduction by methane and oxidation by air.

"Status Report 2: GHG Project," presents data on the equilibrium of iron and manganese compounds during reduction by methane and oxidation by air.

"Status Report 3: GHG Project" presents data on the equilibrium of vanadium compounds during reduction by methane and oxidation by air.

Status Report

Greenhouse Gas Project

Oxides of the following metals were considered in the initial screening, some only momentarily:

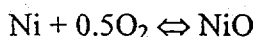
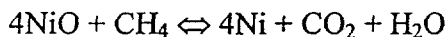
- | | | | |
|----------------|----------------|------------------|----------------|
| 1. Actinium | 21. Gadolinium | 41. Nickel | 61. Sodium |
| 2. Aluminum | 22. Gallium | 42. Niobium | 62. Strontium |
| 3. Americium | 23. Germanium | 43. Osmium | 63. Tantalum |
| 4. Antimony | 24. Gold | 44. Palladium | 64. Technitium |
| 5. Arsenic | 25. Hafnium | 45. Phosphorus | 65. Tellurium |
| 6. Barium | 26. Holmium | 46. Platinum | 66. Terbium |
| 7. Beryllium | 27. Indium | 47. Plutonium | 67. Thallium |
| 8. Bismuth | 28. Iodine | 48. Polonium | 68. Thulium |
| 9. Boron | 29. Iridium | 49. Potassium | 69. Tin |
| 10. Bromine | 30. Iron | 50. Praseodymium | 70. Titanium |
| 11. Cadmium | 31. Lanthanum | 51. Protactinium | 71. Tungsten |
| 12. Calcium | 32. Lead | 52. Radon | 72. Uranium |
| 13. Cerium | 33. Lithium | 53. Rhenium | 73. Vanadium |
| 14. Cesium | 34. Lutetium | 54. Rhodium | 74. Ytterbium |
| 15. Chromium | 35. Magnesium | 55. Rubidium | 75. Yttrium |
| 16. Cobalt | 36. Manganese | 56. Ruthenium | 76. Zinc |
| 17. Copper | 37. Mercury | 57. Samarium | 77. Zirconium |
| 18. Dysprosium | 38. Molybdenum | 58. Scandium | |
| 19. Erbium | 39. Neodymium | 59. Selenium | |
| 20. Europium | 40. Neptunium | 60. Silver | |

As expected, the oxides of nickel and copper, either singly or in combination, are strong candidates. The nickel reaction is clean, i.e., $\text{NiO} \leftrightarrow \text{Ni}$. Reduction of copper occurs stepwise. In the presence of excess CuO the reaction is $\text{CuO} \leftrightarrow \text{Cu}_2\text{O}$. Then $\text{Cu}_2\text{O} \leftrightarrow \text{Cu}$ if demand for oxygen still exists. The reaction of NiO with CH_4 is endothermic while the CuO-CH_4 reaction is exothermic so that mixing the two oxides provides the opportunity for increased flexibility in controlling reactor temperature. One potential problem with both is that formation of aluminates is thermodynamically favored.

Other possibilities identified at this time include chromium, cobalt, iridium, iron, manganese, molybdenum, rhodium, rubidium, tungsten, and vanadium. Obviously, several of these are impractical, but the thermodynamics appear reasonable. More detailed results from the nickel and copper analyses follow.

Nickel

The primary reactions are



With 100% excess NiO (8 mol NiO/mol CH₄), small amounts of carbon may be deposited at $T < 700^\circ\text{C}$ and small amounts of H₂ and CO may be formed throughout the temperature range of $400^\circ\text{C} \leq T \leq 1200^\circ\text{C}$. Results of HSC equilibrium calculations at these conditions are included as Attachment 1 (a), (b), (c), and (d).

The presence of Al₂O₃ favors the formation of NiO*Al₂O₃. HSC equilibrium calculations using initial conditions of 1 mol CH₄, 2.14 mols NiO, and 5.86 mols of NiO*Al₂O₃ are shown as Attachment 2 (a) and (b). The sorbent in this case corresponds to a 50% NiO/50% Al₂O₃ (by weight) mixture with 100% excess NiO as before. The equilibrium composition of the solid phase is more complex and contains (in decreasing amounts) Ni, NiO*Al₂O₃, Al₂O₃, NiO, and C. Of particular interest, the amount of equilibrium C is higher than in the case of no Al₂O₃. The amounts of H and CO in the equilibrium gas are also increased.

Results of three material and energy balance calculations around the reactor system are included as Attachments 3, 4, and 5.

The sorbent in Attachment 3 consists of 50%NiO/50% Al₂O₃ (by weight) but aluminate formation is not allowed. The sorbent circulation rate provides for 100% excess NiO and complete conversion of CH₄ to CO₂ and H₂O is assumed. Both reactors are adiabatic and the maximum system temperature is constrained to ≈ 900 C. The air feed rate to the regenerator required to satisfy the temperature constraint has been calculated. Resultant temperatures and flow rates of the streams are shown on the attachment. The air flowrate is 400% excess over the amount needed to oxidize all Ni to NiO.

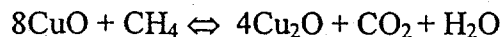
Attachment 4 shows the effect of changing the sorbent composition to 25% NiO/75% Al₂O₃ (by weight). This results in a tripling of the Al₂O₃ circulation rate. The air flowrate was maintained constant and the temperatures of both reactors were calculated. The increased Al₂O₃ circulation rate had a minimal effect on the regenerator, reducing the temperature from 896°C to 892°C , but had a significant effect on the main reactor, increasing the temperature from 746°C to 824°C .

Allowing for NiO*Al₂O₃ formation produced a small effect on the system energy balance as shown in Attachment 5. The conditions in this example are the same as in Attachment 3 except for aluminate formation. The regenerator temperature increased by

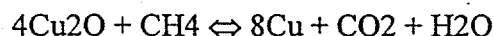
2°C, from 896°C to 898°C, while the main reactor temperature decreased by 10°C, from 746°C to 736°C.

Copper

Reduction of CuO occurs in stages. With excess CuO the primary reaction is



If additional oxygen is needed the Cu₂O is reduced by



During regeneration, most of the copper is oxidized to CuO either by



However, at high temperature some Cu₂O is stable even in an oxidizing atmosphere. Two copper aluminates, CuO*Al₂O₃ and Cu₂O*Al₂O₃, may be formed in the presence of alumina.

Equilibrium compositions as a function of temperature for 100% excess CuO (based on conversion to Cu₂O) and without Al₂O₃ are shown in Attachment 6 (a) and (b). CuO and Cu₂O are the only solid species formed, and decomposition of CuO with the appearance of some free O₂ begins at about 1000C. Oxidation of CH₄ to CO₂ and H₂O is complete throughout the temperature range. Reducing the amount of CuO to stoichiometric (again based on conversion to Cu₂O) eliminates the decomposition of CuO and the formation of O₂, while still resulting in complete oxidation of CH₄ to CO₂ and H₂O as shown in Attachment 7 (a) and (b).

Addition of Al₂O₃ and allowing the formation of copper aluminates complicates the equilibrium solid phase as shown in Attachment 8 (a) but has little effect on the gas phase (Attachment 8 (b)). The initial mixture contains 100% excess CuO and O₂ appears in the gas at about 1000C as in the case of Attachment 6. The solid phase contains (in decreasing amount) Al₂O₃, CuO, CuO*Al₂O₃, Cu₂O*Al₂O₃, and Cu₂O.

Material and energy balance results for three cases involving copper sorbents are presented as Attachments 9, 10, and 11.

The first case (Attachment 9) utilizes a sorbent containing 50%CuO/50%Al₂O₃ (by weight) but with aluminate formation not allowed. 100% excess copper (based on CuO to Cu₂O) is added to the CH₄. Complete conversion of CuO to Cu₂O in the primary reactor and of Cu₂O to CuO in the regenerator is assumed. The flow rate of air

to the regenerator needed to produce the maximum system temperature at ≈ 900 C has been calculated. 500% excess air is required. Note that the maximum temperature of 892 C is now associated with the primary reactor, opposite the situation with nickel where the maximum temperature is in the regenerator.

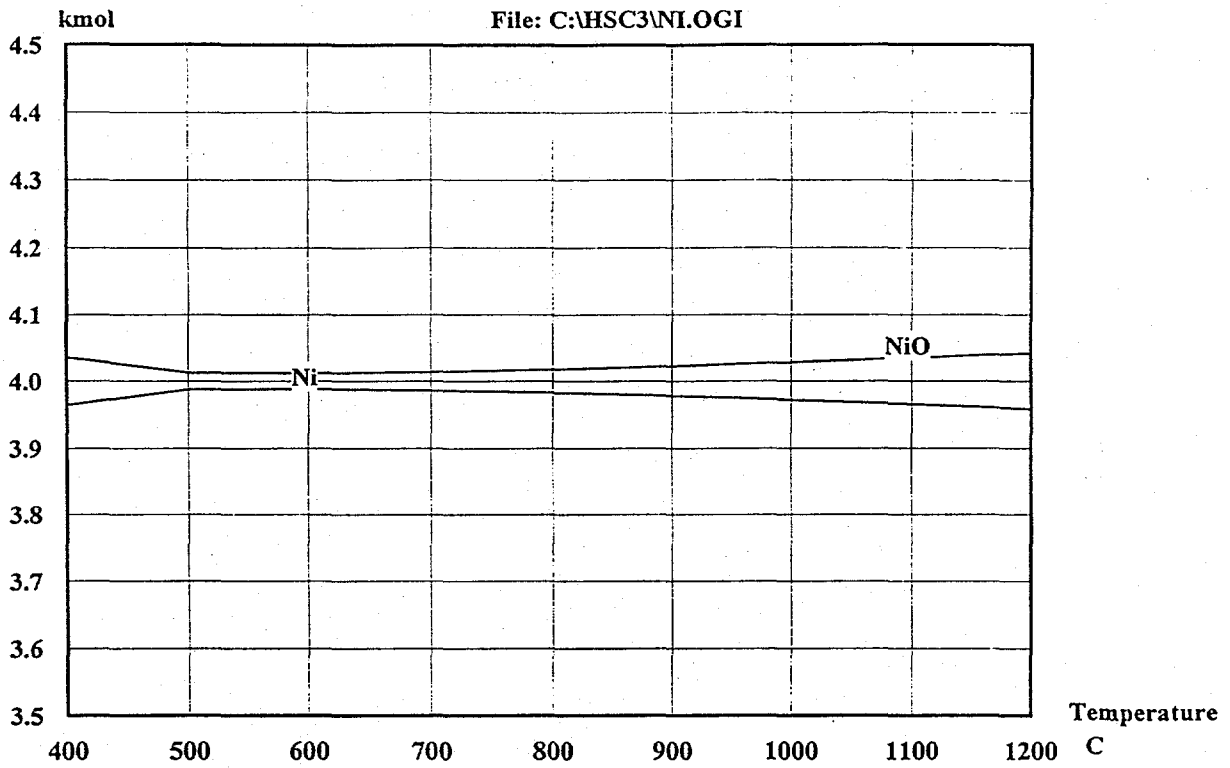
In Attachment 10, the copper content of the sorbent is reduced to 30%(by weight). This increases the circulation rate of Al_2O_3 and tends to equalize the temperatures in the two reactors. The air flow rate was decreased to 450% excess to satisfy the maximum temperature constraint. Complete conversion of CuO to Cu_2O in the primary reactor and of Cu_2O to CuO in the regenerator were assumed.

Attachment 11 shows results of a more complex case in which copper aluminate formation is permitted. The solid feed to the primary reactor and regenerator contains CuO , Cu_2O , $CuO \cdot Al_2O_3$, $Cu_2O \cdot Al_2O_3$, and Al_2O_3 with the quantities corresponding to equilibrium at 900C. The total copper is 100% excess of the amount required for complete conversion of CuO to Cu_2O , and the proportions of CuO and Al_2O_3 correspond to a 50-50 mixture by weight. The case is equivalent to that in Attachment 9 except that aluminate formation is allowed. The resulting temperatures are significantly different.

Copper-Nickel Mixture

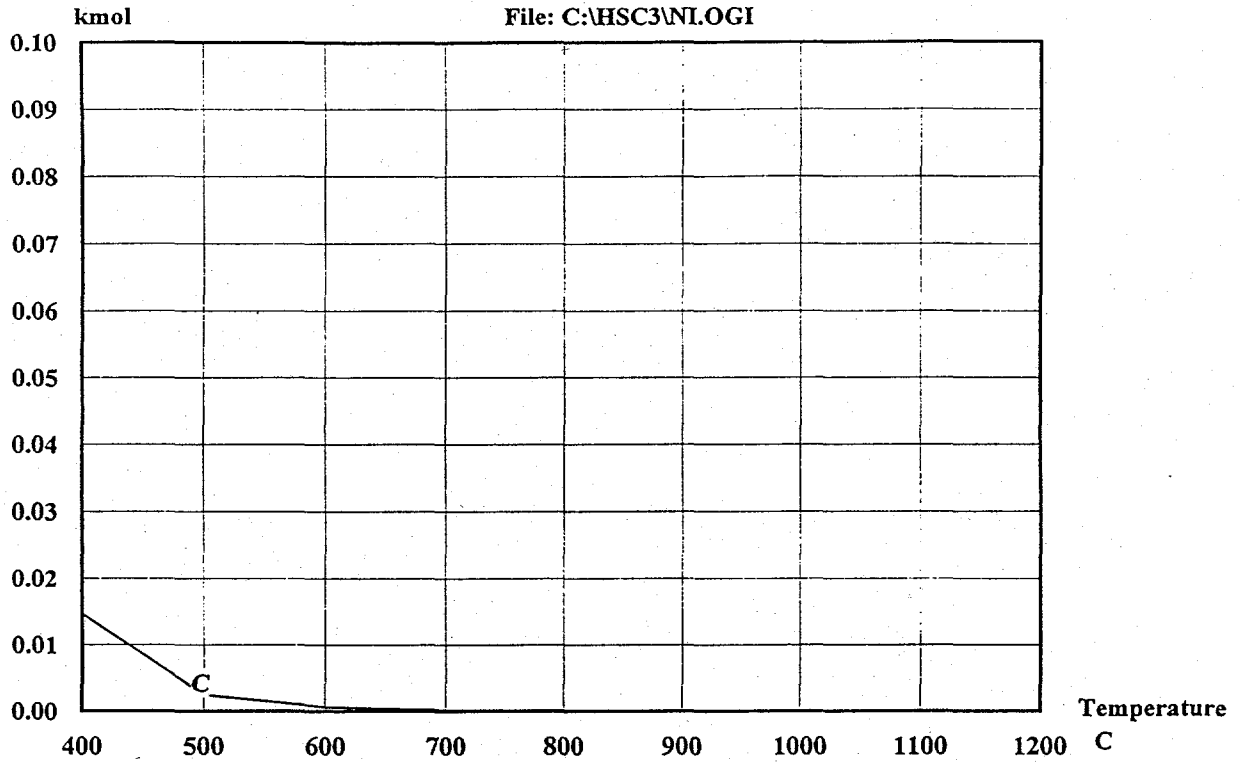
Combining the exothermic $CuO-CH_4$ and endothermic $NiO-CH_4$ reactions provides additional flexibility in controlling reactor temperatures. If the proportions of Cu and Ni reacting can be controlled, it will be possible to operate both reactors at equal temperatures and the sorbent temperature will not change as it circulates between the primary reactor and regenerator. However, equilibrium calculations involving excess reactants are not possible. The $Cu-CH_4$ reaction is more strongly favored thermodynamically than the $Ni-CH_4$ reaction. Hence, if the initial system contains excess Cu , thermodynamic analysis will show that the $Cu-CH_4$ reaction will go to completion before any Ni begins to react.

An "isothermal" case using stoichiometric CuO plus NiO with both reactors operating at 900 C is illustrated in Attachment 12. No aluminate formation is permitted. These conditions can be achieved if 1.81 mol of NiO plus 2.19 mol of CuO (the amount of Al_2O_3 is not important) react to completion with 1 mol CH_4 , and if 9.7 mols or O_2 are used for regeneration. Results of equilibrium calculations at these conditions in Attachment 13 (a) and (b) shown that all Cu and most of the Ni would react. However, small amounts of NiO would remain and the equilibrium gas would also contain some H_2 and CO .



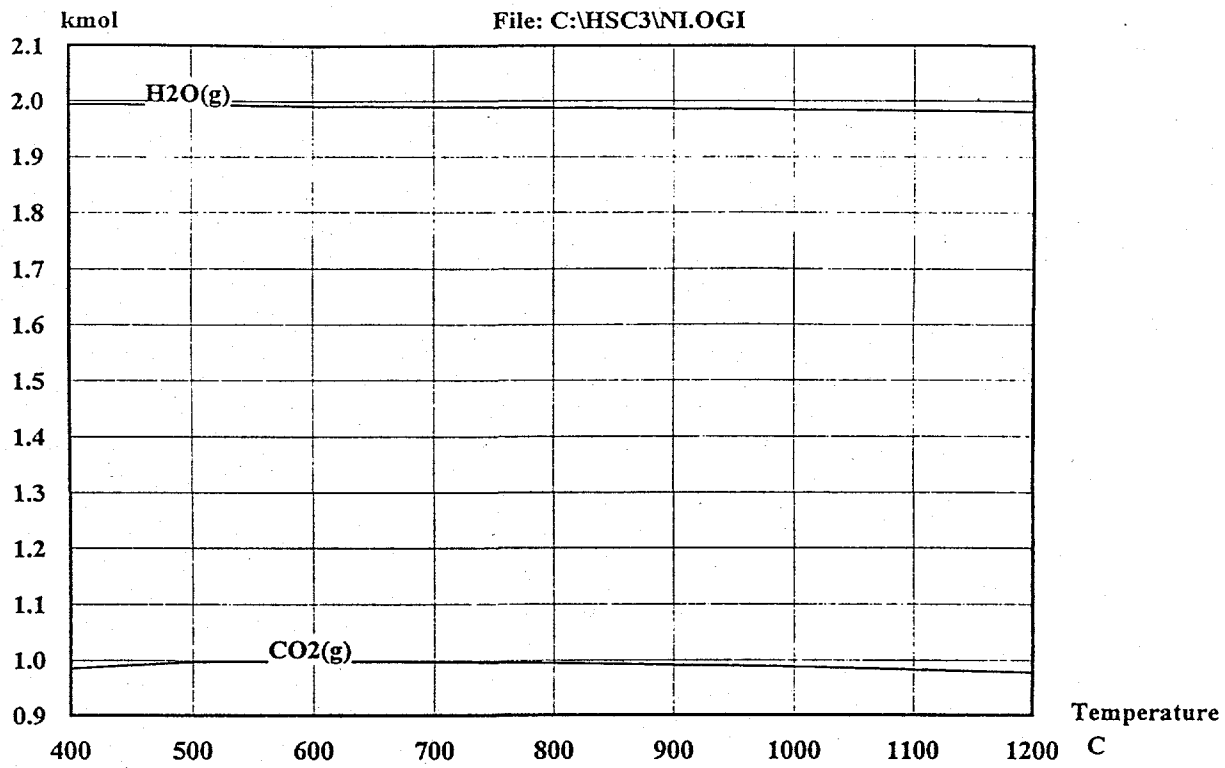
Temperature: 673.150 K
 Pressure: 15.000 bar
 Raw Materials: kmol
 CH4(g) 1.0000E+00
 NiO 8.0000E+00

Attachment 1 (a)



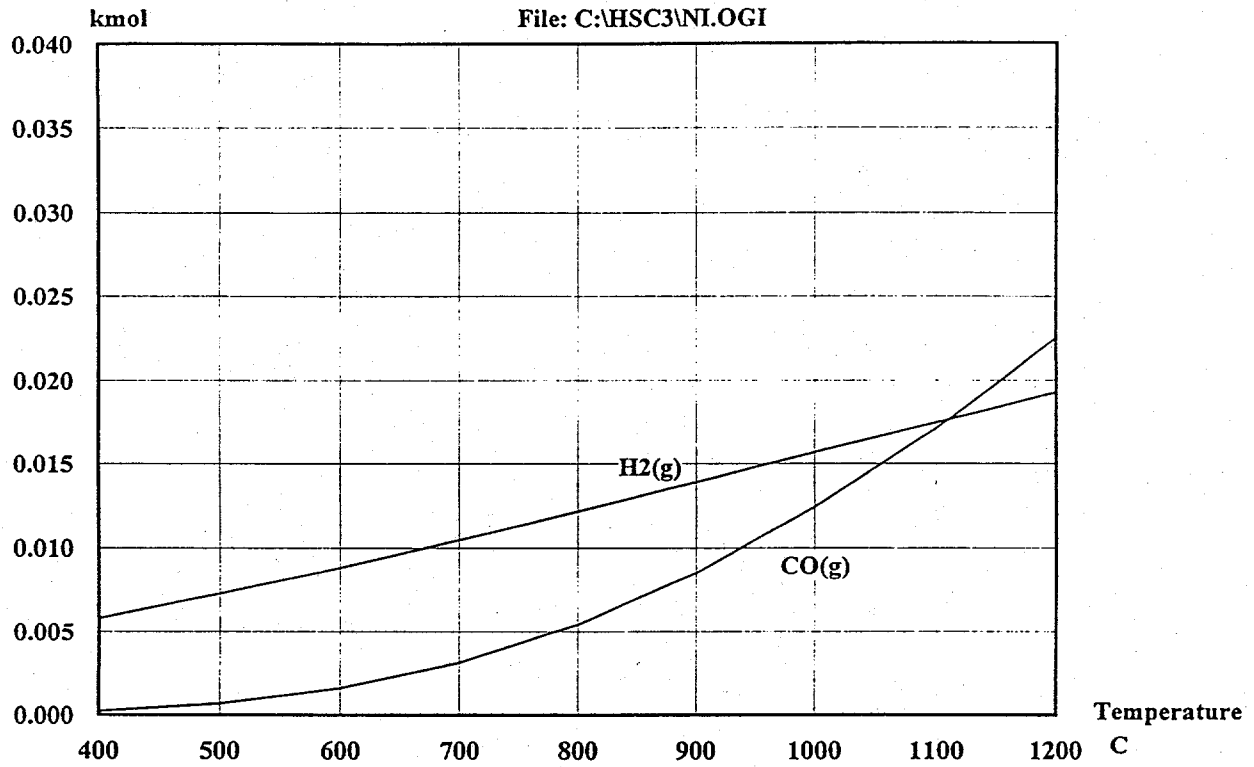
Temperature: 673.150 K
 Pressure: 15.000 bar
 Raw Materials: kmol
 CH₄(g) 1.0000E+00
 NiO 8.0000E+00

Attachment 1 (b)



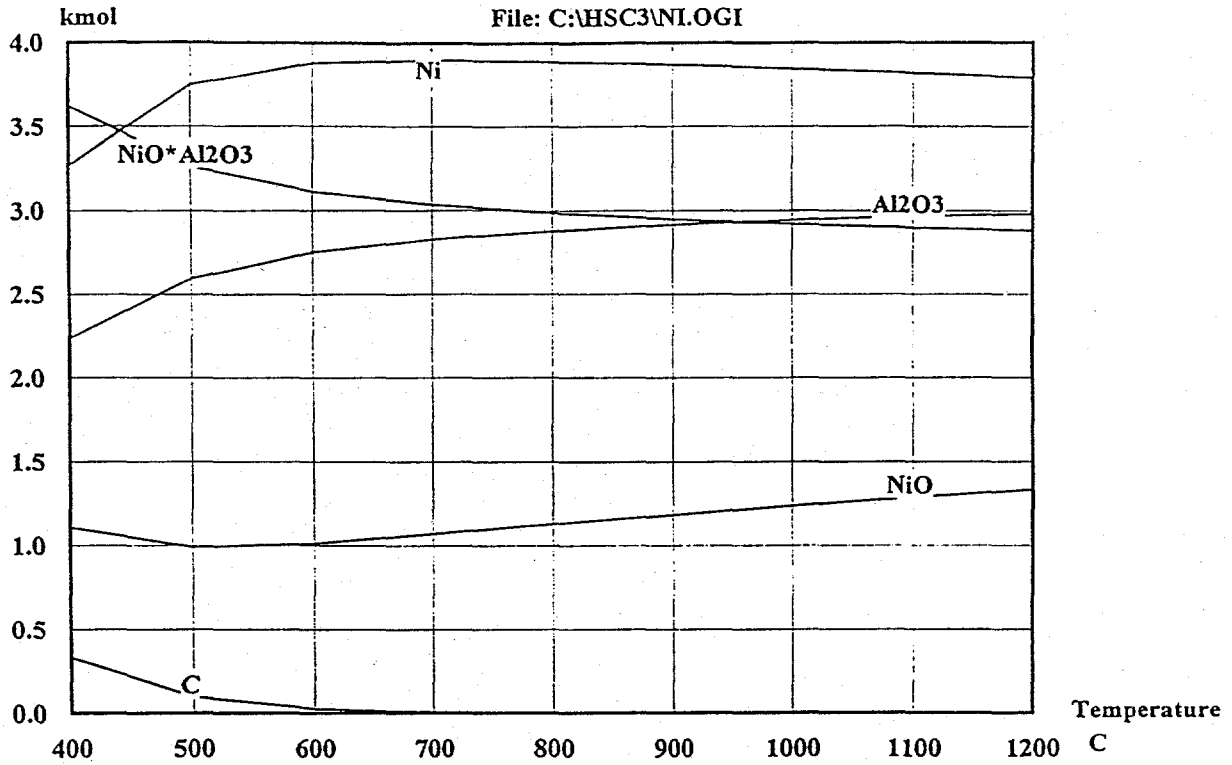
Temperature: 673.150 K
 Pressure: 15.000 bar
 Raw Materials: kmol
 CH₄(g) 1.0000E+00
 NiO 8.0000E+00

Attachment 1 (c)



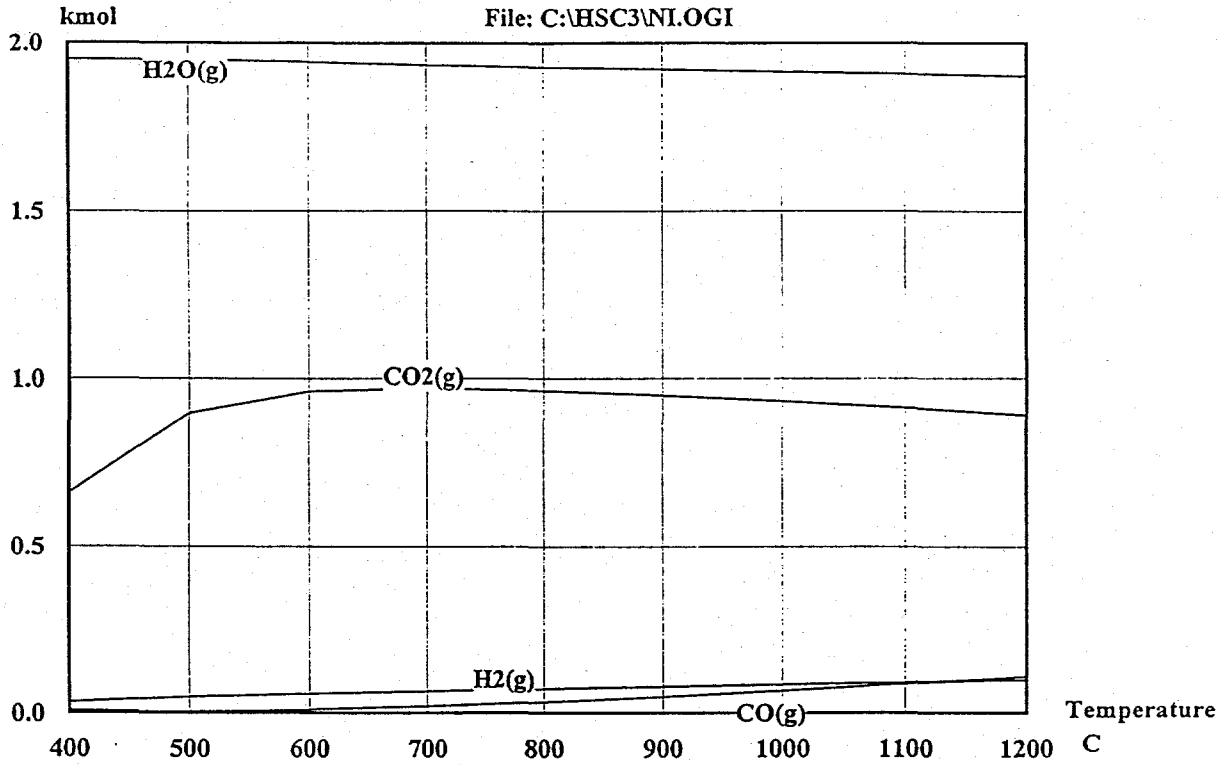
Temperature: 673.150 K
 Pressure: 15.000 bar
 Raw Materials: kmol
 CH₄(g) 1.0000E+00
 NiO 8.0000E+00

Attachment 1 (d)



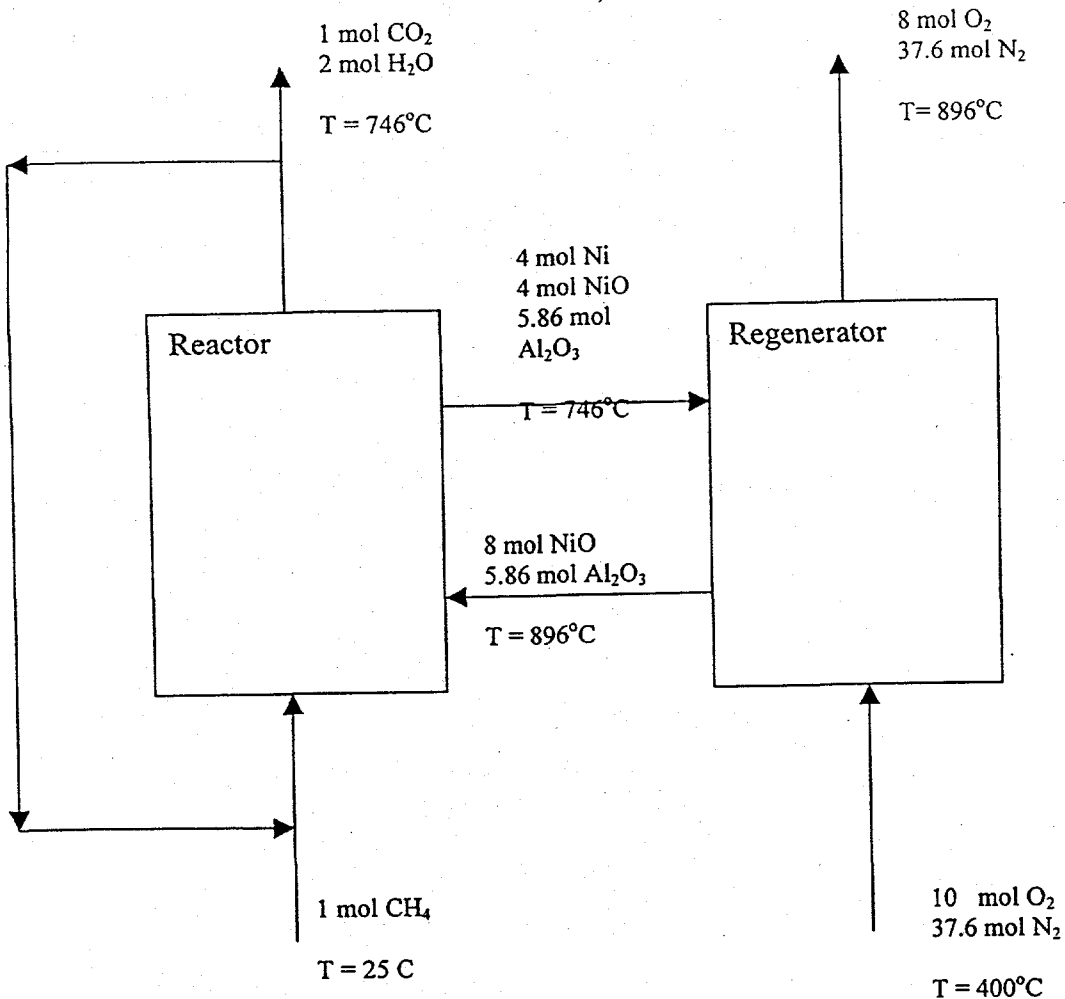
Temperature: 673.150 K
 Pressure: 15.000 bar
 Raw Materials: kmol
 CH₄(g) 1.0000E+00
 NiO 2.1400E+00
 NiO*Al₂O₃ 5.8600E+00

Attachment 2 (a)



Temperature: 673.150 K
 Pressure: 15.000 bar
 Raw Materials: kmol
 CH₄(g) 1.0000E+00
 NiO 2.1400E+00
 NiO*Al₂O₃ 5.8600E+00

Attachment 2 (b)



Attachment 3

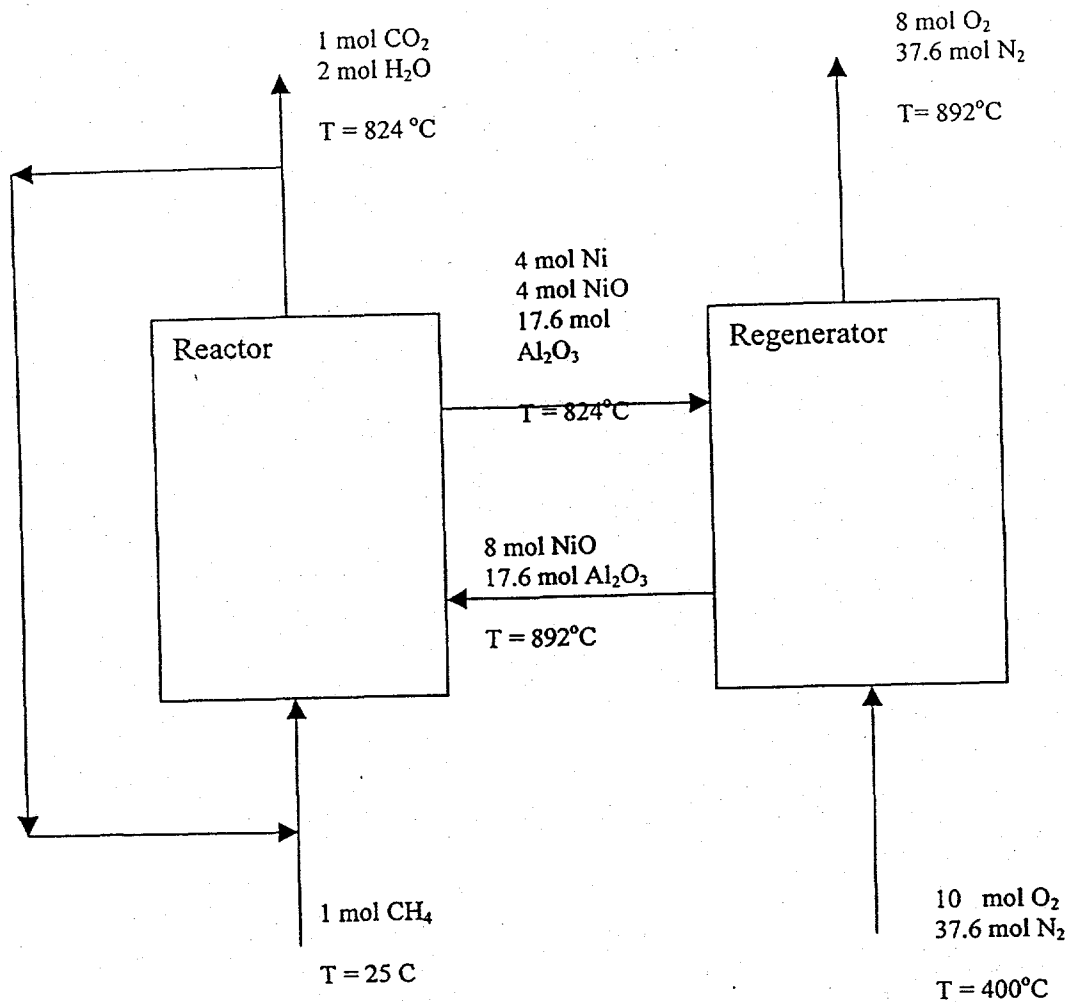
NiO Sorbent

50 % NiO/50% Al₂O₃ (wt)

100% excess NiO

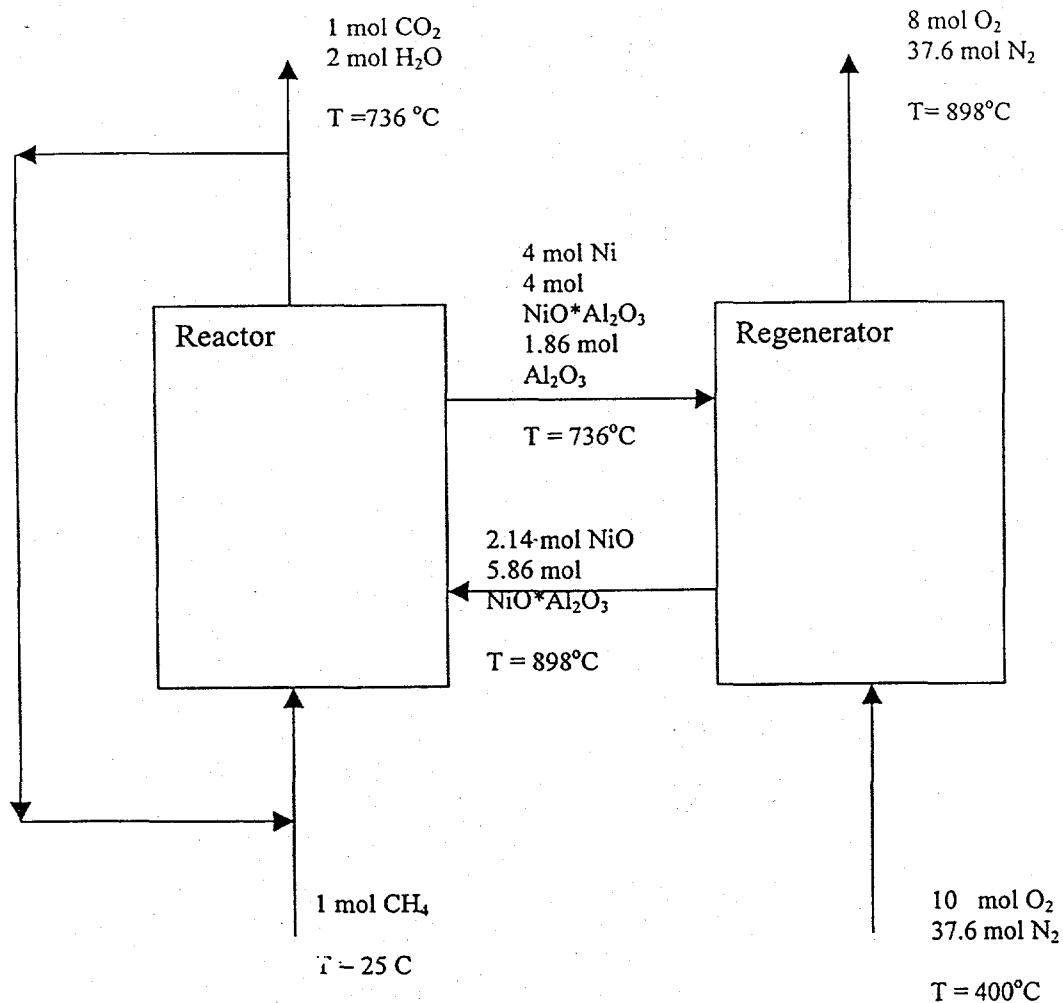
400% excess air

No aluminate



Attachment 4

NiO Sorbent
 25 % NiO/75% Al_2O_3 (wt)
 100% excess NiO
 400% excess air
 No aluminate



Attachment 5

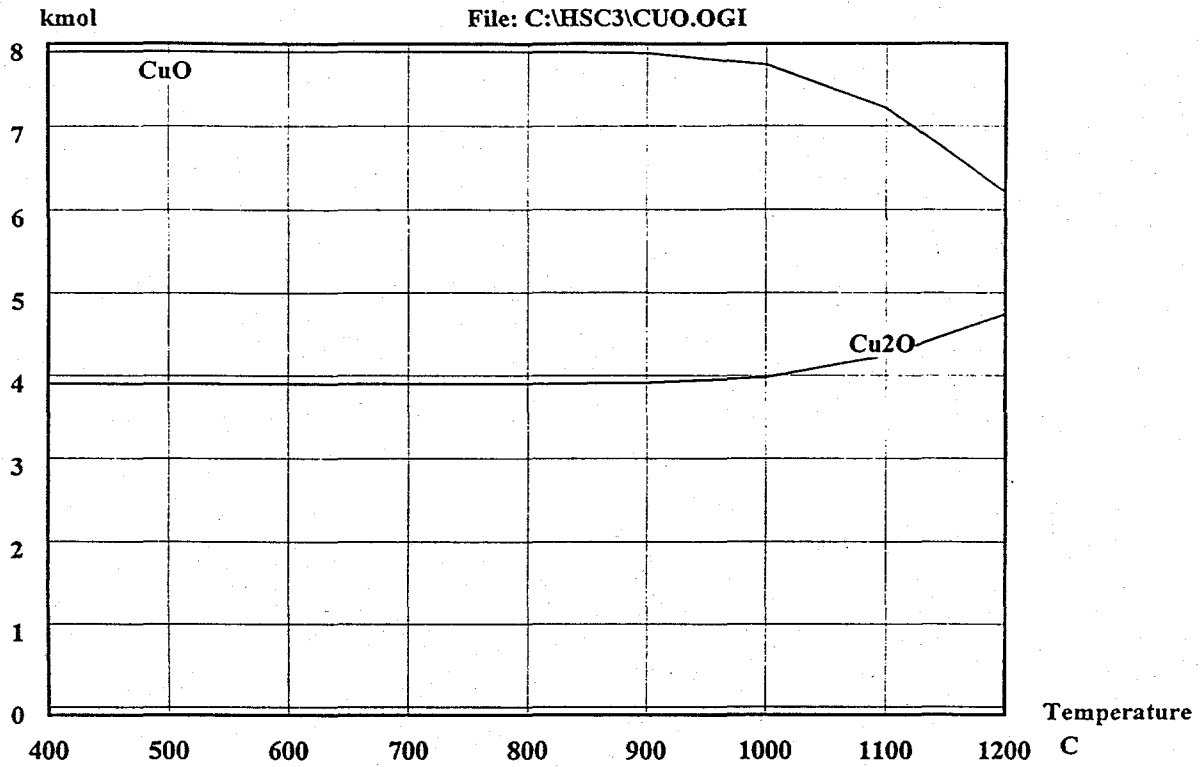
NiO Sorbent

50 % NiO/50% Al_2O_3 (wt)

100% excess NiO

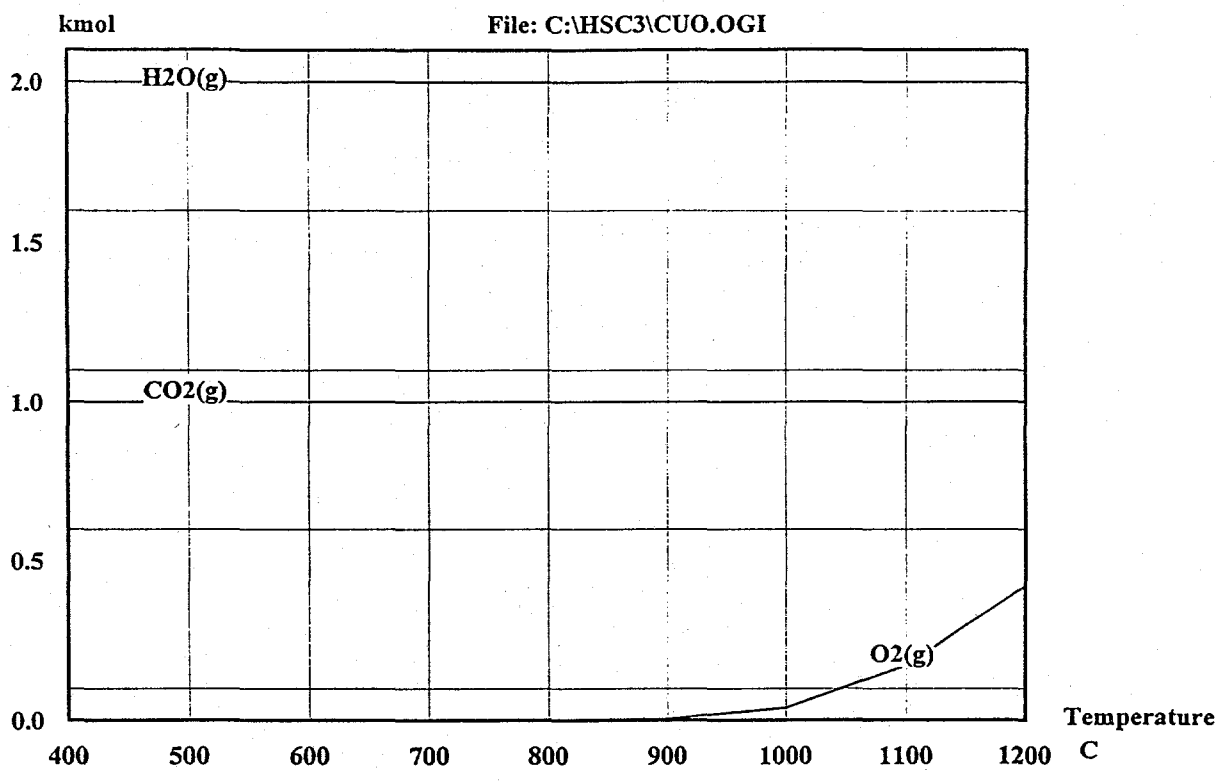
400% excess air

With aluminate



Temperature: 673.150 K
 Pressure: 15.000 bar
 Raw Materials: kmol
 CH₄(g) 1.0000E+00
 CuO 1.6000E+01

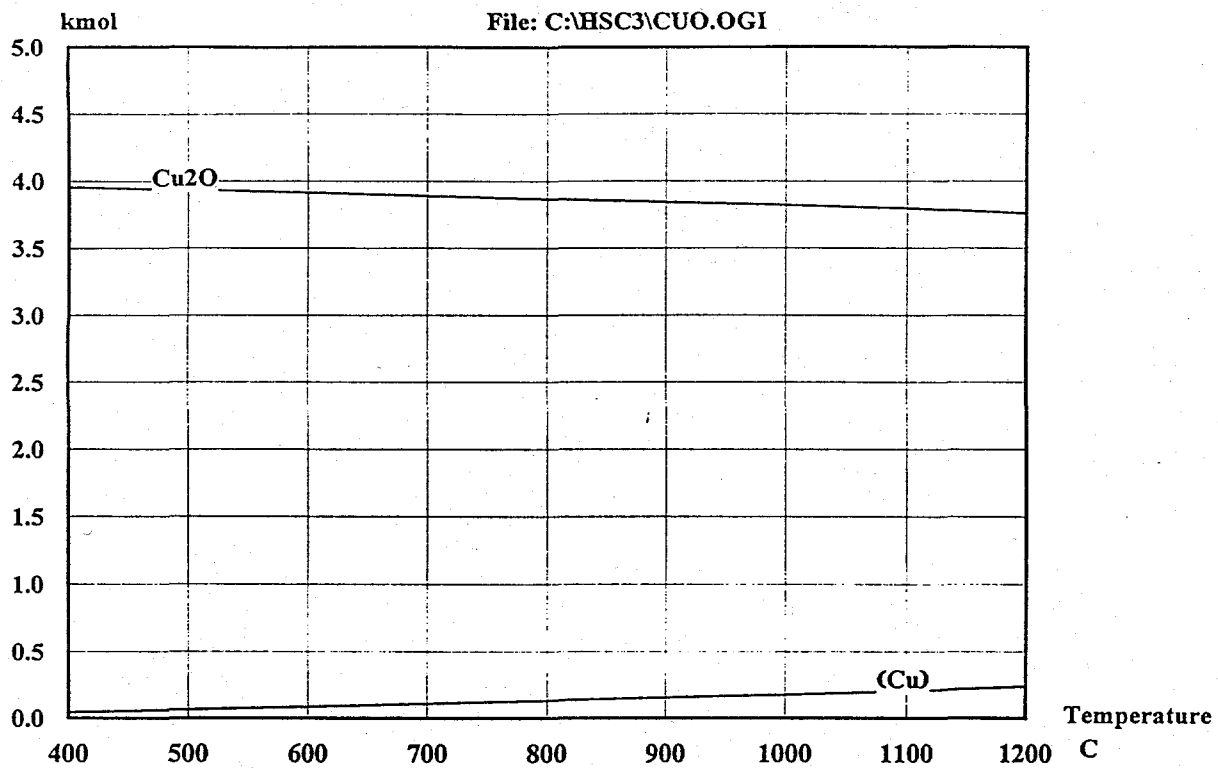
Attachment 6 (a)



Temperature: 673.150 K
Pressure: 15.000 bar
Raw Materials: kmol
CH₄(g) 1.0000E+00
CuO 1.6000E+01

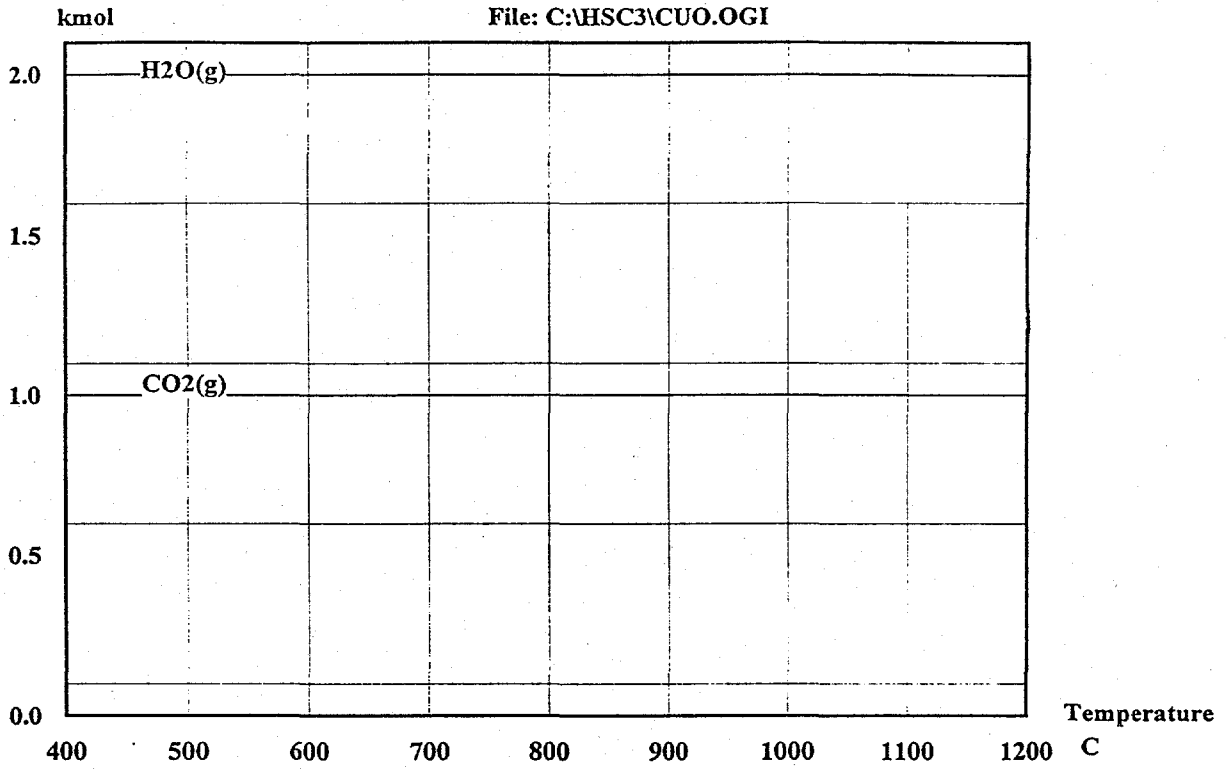
Attachment 6(b)

File: C:\HSC3\CUO.OGI



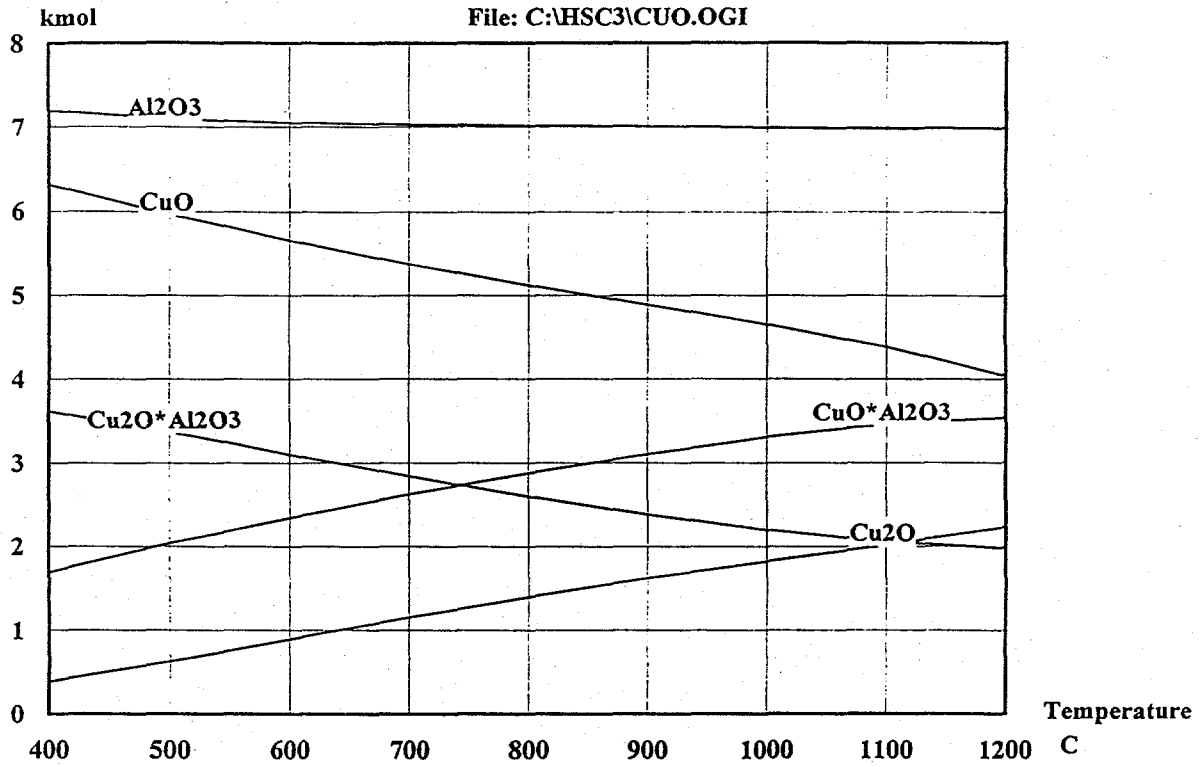
Temperature: 673.150 K
Pressure: 15.000 bar
Raw Materials: kmol
CH₄(g) 1.0000E+00
CuO 8.0000E+00

Attachment 7(a)



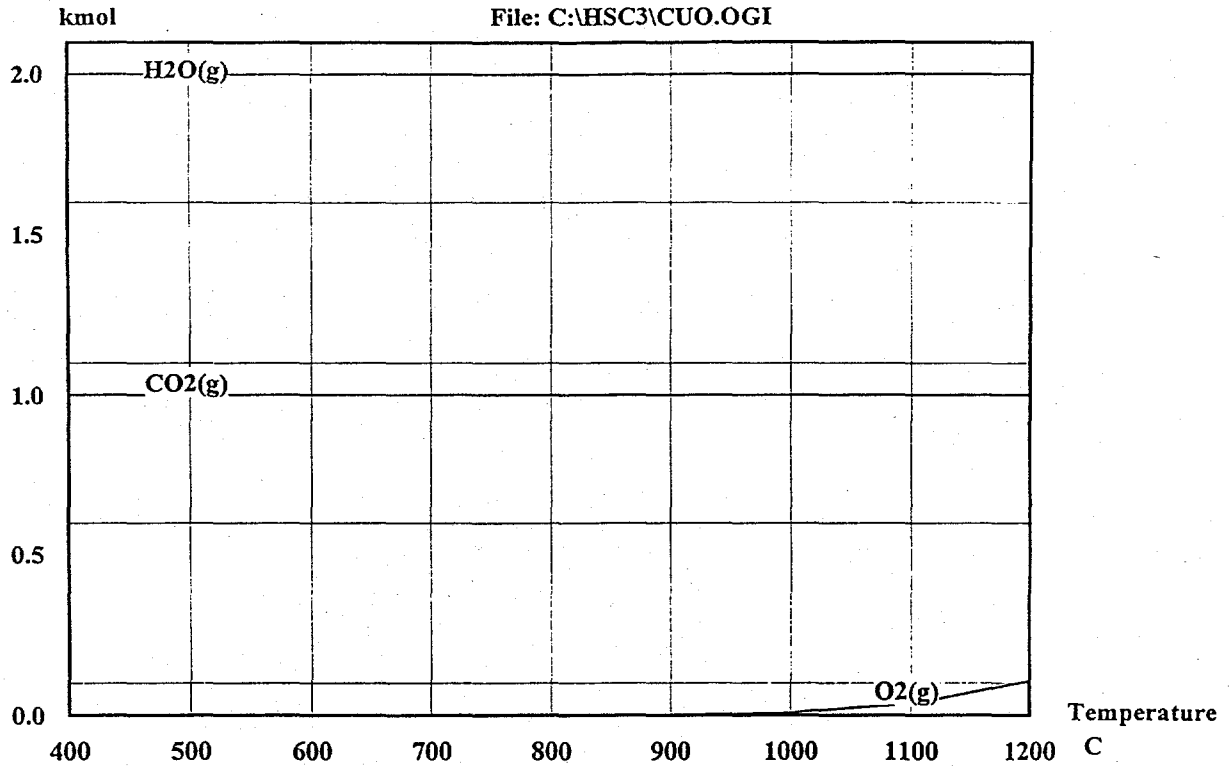
Temperature: 673.150 K
 Pressure: 15.000 bar
 Raw Materials: kmol
 CH4(g) 1.0000E+00
 CuO 8.0000E+00

Attachment 7(b)



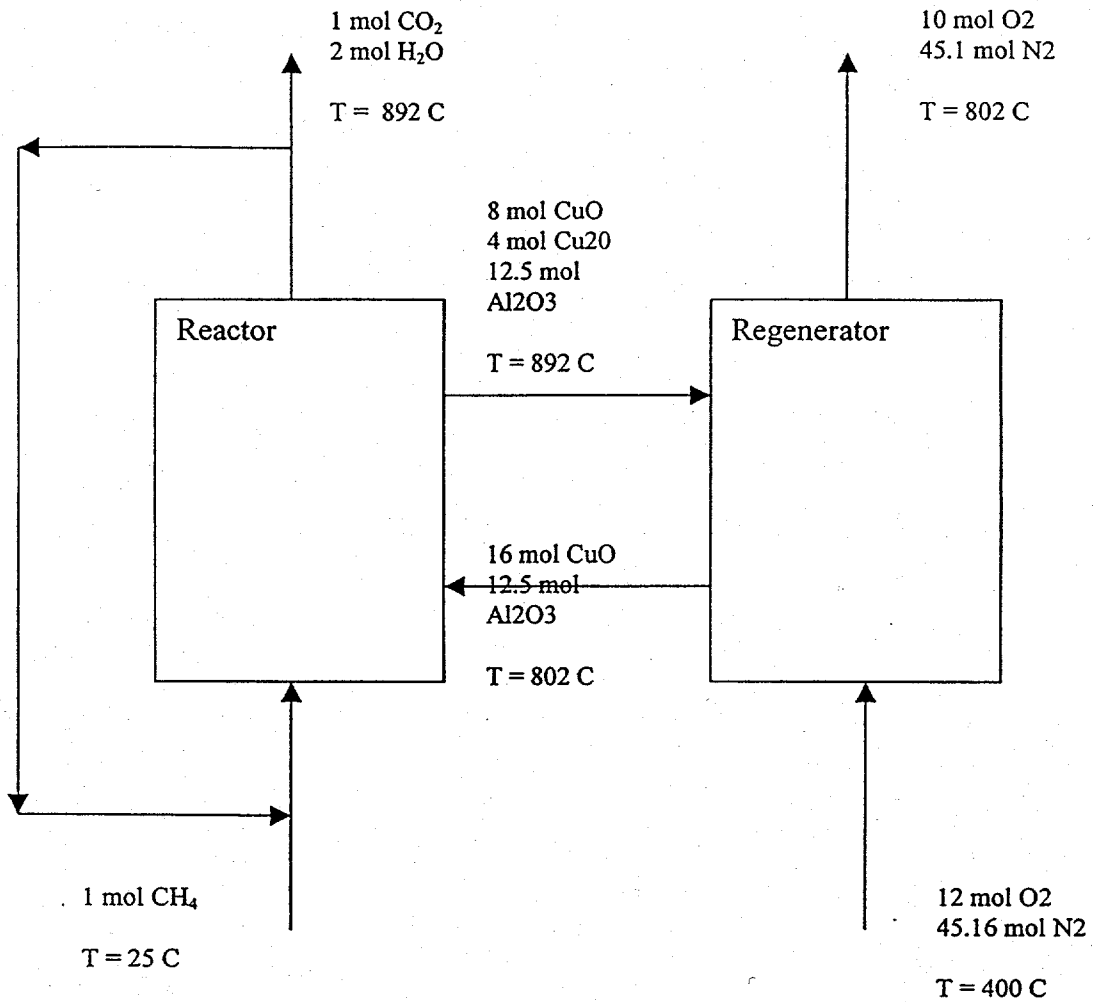
Temperature: 673.150 K
 Pressure: 15.000 bar
 Raw Materials: kmol
 CH₄(g) 1.0000E+00
 Al₂O₃ 1.2500E+01
 CuO 1.6000E+01

Attachment 8 (A)



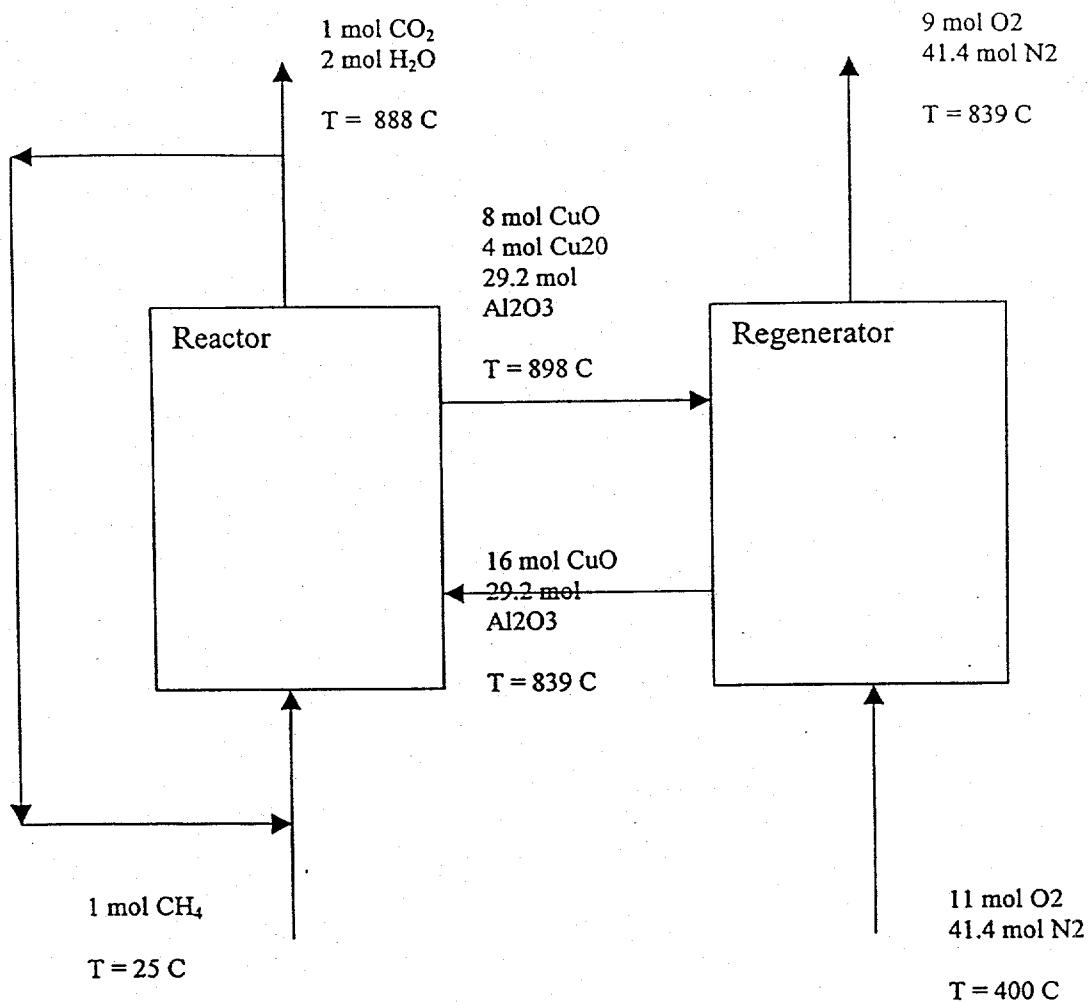
Temperature: 673.150 K
 Pressure: 15.000 bar
 Raw Materials: kmol
 CH₄(g) 1.0000E+00
 Al₂O₃ 1.2500E+01
 CuO 1.6000E+01

Attachment 8(b)



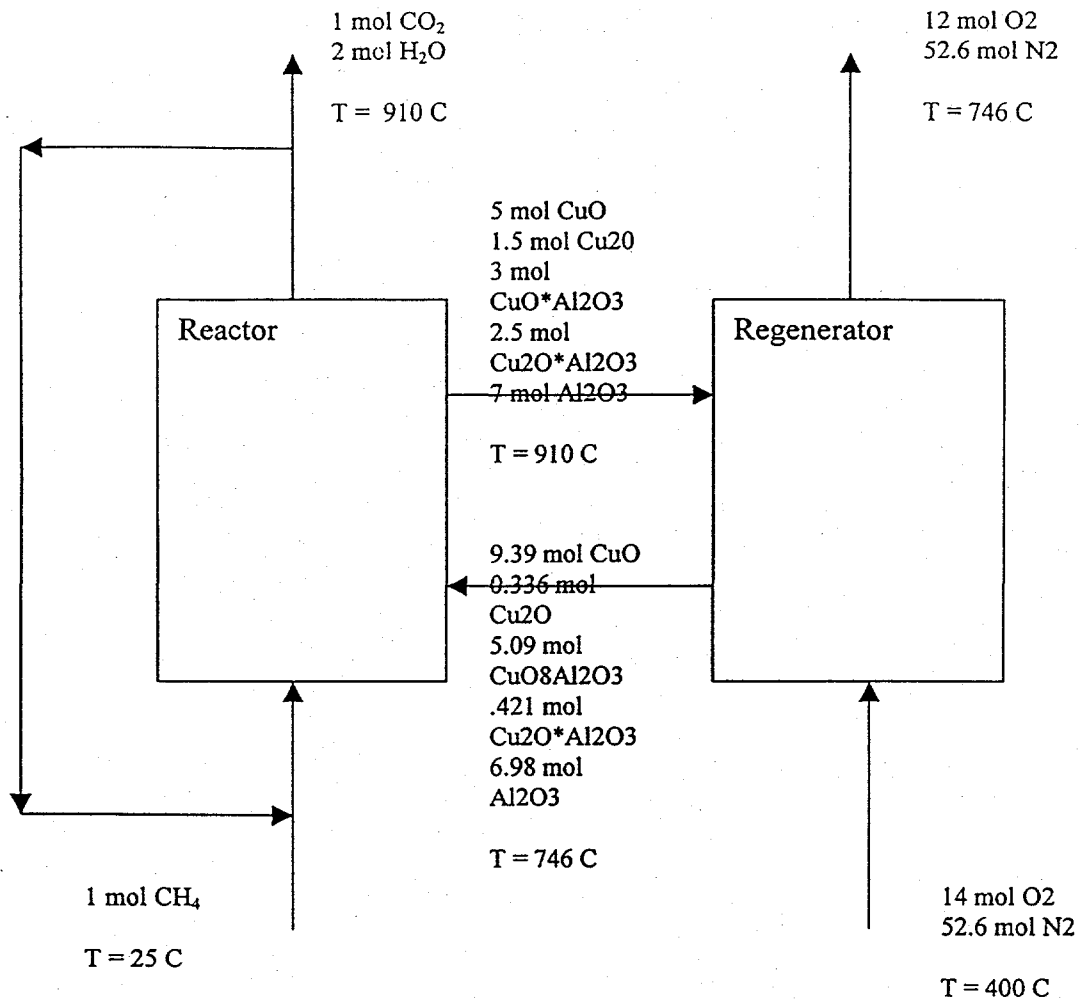
Attachment 09

CuO Sorbent
 50% CuO /50% Al_2O_3 (wt)
 100% Excess Cu
 500% Excess Air
 Without Aluminate



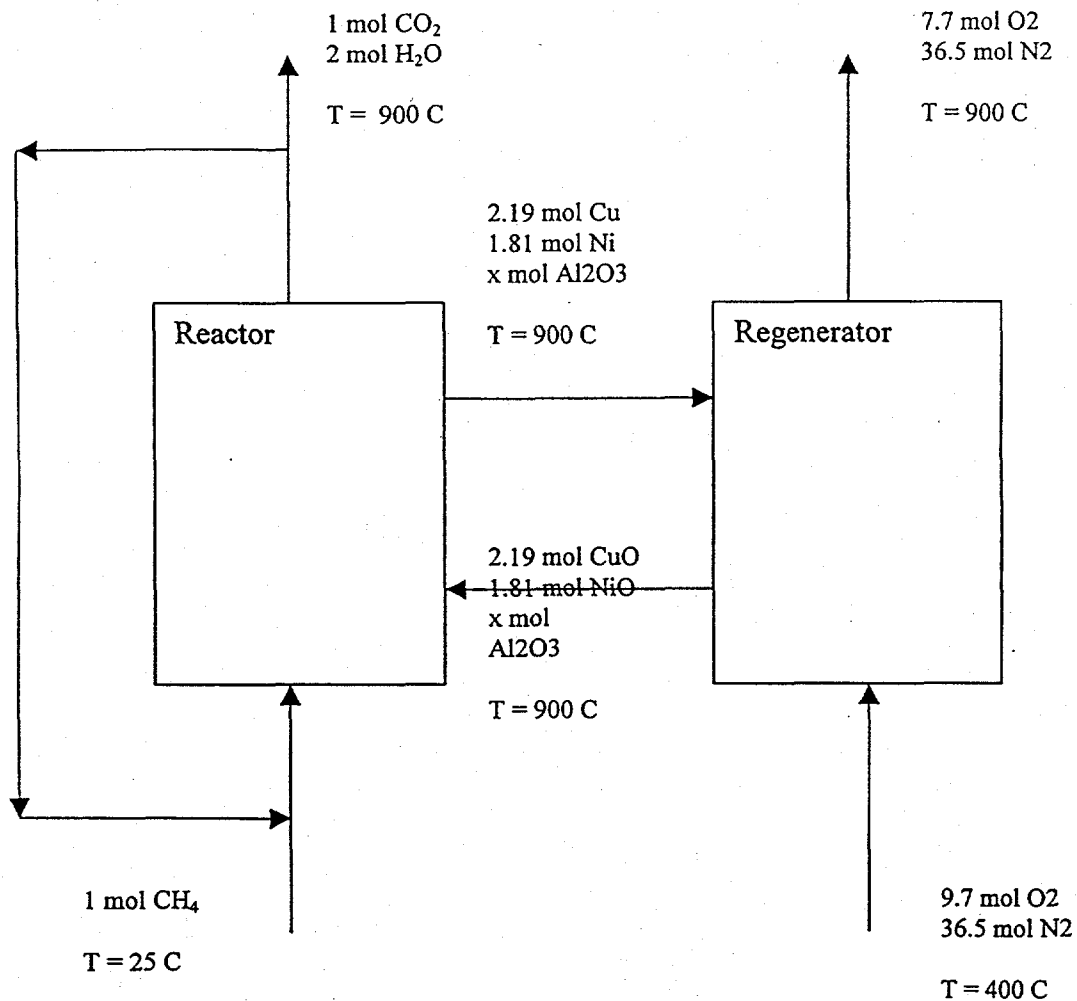
Attachment 010

CuO Sorbent
 30% CuO /70% Al_2O_3 (wt)
 100% Excess Cu
 450% Excess Air
 Without Aluminate



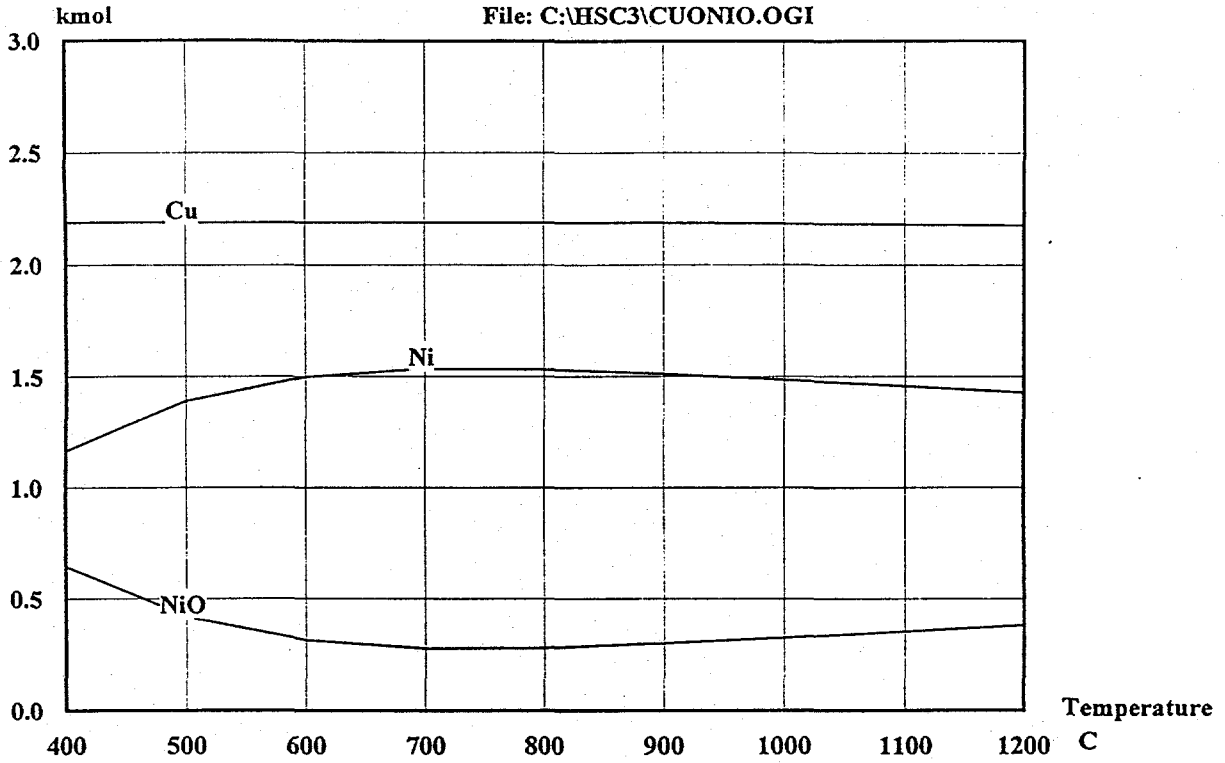
Attachment 011

CuO Sorbent
 50% CuO/50% Al₂O₃ (wt)
 100% Excess Cu
 600% Excess Air
 With Aluminate



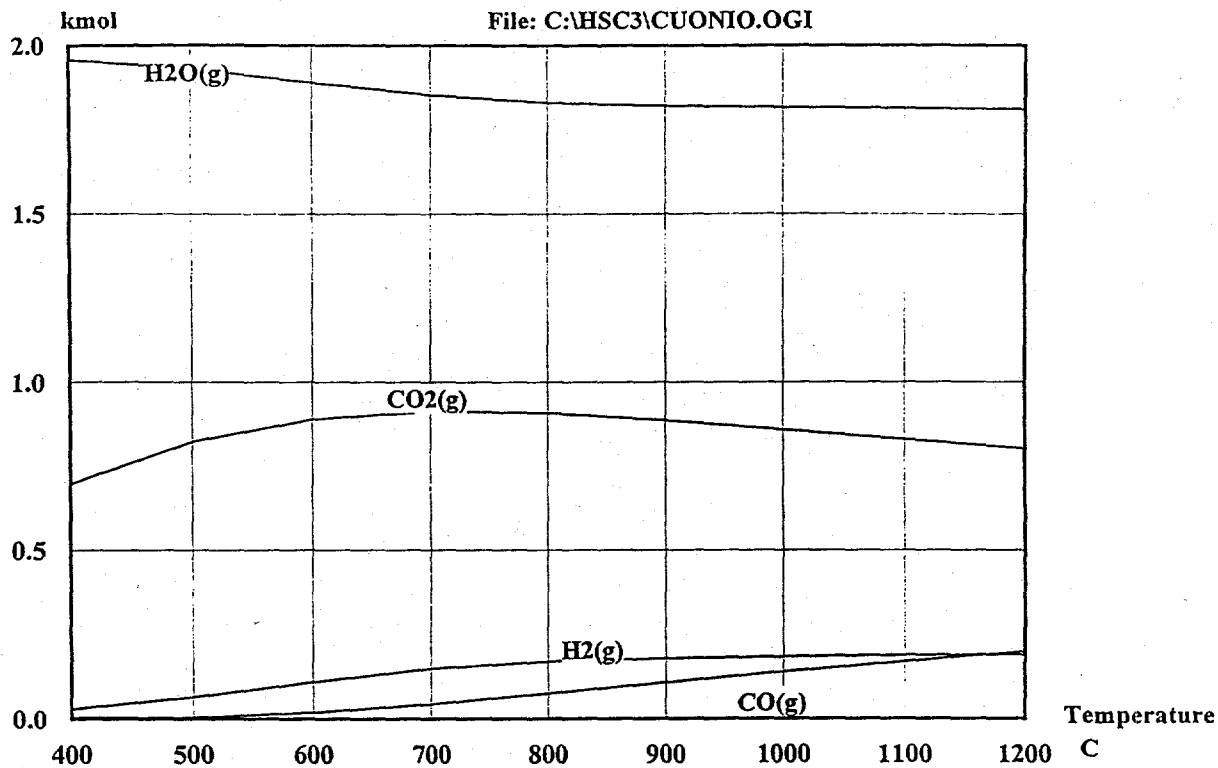
Attachment 12

CuO-NiO Sorbent
 Stoichiometric (Cu+Ni)
 Proportion of Cu to Ni and
 amount of regeneration air chosen so
 that both reactors are at 900C
 Without aluminate (amount of
 Al_2O_3 is not important)



Temperature: 673.150 K
Pressure: 15.000 bar
Raw Materials: kmol
 CH4(g) 1.0000E+00
 Al2O3 1.0000E+01
 CuO 2.1900E+00
 NiO 1.8100E+00

Attachment 13 (a)



Temperature: 673.150 K
 Pressure: 15.000 bar
 Raw Materials: kmol
 CH₄(g) 1.0000E+00
 Al₂O₃ 1.0000E+01
 CuO 2.1900E+00
 NiO 1.8100E+00

Attachment 13 (b)

Status Report 2

GHG Project

IRON

The endothermic reaction with iron is relatively complex because of the multiple oxidation states – Fe_2O_3 , Fe_3O_4 , and FeO – which may exist. FeAl_2O_4 formation is also favored but complete reduction to Fe does not seem to be favored at any conditions of interest. Similarly, decomposition of Fe_xO_y to liberate O_2 does not appear to be a problem. Free oxygen would contaminate the CO_2 product and complicate the disposal problem.

Attachment 1: Complete conversion of CH_4 to CO_2 and H_2O is favored from 400°C to 1200°C in the presence of excess Fe_2O_3 . Much of the excess iron remains as Fe_2O_3 while the reduced iron is primarily Fe_3O_4 along with a small amount of FeO .

Attachment 2: At 900°C , complete reaction of CH_4 to CO_2 and H_2O is favored whenever the Fe_2O_3 to CH_4 ratio is equal to or greater than 11. As the Fe_2O_3 to CH_4 ratio increases the equilibrium quantity of FeO decreases while Fe_3O_4 and Fe_2O_3 increase.

Attachment 3: During regeneration with excess O_2 , essentially all iron is oxidized to Fe_2O_3 up to 800°C . Above 800°C , appreciable quantities of Fe_3O_4 may be formed, but even at 1200°C the amount of Fe_2O_3 is still significantly larger than Fe_3O_4 .

Attachment 4: Regeneration at 900°C with varying quantities of excess O_2 does not alter the Fe_2O_3 to Fe_3O_4 ratio which is about 20 to 1 throughout.

Attachment 5: Allowing for the formation of FeAl_2O_4 alters the distribution of iron species, but complete conversion of CH_4 to CO_2 and H_2O is still favored over the entire temperature range. However, very little Fe_3O_4 may be formed when FeAl_2O_4 is present (compare to Attachment 1). Instead, there is more Fe_2O_3 in the equilibrium product and the majority of reduced iron is combined as FeAl_2O_4 .

Attachment 6: Little FeAl_2O_4 remains after exposure to excess O_2 in the regenerator. At low temperatures ($<700^\circ\text{C}$) all iron is oxidized to Fe_2O_3 . Above 700°C , relatively small amounts of Fe_3O_4 and FeAl_2O_4 are favored.

Attachment 7: This shows an approximate material and energy balance for a sorbent consisting of 50% Fe_2O_3 /50% Al_2O_3 (wt) without aluminate formation. The atomic ratio of Fe to C in the reactor feed is 32 to 1. Air to the regenerator is adjusted to give a regenerator outlet temperature just below 900°C .

Attachment 8: This material and energy balance is similar to that shown in Attachment 7 except that FeAl_2O_4 is permitted. The sorbent composition and the ratio of Fe to C are the same. The reaction $\text{FeO} + \text{Al}_2\text{O}_3 \Rightarrow \text{FeAl}_2\text{O}_4$ is exothermic so that both reactors will

operate at about the same temperature (887°C for the reactor and 882°C for the regenerator). This creates interesting possibilities.

MANGANESE

The exothermic manganese-CH₄ reaction is more complex than the reaction with iron. MnO₂, Mn₂O₃, Mn₃O₄, and MnO co-exist at certain conditions of interest. MnO*Al₂O₃ may also be formed. Complete reduction to Mn has not been observed at conditions of interest. However, decomposition of higher oxides to liberate O₂ may occur. This potential problem is most severe with MnO₂ and Mn₂O₃ but also is favored to a limited extent with Mn₃O₄.

Attachment 9: This shows the potential problem with decomposition of Mn₃O₄ in N₂. Free O₂ is released at T ≥ 900°C and a mixture of manganese compounds is favored. Mn₃O₄ decreases with increasing temperature while the amounts of Mn₂O₃ and MnO₂ increase with increasing temperature.

Attachment 10: Complete conversion of CH₄ to CO₂ and H₂O is favored at T ≥ 500°C when 1 mol of CH₄ is in equilibrium with 8 mols of Mn₃O₄. The excess manganese forms three compounds with MnO > Mn₃O₄ > Mn₂O₃.

Attachment 11: Complete conversion of CH₄ to CO₂ and H₂O is favored at 900°C when the initial amount of Mn₃O₄ is varied between 4 and 8 mols. Excess manganese is present primarily as MnO which is relatively independent of the amount of Mn₃O₄. Lesser quantities of Mn₃O₄ and Mn₂O₃ are favored and the amount of each increases with increasing Mn₃O₄.

Attachment 12: Regeneration of mixed reduced manganese oxides in excess O₂ produces a mixture of higher oxides. Total oxidation to MnO₂ is favored at 400°C, but the quantity decreases with increasing temperature. Mn₂O₃ is formed in the largest amount for 600°C ≤ T ≤ 1100°C with Mn₃O₄ favored above 1100°C. However, all four oxides may co-exist throughout much of the temperature range.

Attachment 13: This shows the effect of increasing the quantity of O₂ used for regeneration at 900°C. Once excess O₂ is present, the distribution of manganese oxides is relatively flat with Mn₂O₃ > Mn₃O₄ > MnO₂ > MnO.

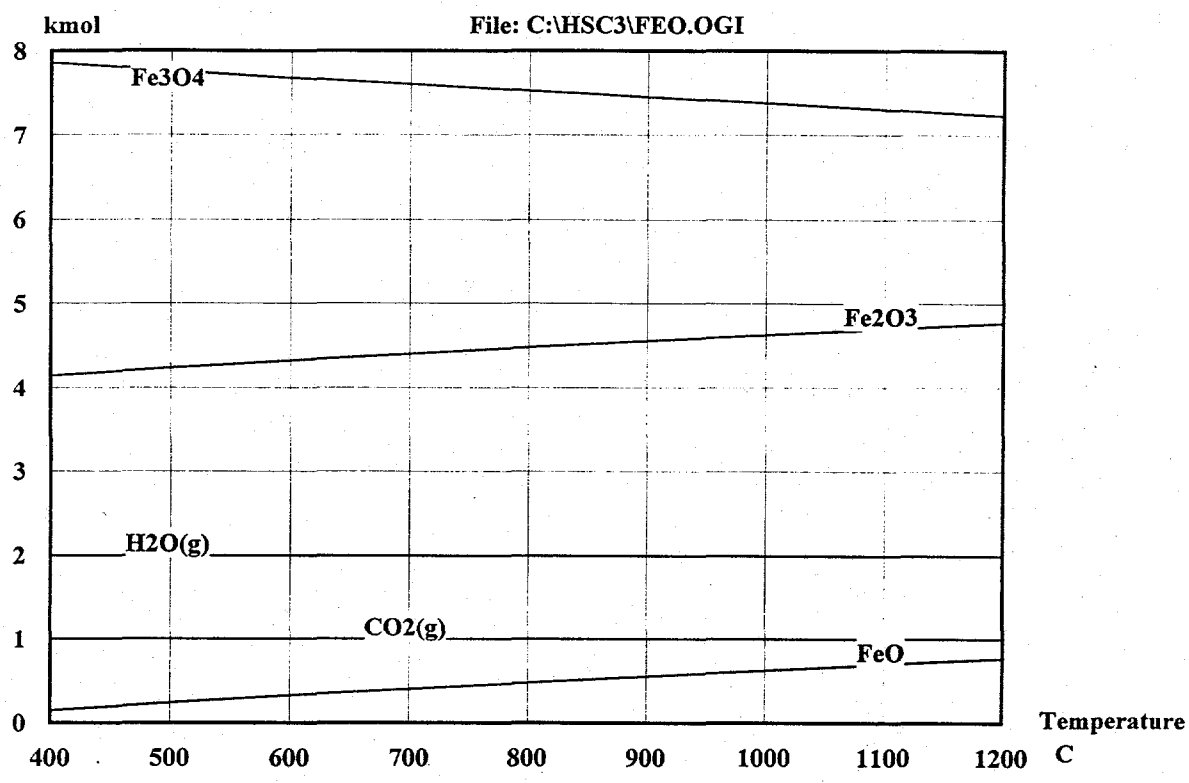
Attachment 14: MnO*Al₂O₃ may be formed along with free Al₂O₃, MnO_x, and O₂ in a neutral atmosphere. That is, aluminate formation does not prevent decomposition of MnO_x. This is true for various initial oxidation states – MnO₂, Mn₂O₃, and Mn₃O₄.

Attachment 15: Formation of MnO*Al₂O₃ does not prevent complete oxidation of CH₄ to CO₂ and H₂O over the entire temperature range. Note that free Al₂O₃ and MnO_x are also present throughout the temperature range.

Attachment 16: Oxidizing a mixture of reduced manganese oxides, including $\text{MnO} \cdot \text{Al}_2\text{O}_3$, with excess O_2 results in the formation of mixed oxides in a higher oxidation state. At 900°C , the product oxides in descending order are $\text{MnO} \cdot \text{Al}_2\text{O}_3 \approx \text{Mn}_2\text{O}_3 > \text{MnO}_2 \approx \text{Mn}_3\text{O}_4 > \text{MnO}$.

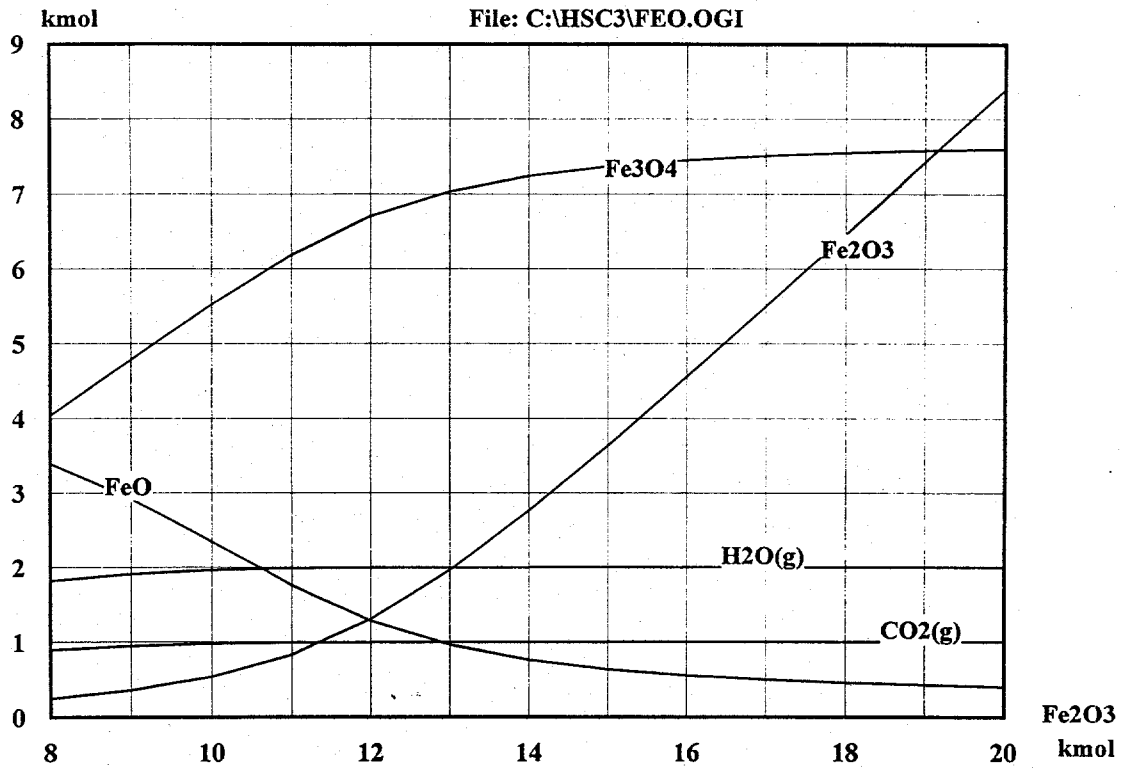
Attachment 17: This figure shows material and energy balance results when CH_4 reacts with mixed manganese oxides (including $\text{MnO} \cdot \text{Al}_2\text{O}_3$). The sorbent is based on an initial composition of 50% Mn_3O_4 /50% Al_2O_3 (wt) and a ratio of Mn to C of 24 to 1 is used. Air flow to the regenerator is fixed so that the maximum temperature (in this case the reactor) is just less than 900°C . Note that the reaction $\text{MnO} + \text{Al}_2\text{O}_3 \Rightarrow \text{MnO} \cdot \text{Al}_2\text{O}_3$ is exothermic.

Attachment 18: This material and energy balance calculation is equivalent to that shown in Attachment 17 except that $\text{MnO} \cdot \text{Al}_2\text{O}_3$ formation is not permitted. The overall sorbent composition, the ratio of Mn to C, and the air feed rate to the regenerator are the same. The most significant difference is the reactor exit temperature is reduced by about 50°C , due to the fact that the heat of reaction associated with $\text{MnO} \cdot \text{Al}_2\text{O}_3$ is no longer present.



Temperature: 673.150 K
 Pressure: 15.000 bar
 Raw Materials: kmol
 CH4(g) 1.0000E+00
 Fe2O3 1.6000E+01

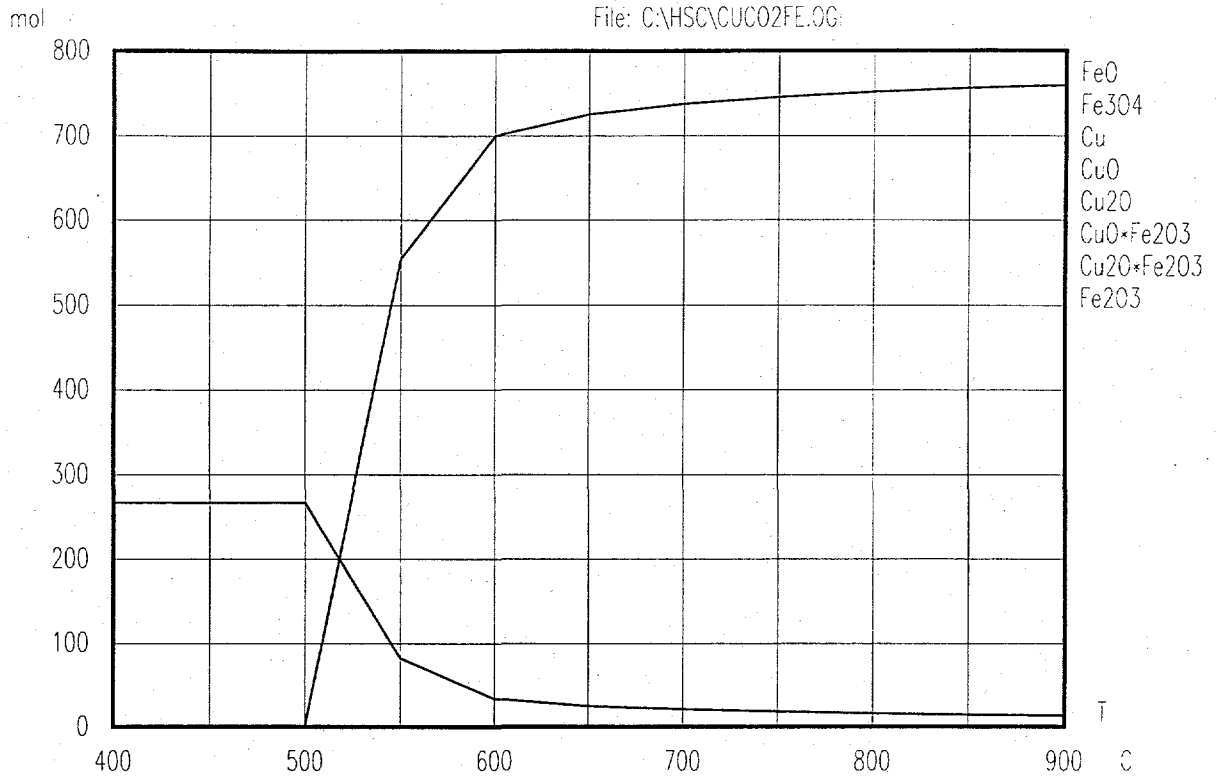
Attachment 1



Temperature: 1173.150 K
 Pressure: 15.000 bar
 Raw Materials: kmol
 CH4(g) 1.0000E+00
 Fe2O3 8.0000E+00

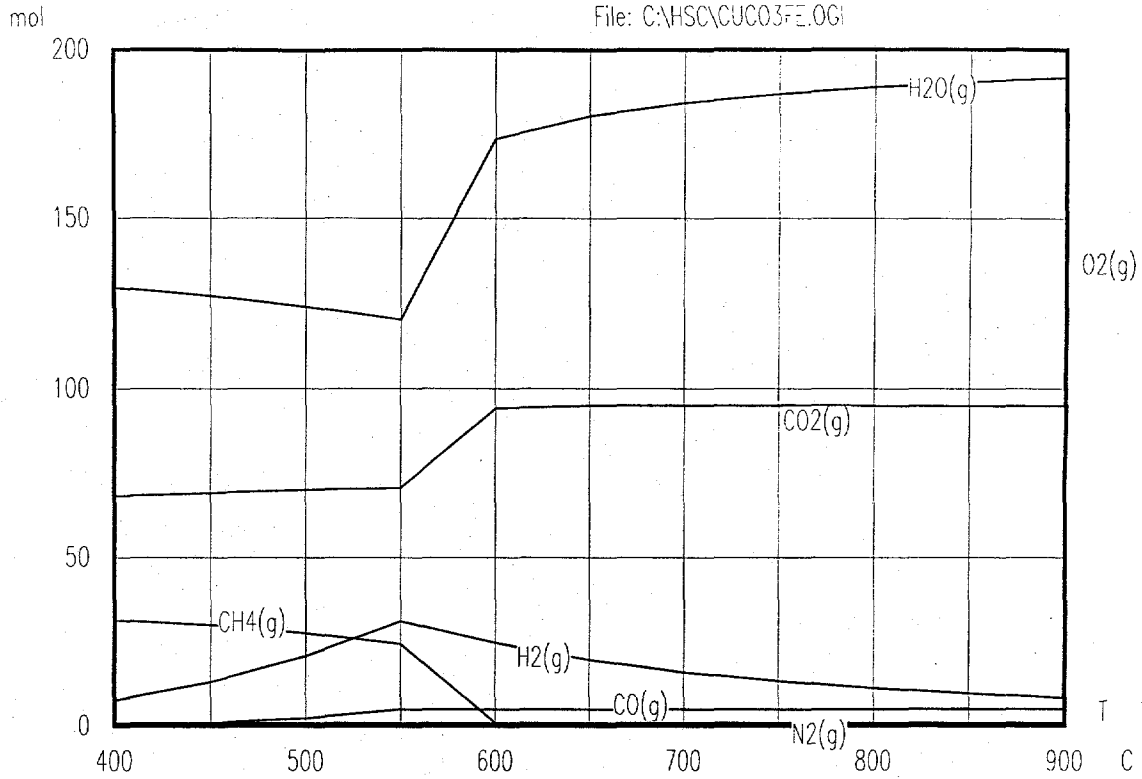
Attachment 2

File: C:\HSC\CUCO2FE.00

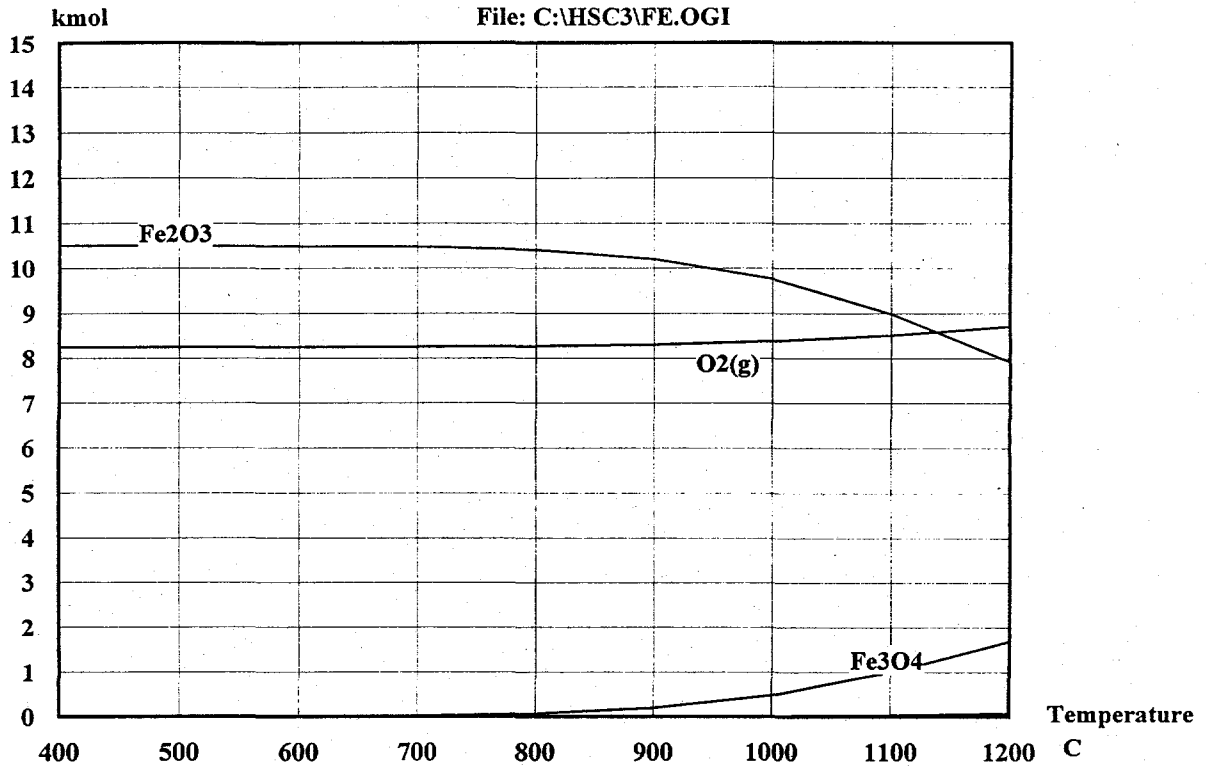


Temperature: 673.150 K
 Pressure: 10.000 bar
 Raw Materials: mol
 CH4(g) 1.0000E+02
 N2(g) 1.0000E+00
 Fe2O3 4.0000E+02
 Cu 1.0000E+00

File: C:\HSC\CUCO3FE.0G1

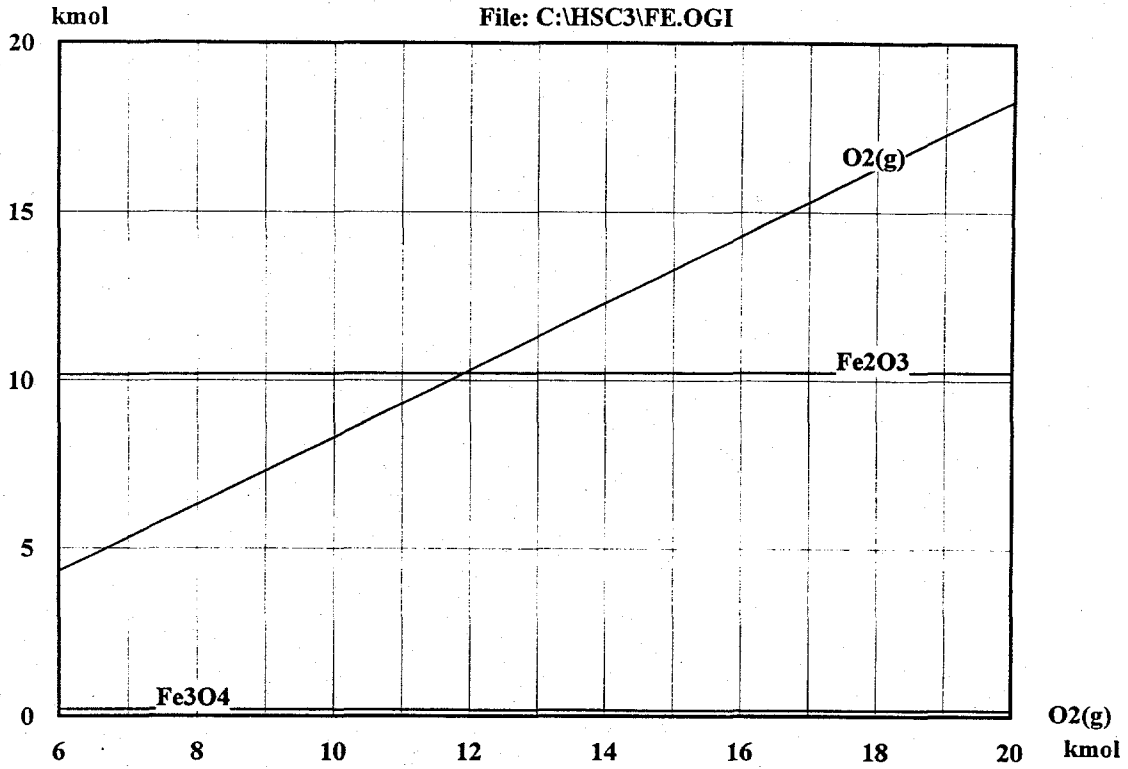


Temperature: 673.150 K
Pressure: 10.000 bar
Raw Materials: mol
CH4(g) 1.0000E+02
N2(g) 1.0000E+00
Fe2O3 8.0000E+02
Cu 1.0000E+00



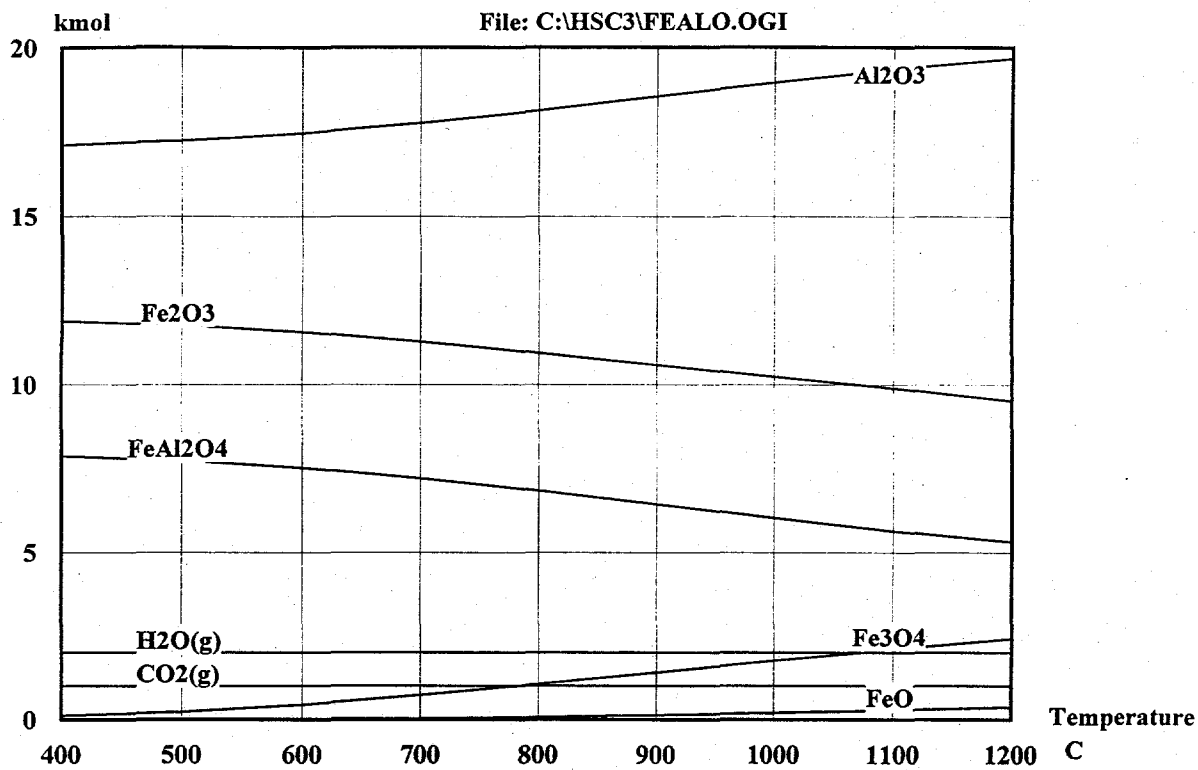
Temperature: 673.150 K
 Pressure: 15.000 bar
 Raw Materials: kmol
 N2(g) 3.7600E+01
 O2(g) 1.0000E+01
 FeO 1.5000E+00
 Fe2O3 1.5000E+00
 Fe3O4 5.5000E+00

Attachment 3



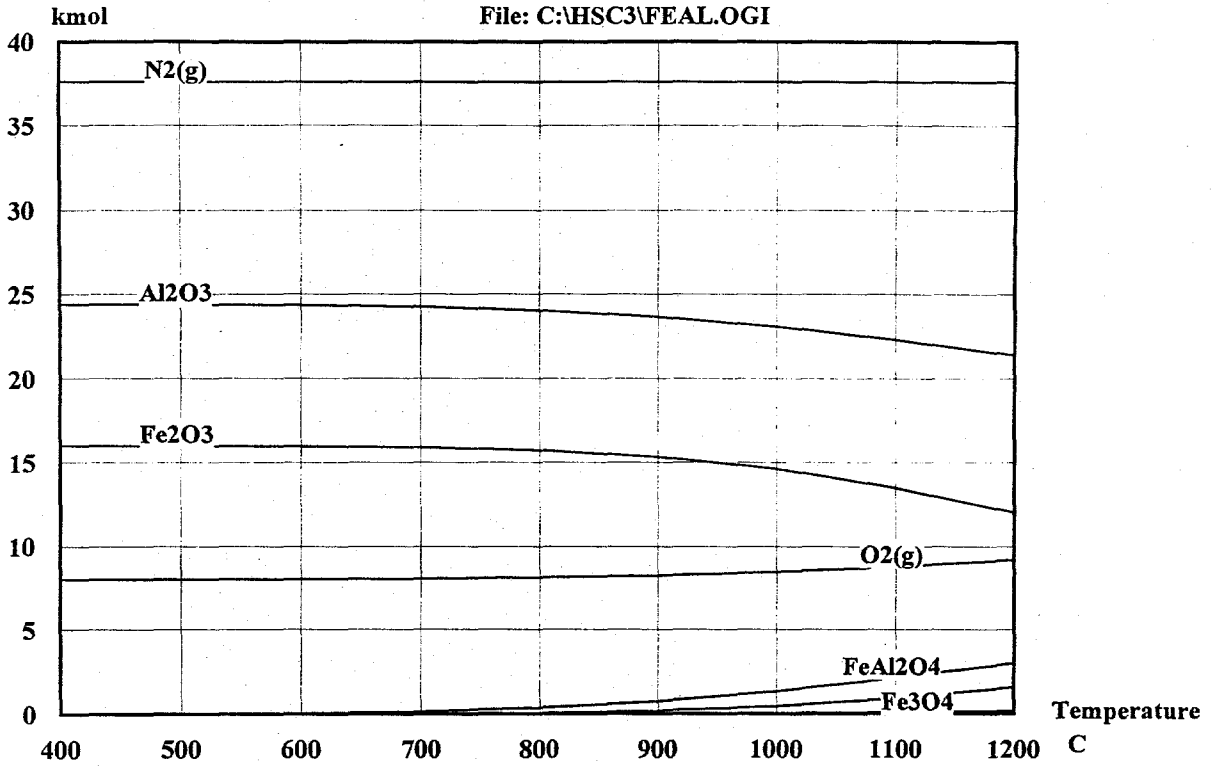
Temperature:	1173.150 K
Pressure:	15.000 bar
Raw Materials:	kmol
$\text{N}_2(\text{g})$	3.7600E+01
$\text{O}_2(\text{g})$	6.0000E+00
FeO	1.5000E+00
Fe_2O_3	1.5000E+00
Fe_3O_4	5.5000E+00

Attachment 4



Temperature: 673.150 K
 Pressure: 15.000 bar
 Raw Materials: kmol
 CH₄(g) 1.0000E+00
 Al₂O₃ 2.5000E+01
 Fe₂O₃ 1.6000E+01

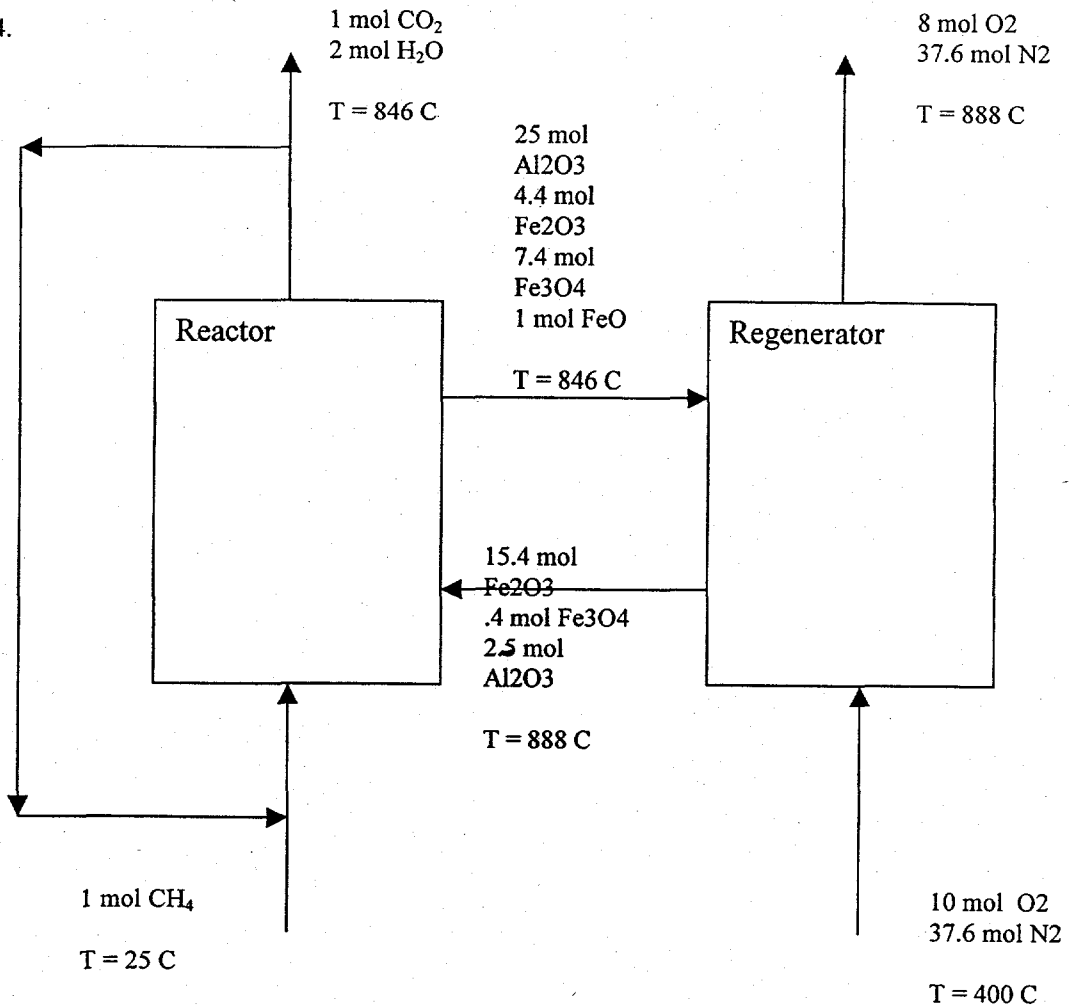
Attachment 5



Temperature: 673.150 K
 Pressure: 15.000 bar
 Raw Materials: kmol
 N2(g) 3.7600E+01
 O2(g) 1.0000E+01
 Al2O3 1.8000E+01
 FeAl2O4 6.4000E+00
 FeO 1.0000E-01
 Fe2O3 1.0500E+01
 Fe3O4 1.5000E+00

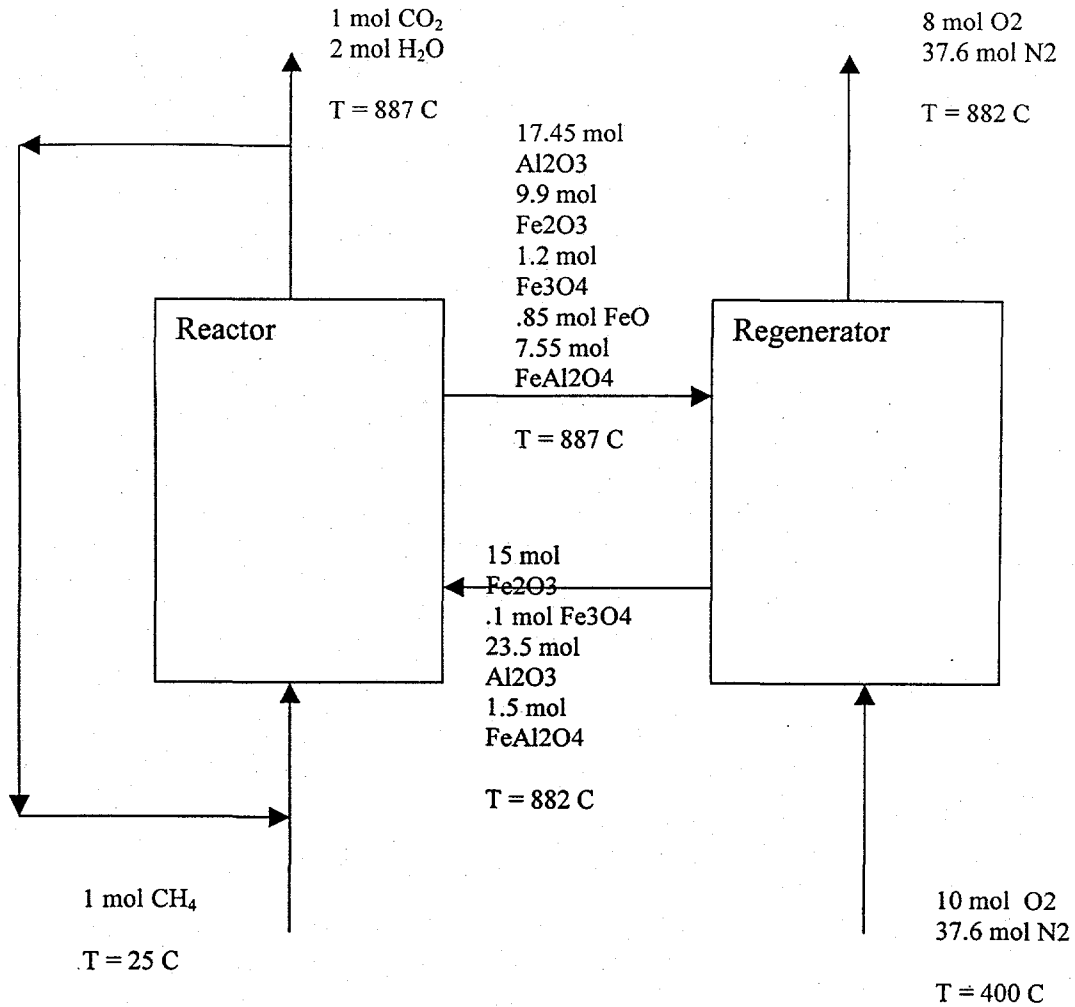
Attachment 6

4.



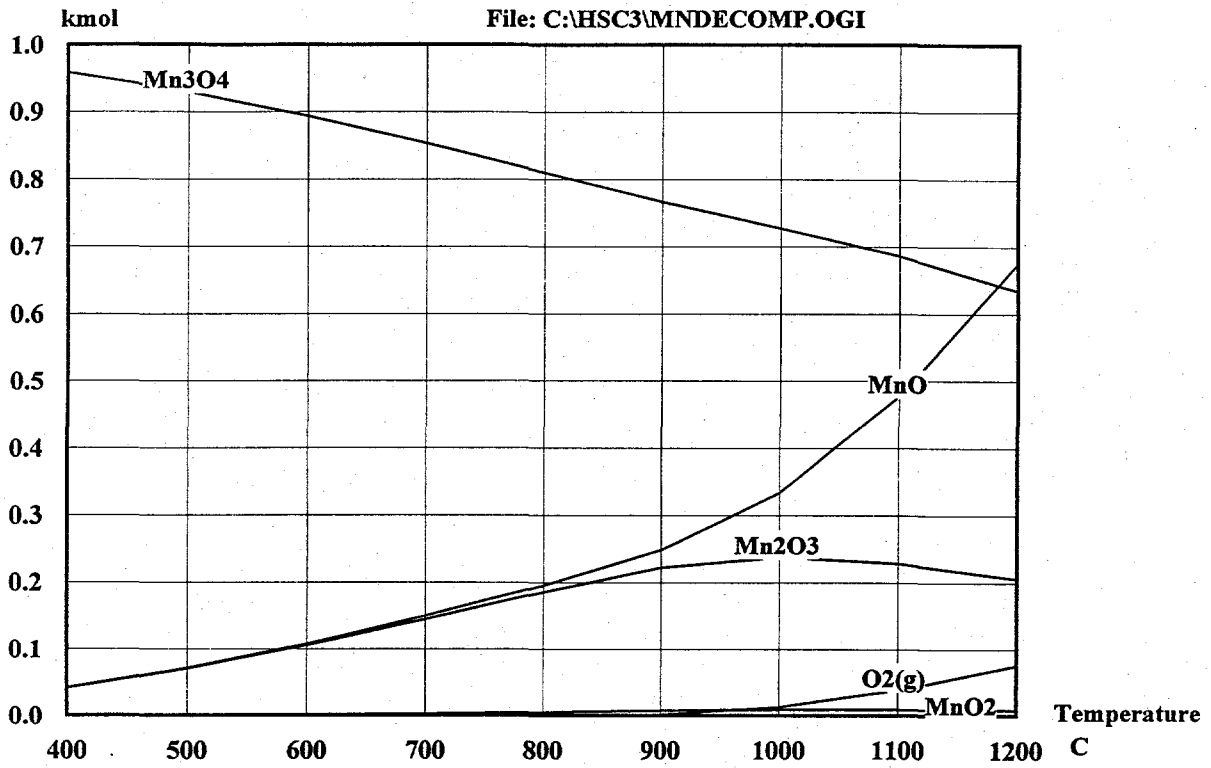
Attachment 7

Fe_xO_y Sorbent (without
aluminate formation)
50%Fe₂O₃/50% Al₂O₃ (wt)



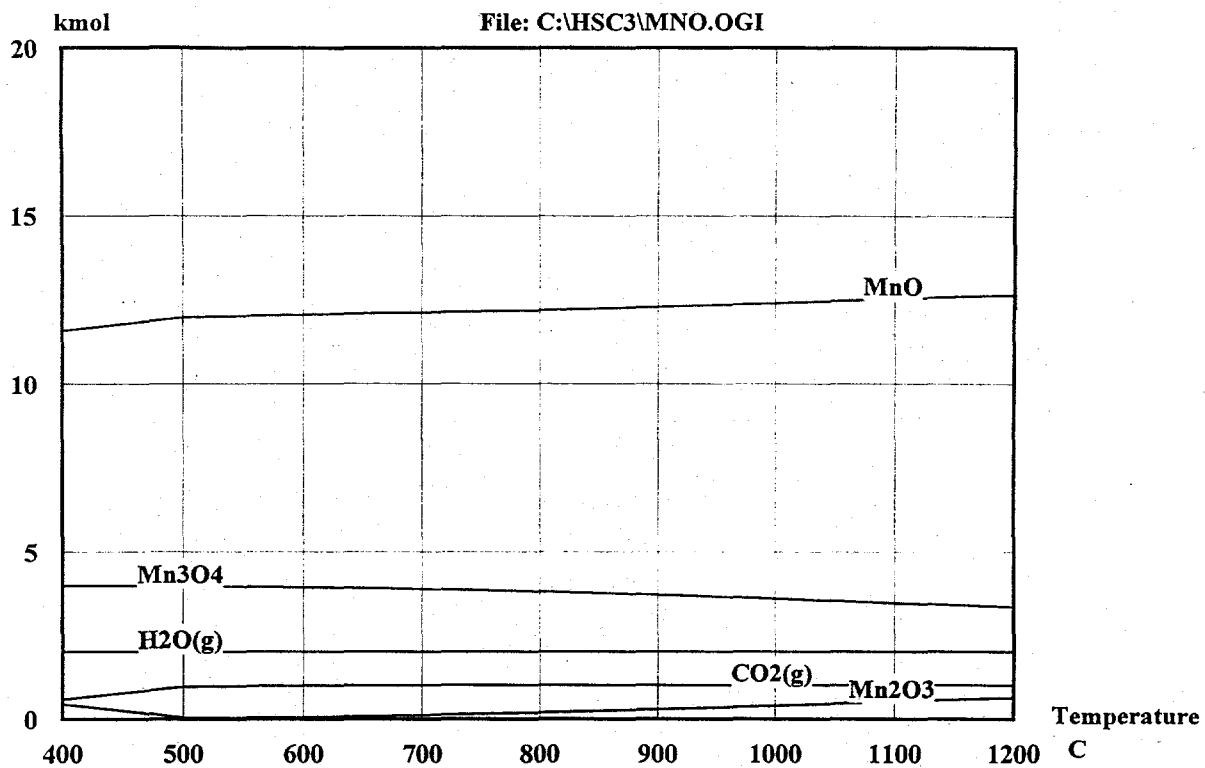
Attachment 8

FexOy Sorbent (without
aluminate formation)
50%Fe₂O₃/50% Al₂O₃ (wt)



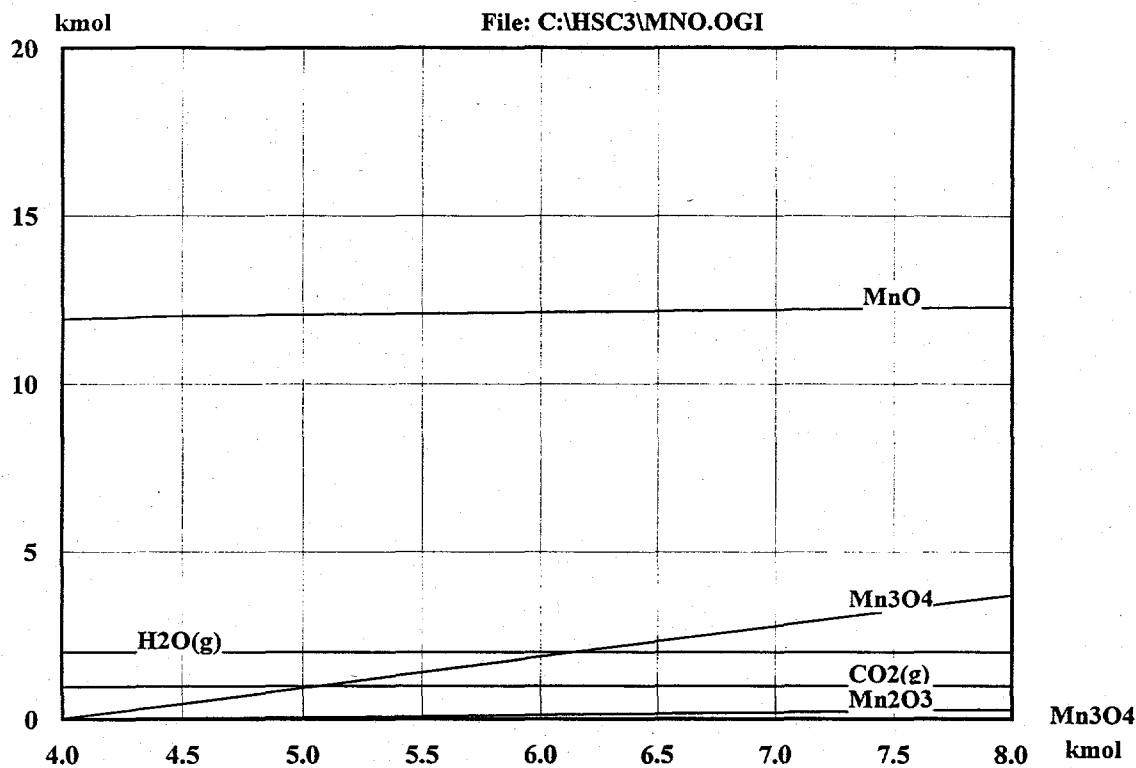
Temperature: 673.150 K
 Pressure: 1.000 bar
 Raw Materials: kmol
 N2(g) 1.0000E+01
 Mn3O4 1.0000E+00

Attachment 9



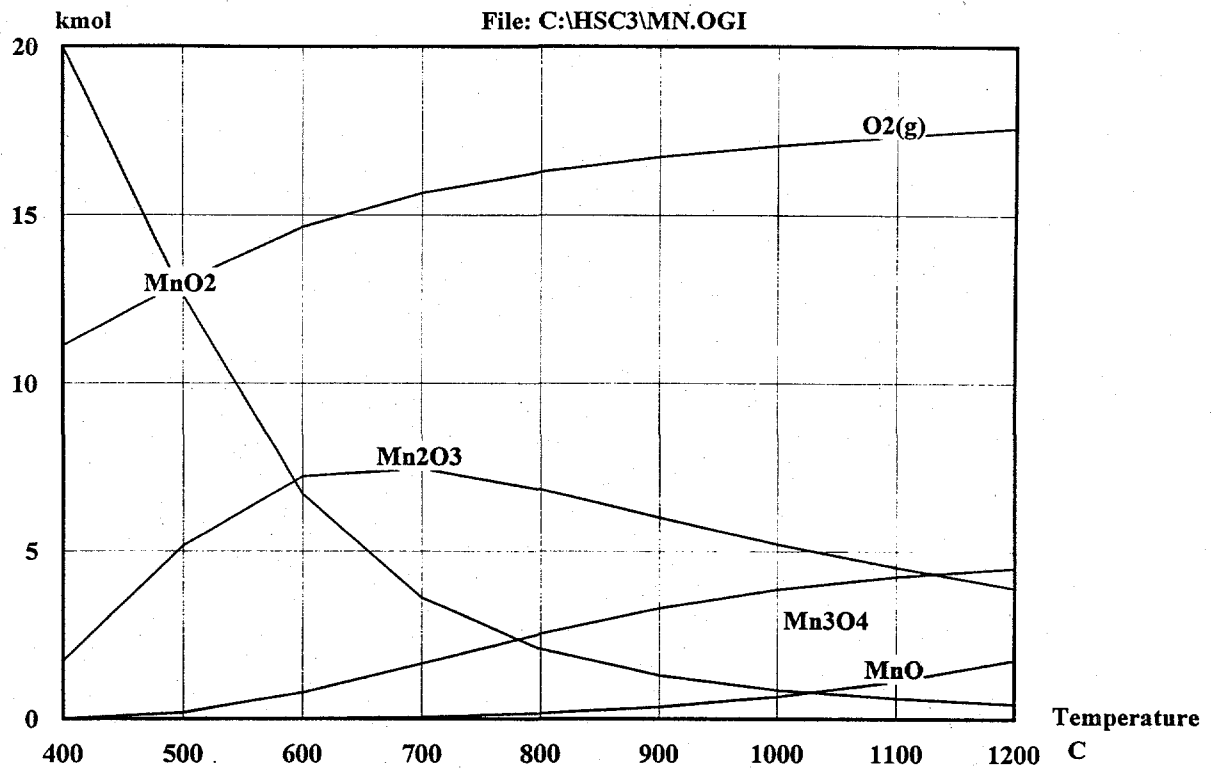
Temperature: 673.150 K
 Pressure: 1.000 bar
 Raw Materials: kmol
 CH₄(g) 1.0000E+00
 Mn₃O₄ 8.0000E+00

Attachment 10



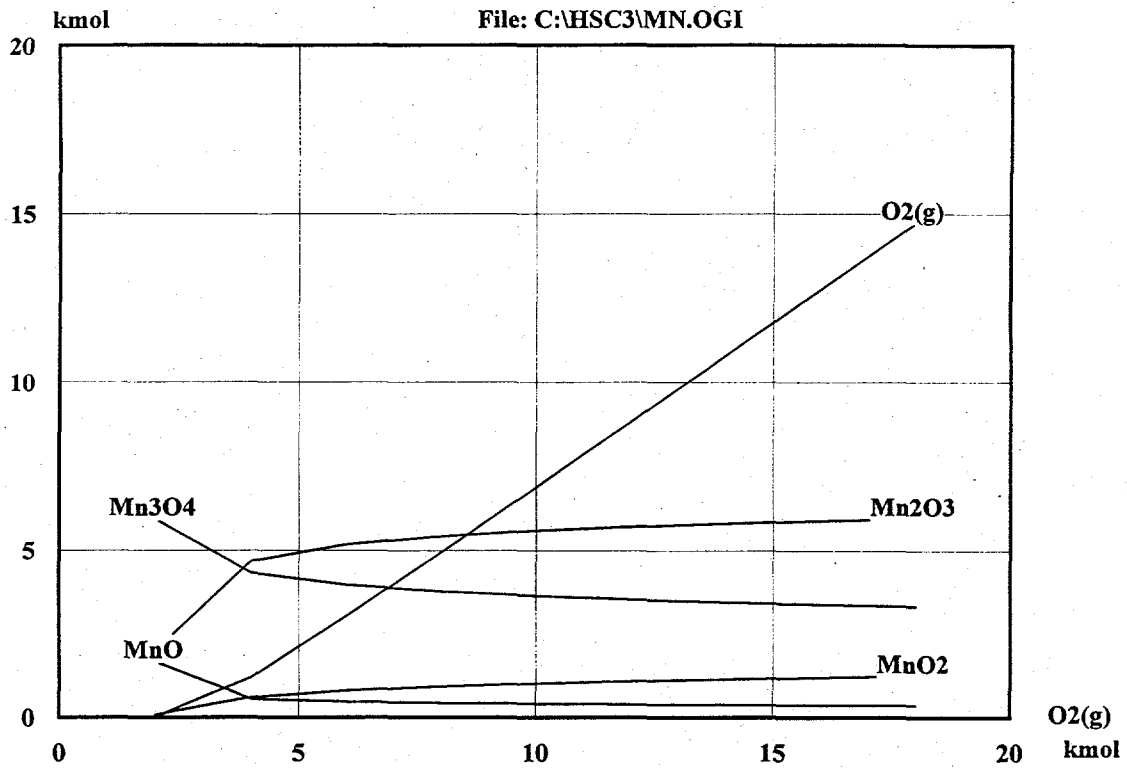
Temperature: 1173.150 K
 Pressure: 1.000 bar
 Raw Materials: kmol
 CH4(g) 1.0000E+00
 Mn3O4 4.0000E+00

Attachment 11



Temperature: 673.150 K
 Pressure: 15.000 bar
 Raw Materials: kmol
 O2(g) 2.0000E+01
 N2(g) 7.5000E+01
 MnO 1.2000E+01
 Mn2O3 5.0000E-01
 Mn3O4 3.5000E+00

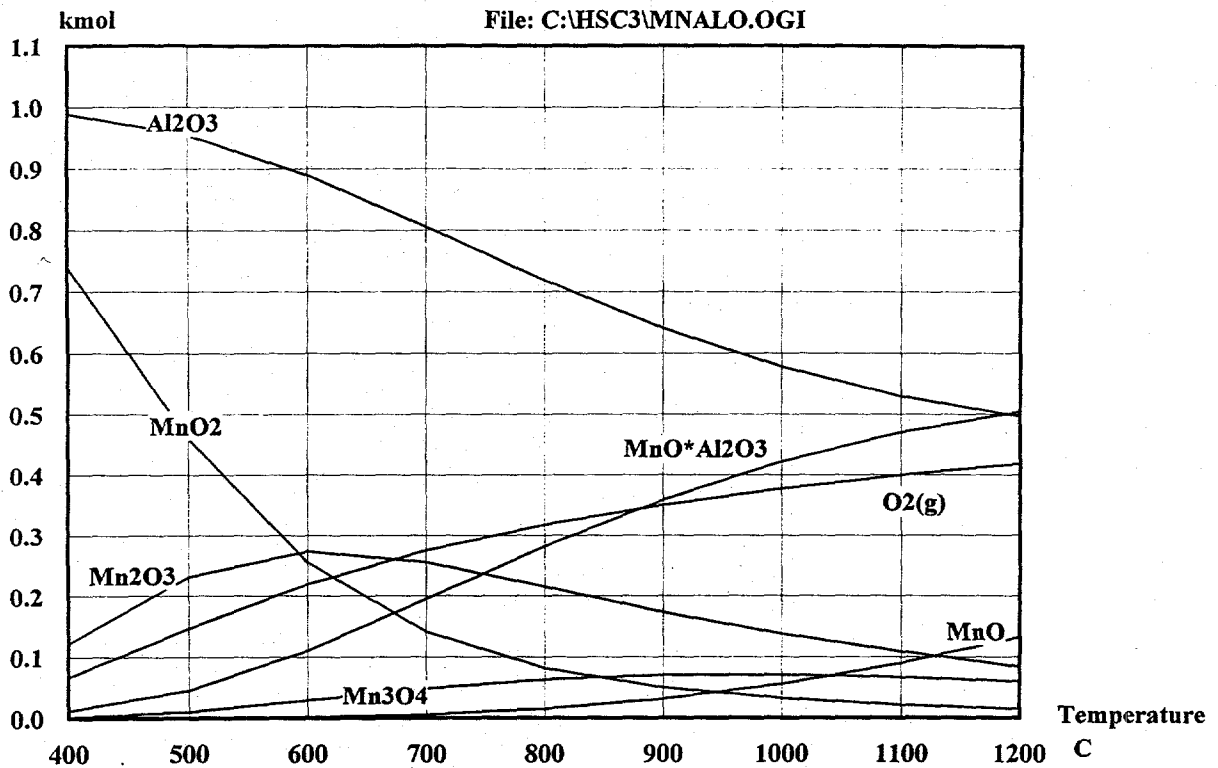
Attachment 12



Temperature: 1173.150 K
 Pressure: 15.000 bar
 Raw Materials: kmol
 O₂(g) 2.0000E+00
 N₂(g) 7.5000E+01
 MnO 1.2000E+01
 Mn₂O₃ 5.0000E-01
 Mn₃O₄ 3.5000E+00

Attachment 13

File: C:\HSC3\MNALO.OGI

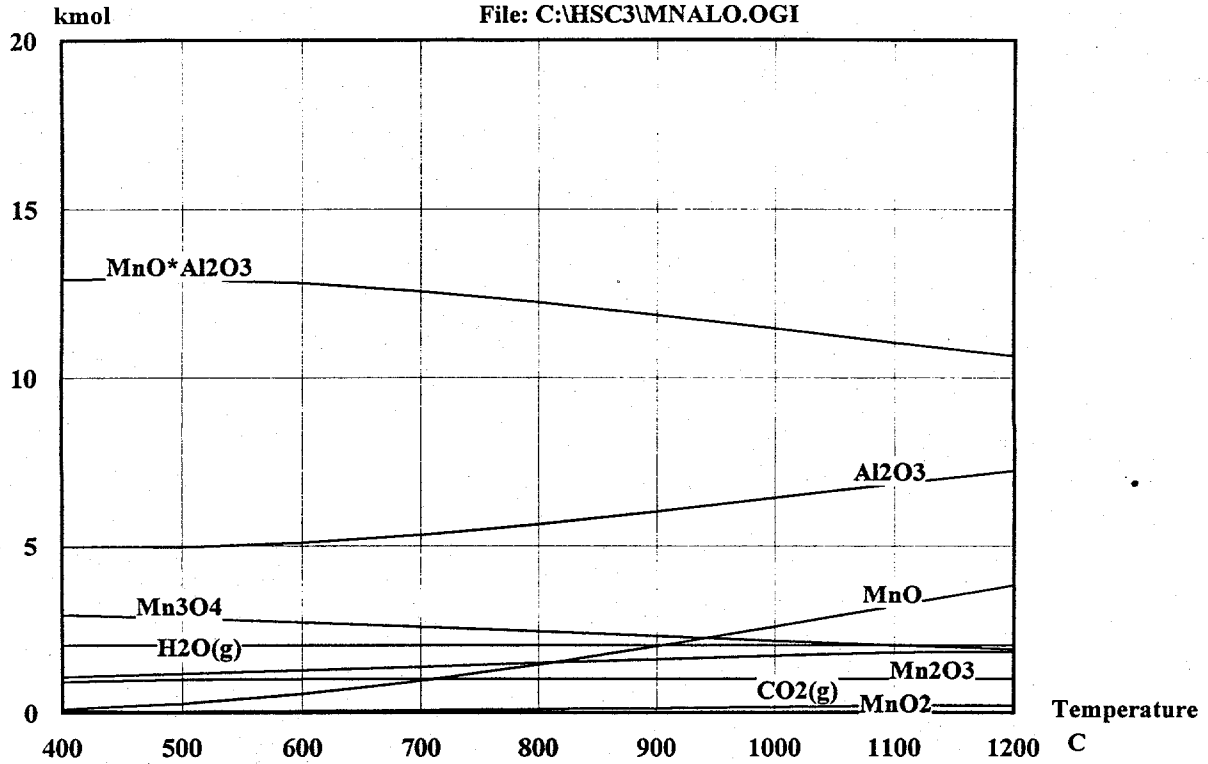


9

Temperature: 673.150 K
 Pressure: 15.000 bar
 Raw Materials: kmol
 CH₄(g) 1.0000E-03
 N₂(g) 1.0000E+01
 Al₂O₃ 1.0000E+00
 MnO₂ 1.0000E+00

Attachment 14

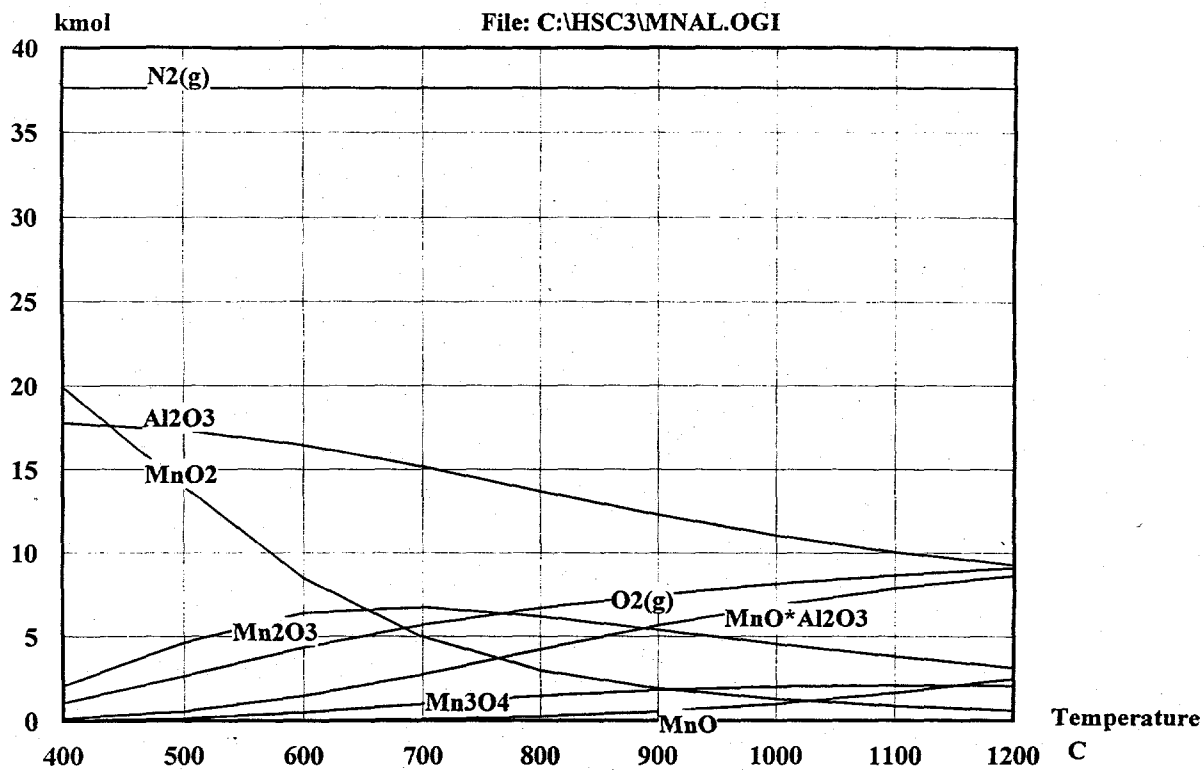
File: C:\HSC3\MNALO.OGI



9

Temperature: 673.150 K
 Pressure: 15.000 bar
 Raw Materials: kmol
 CH₄(g) 1.0000E+00
 Al₂O₃ 1.7900E+01
 Mn₃O₄ 8.0000E+00

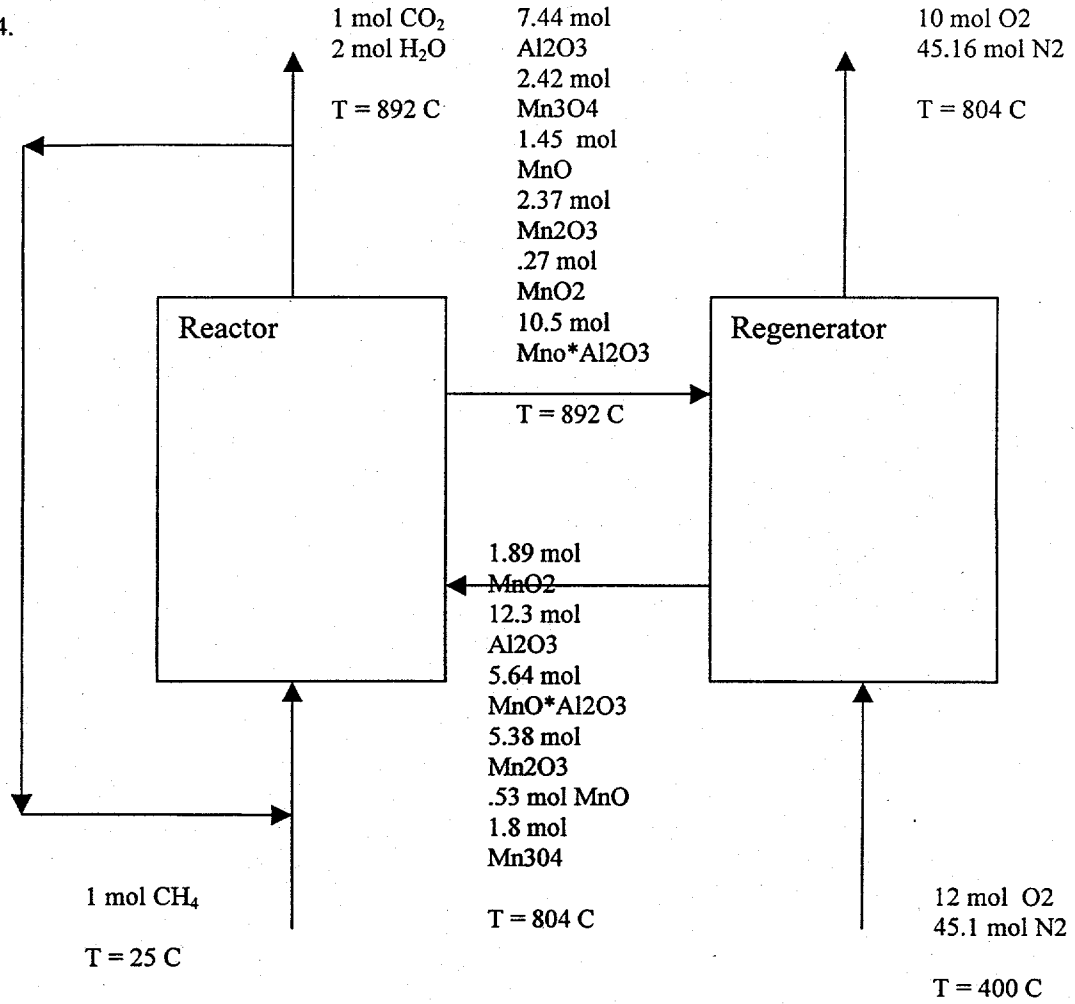
Attachment 15



Temperature: 673.150 K
 Pressure: 15.000 bar
 Raw Materials: kmol
 N2(g) 3.7600E+01
 O2(g) 1.0000E+01
 Al2O3 5.9000E+00
 MnO 2.0500E+00
 MnO2 2.0000E-01
 Mn2O3 1.6000E+00
 Mn3O4 2.2500E+00
 MnO*Al2O3 1.2000E+01

Attachment 16

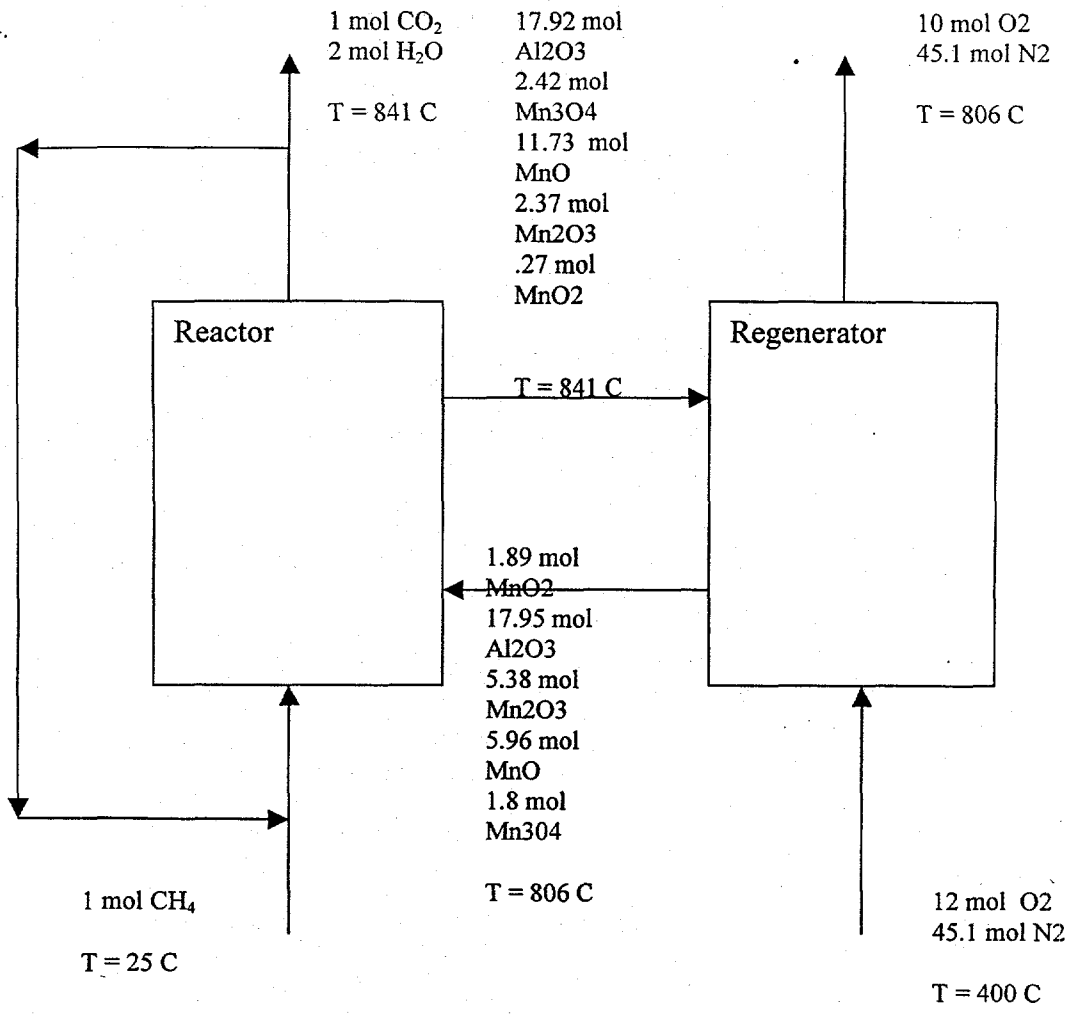
4.



Attachment 17

Mn_xO_y Sorbent (with aluminate formation)
50%Mn₃O₄/50% Al₂O₃ (wt)

4.



Attachment 18

Mn_xO_y Sorbent (without aluminate formation)
50%Mn₃O₄/50% Al₂O₃ (wt)

Status Report 3

GHG Project

VANADIUM

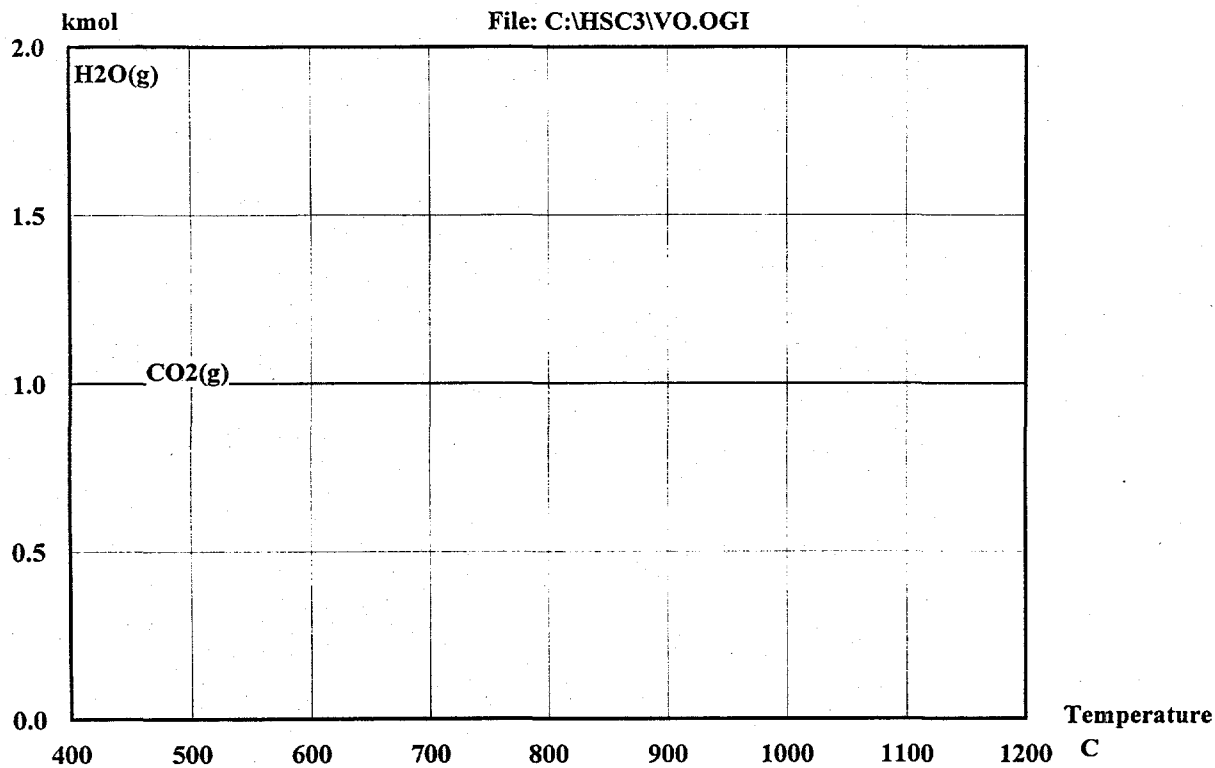
Vanadium is probably not a good candidate based on its thermodynamics. V_2O_5 is the dominant equilibrium product when any reduced oxide is regenerated in air. The reaction between V_2O_5 and CH_4 to form V_xO_y is exothermic for all $y > x$. When the reduced oxide is VO ($y = x$) the reaction is endothermic. However, VO formation is not favored at any reasonable reaction conditions.

Attachments 1 & 2: These figures show the product distribution when a large excess of V_2O_5 reacts with CH_4 (5 mols V_2O_5 per 1 mol CH_4). Only H_2O and CO_2 appear in the gas phase (Attachment 1). The equilibrium solid phase (Attachment 2) consists of a mixture of oxides with $V_2O_4 > VO_2 > V_2O_5 > V_3O_5$. The oxygen transfer between V_2O_5 and VO_2 is only 8.8%, so that the cost of vanadium per pound of O_2 transferred will be quite high.

Attachments 3 & 4: The quantity of V_2O_5 is reduced by 40% so that the initial conditions are 3 mol V_2O_5 per 1 mol of CH_4 . Complete conversion of CH_4 to H_2O and CO_2 is favored as shown in Attachment 3. The solid phase (Attachment 4) is again a mixture of oxides with $V_2O_4 > VO_2 > V_3O_5 > V_2O_3 > V_4O_7$. Note that there is no V_2O_5 in the equilibrium solid at these conditions.

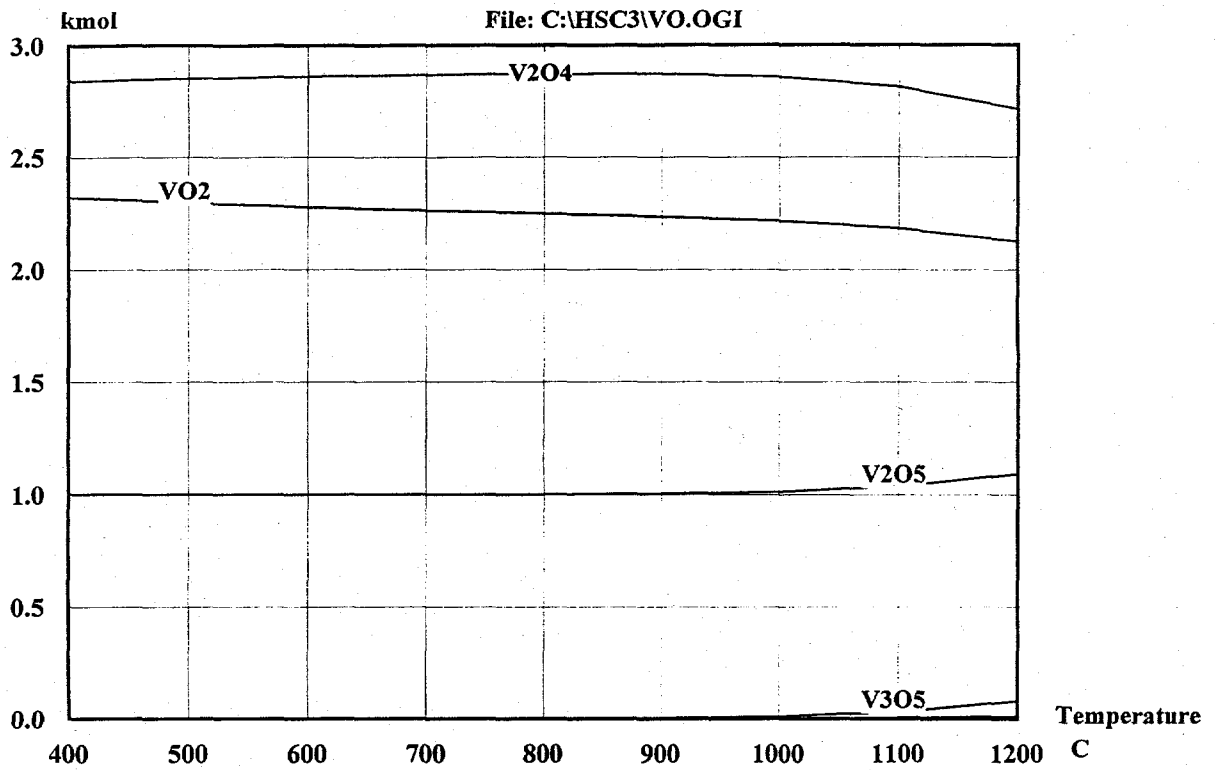
Attachments 5 & 6: The quantity of V_2O_5 is again reduced to 1.5 mol V_2O_5 per 1 mol CH_4 (just slightly in excess of the stoichiometric quantity required for $V_2O_5 \Rightarrow VO$). Oxidation of CH_4 is incomplete at all temperatures (Attachment 5). Unreacted CH_4 exists $T < 800^\circ C$ and both H_2 and CO are favored throughout the temperature range. Once again, all V_2O_5 is reduced to a mixture of oxides with $V_2O_3 > V_3O_5 > VO_2 \approx VO$ (Attachment 6).

Attachment 7: This regeneration analysis shows that V_2O_5 should be the dominant product when a mixture of reduced oxides is oxidized in excess air. The initial mixture of oxides corresponds to the equilibrium distribution achieved using 3 mol V_2O_5 to 1 mol CH_4 at $900^\circ C$. In addition to the dominant V_2O_5 , small amounts of VO_2 and V_2O_4 are favored with both amounts increasing slightly with increasing temperature.



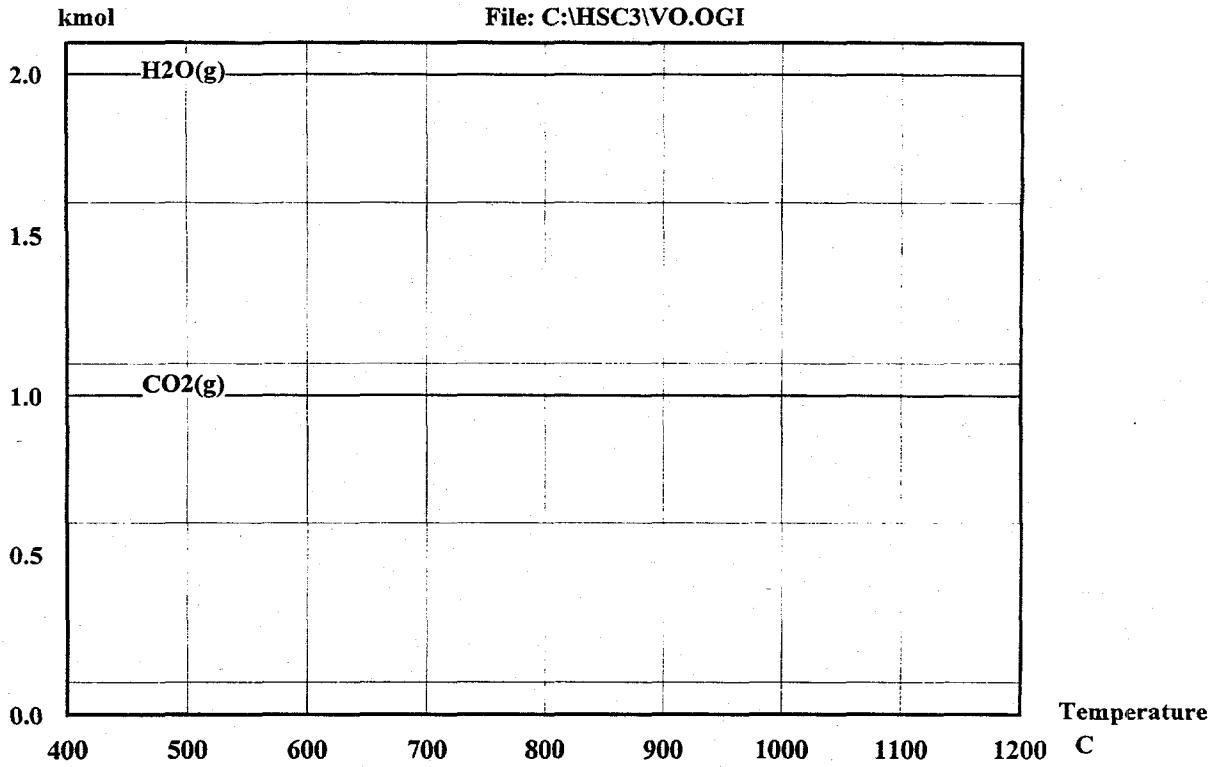
Temperature: 673.150 K
Pressure: 15.000 bar
Raw Materials: kmol
CH4(g) 1.0000E+00
V2O5 5.0000E+00

Attachment 1



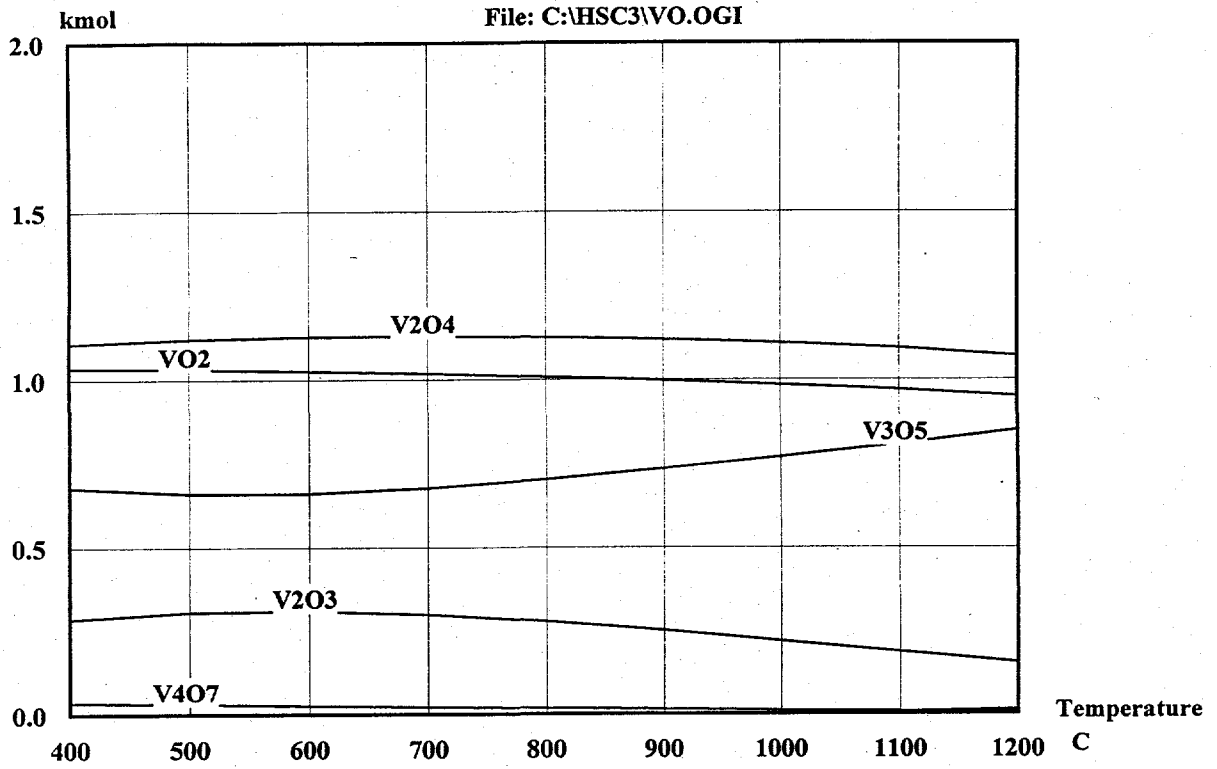
Temperature: 673.150 K
 Pressure: 15.000 bar
 Raw Materials: kmol
 CH4(g) 1.0000E+00
 V2O5 5.0000E+00

Attachment 2



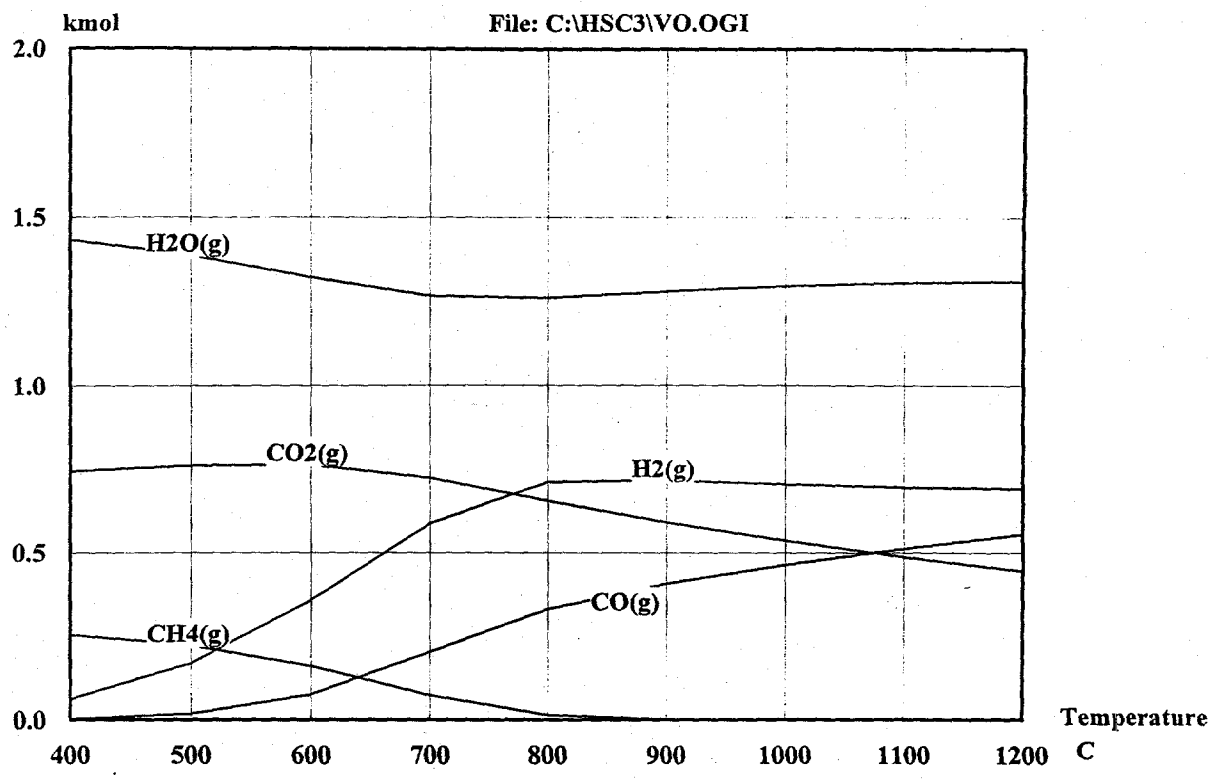
Temperature: 673.150 K
Pressure: 15.000 bar
Raw Materials: kmol
CH4(g) 1.0000E+00
V2O5 3.0000E+00

Attachment 3



Temperature: 673.150 K
Pressure: 15.000 bar
Raw Materials: kmol
 CH4(g) 1.0000E+00
 V2O5 3.0000E+00

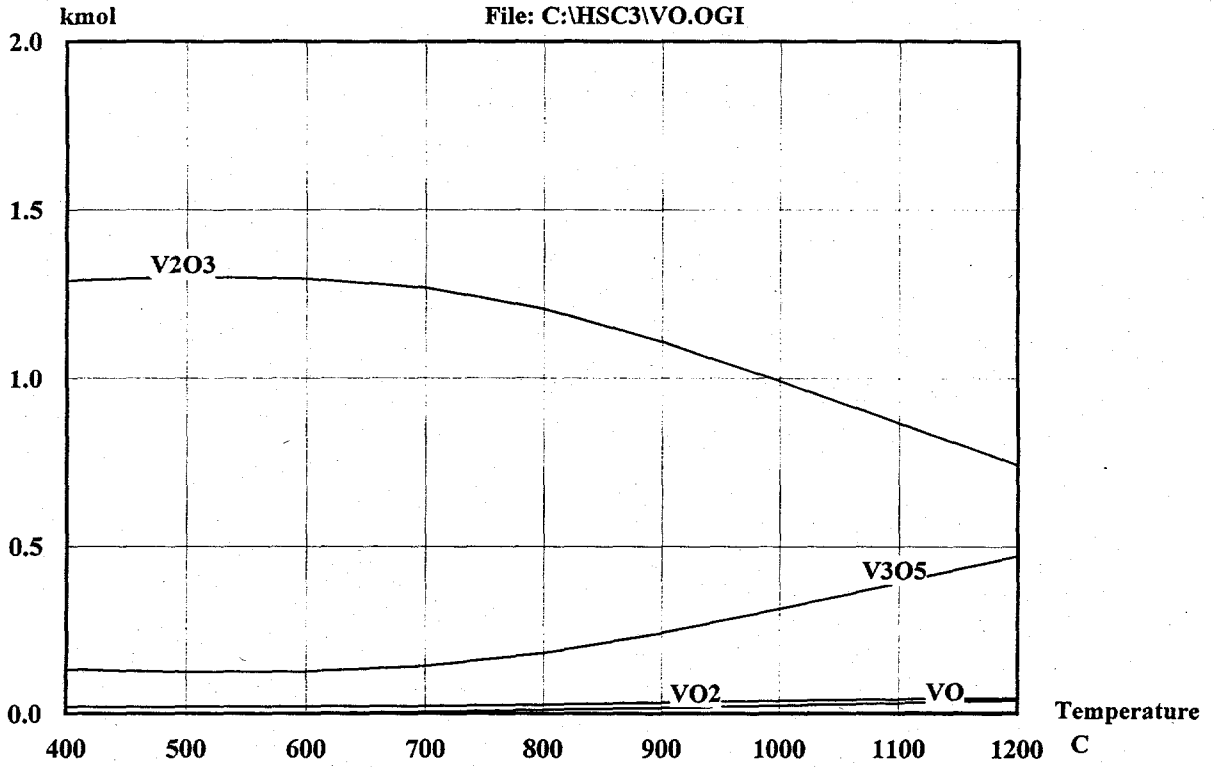
Attachment 4



Temperature: 673.150 K
 Pressure: 15.000 bar
 Raw Materials: kmol
 CH4(g) 1.0000E+00
 V2O5 1.5000E+00

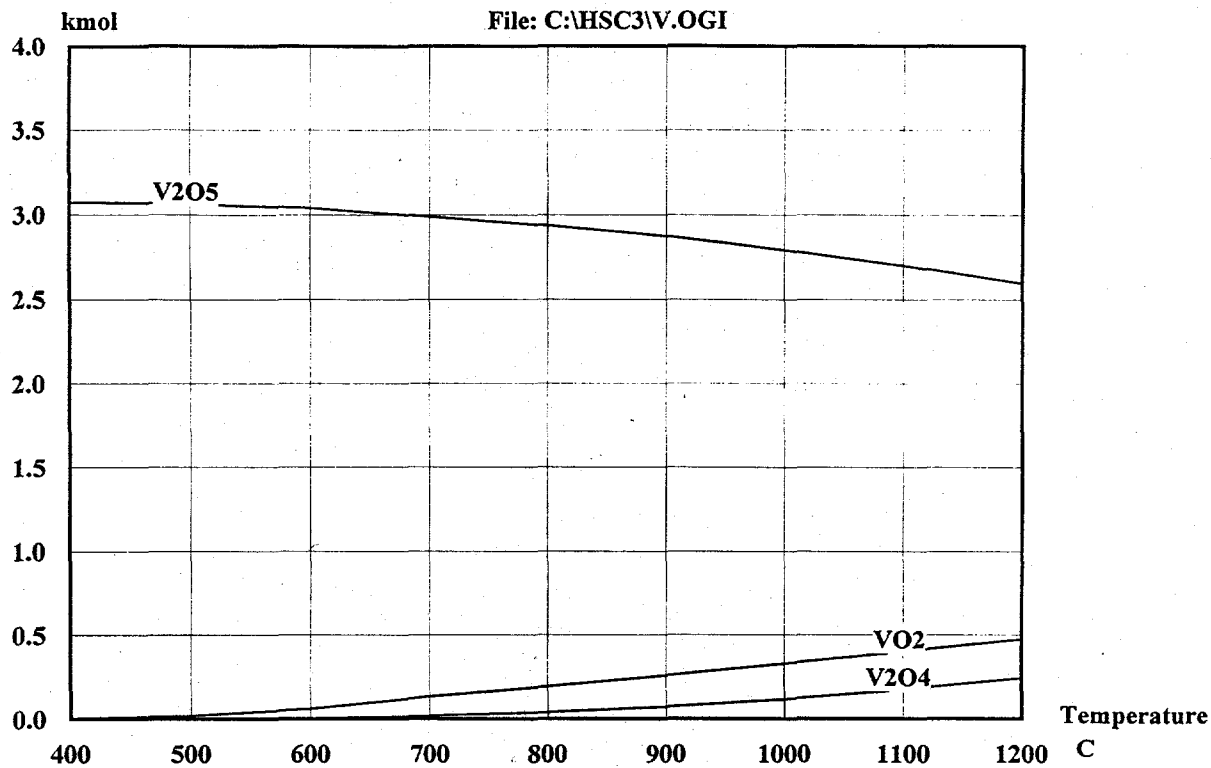
Attachment 5

6



Temperature: 673.150 K
Pressure: 15.000 bar
Raw Materials: kmol
CH4(g) 1.0000E+00
V2O5 1.5000E+00

Attachment 6



Temperature:	673.150 K
Pressure:	15.000 bar
Raw Materials:	kmol
N2(g)	7.5200E+01
O2(g)	2.0000E+01
VO2	1.0000E+00
V2O3	2.5000E-01
V2O4	1.2000E+00
V3O5	7.5000E-01

Attachment 7